EXPLORING CONTAMINANT FATE WITHIN PLASTIC WATER INFRASTRUCTURE: THE NEXUS OF ENVIRONMENTAL ENGINEERING AND MATERIAL SCIENCE FRONTIERS

by

Maryam Salehi Esfandarani

A Dissertation

Submitted to the Faculty of Purdue University

In Partial Fulfillment of the Requirements for the degree of

Doctor of Philosophy

Department of Civil Engineering

West Lafayette, Indiana

August 2017

THE PURDUE UNIVERSITY GRADUATE SCHOOL
STATEMENT OF DISSERTATION APPROVAL

Dr. Andrew J Whelton, Chair

Lyles School of Civil Engineering, Purdue University

Division of Environmental and Ecological Engineering, Purdue University

Dr. Chad T Jafvert

Lyles School of Civil Engineering, Purdue University

Division of Environmental and Ecological Engineering, Purdue University

Dr. Jeffery P Youngblood

School of Material Engineering, Purdue University

Dr. Marc A Edwards

The Charles E. Via, Jr. Department of Civil & Environmental Engineering, Virginia Tech

Approved by:

Dr. Dulcy Abraham

Head of the Departmental Graduate Program

Dedicated to

My Beautiful Daughter ***Tina***

and

My Loving Husband ***Ali***

ACKNOWLEDGMENTS

First and foremost I would like to express my sincere gratitude to my advisor Dr. Andrew Whelton. It was an honor to be his first Ph.D. student. I appreciate all his contribution in terms of time, idea and funding to make my Ph.D. experience inspiring and productive. I am evermore grateful to my committee members Dr. Chad Jafvert, Dr. Jeffery Youngblood and Dr. Marc Edwards for their recommendations and technical inputs on my work.

I would like to thank my family for all their love and encouragement. Thanks to my husband Ali, who supports me in every step of my dissertation, and to my beautiful daughter Tina, who shared the joy and suffered difficulty through with me for attainment of this degree. I am truly grateful to my parents' wisdom and support who raised me with love in science.

I would like to thank the following individuals for their technical assistance during this work.

Government Agencies

National Institute for Standards and Technology: Dr. Ajay Krishnamurthy, Dr. Aaron M. Forster

Companies

Tony Hahn Plumbing: Tony Hahn

Whirlpool Corporation: Eric Bowler

American Water

Purdue University

Administration: Jennifer Ricksy

Lyles School of Civil Engineering: Dr. Ernest Blatchley, Dr. George Zhou, Dr. Nadezhda Zyaykina, Mahboobeh Teimouri, Mahsa Modiri, Mian Wang

Division of Environmental and Ecological Engineering: Xianzhen Li, Jessica Yaputri, Celeste Bronson, Jesse Li, Jackson Coleman, Jason Hawes

School of Material Engineering: Dr. John Howarter, Dr. Lia Stanciu, Gamini Mendis

School of Chemical Engineering: Dr. Stephen Beaudoin, Darby Hoss, Chiebuka Egwuonwu

School of Mechanical Engineering: Stephen Caskey

Collage of Pharmacy: Dr. Keith Chadwick, Mitul Patal Kumar

Department of Agronomy: Dr. Chloe De Perre

Birck Nanotechnolgy Center: Dr. Rosa Diaz, Dr. Dmitry Zemlyanov

Other Academic Institutions

Michigan State University: Dr. Amir Pouyan Nejadhashemi, Dr. Jade Mitchell, Dr. Mohammad Abouali

University of South Alabama: Dr. Kuang–Ting Hsiao, Keven Kelley

Clemson University: Dr. David Ladner

Dauphin Island Sea Lab: Ms. Laura Linn

Funding for this research

The authors thank the National Science Foundation (NSF) for funding this research under grant CBET-1228615 and US Environmental Protection Agency (EPA) grant R836890. Partial project support was provided by the Birck Nanotechnology Center, US National Aeronautics and Space Administration (NASA) EPSCoR #NNX10AN26A, US National Science Foundation EPSCoR #1158862, and National Institute of Standards and Technology. I am grateful to the National Science Foundation, US EPA, NASA and NIST for their support.

TABLE OF CONTENTS

LIST OF TABLES

LIST OF FIGURES

ABSTRACT

Author: Salehi, Maryam. Ph.D.
Institution: Purdue University
Degree Received: August 2017
Title: Exploring Contaminant Fate Within Plastic Water Infrastructure: The Nexus of Environmental Engineering and Material Science Frontiers
Major Professor: Andrew Whelton

Plastic pipes are increasingly being used in potable water systems as corrosion resistant low cost materials. Despite the growth and installation of plastic pipes, gaskets, coatings, and liners in drinking water systems there are many knowledge-gaps with these materials. Lack of knowledge regarding contaminant fate within plastic water infrastructure systems present a possible emerging public health problem. For example, polyethylene plastic pipes are being installed in 75% of new building construction, and buried water service. For this dissertation research, water chemistry, environmental engineering, polymer and surface science and principles were applied to address several knowledge-gaps regarding plastic pipes. The first chapter of this dissertation focusses on reinforced plastic composites, materials sometimes used for water piping. Chapter 1 describes the influence of carbon nanofiber reinforcements on polyester composite water uptake and organic contaminant release. The experiments revealed that oxidized carbon nanofibers (CNFs) in the polyester composites significantly influenced water-composite interactions and organic contaminant leaching. Chapter 2 of this dissertation describes an investigation of the linkage between fixture water use and drinking water quality in a new green building. It was found that at the basement fixture, where the least amount of water use events occurred, greater organic carbon, bacteria, and heavy metal concentrations were detected. Different fixture use patterns resulted in disparate drinking water quality within the same residential building. Within Chapter 3, results of experiments conducted to determine the factors that influence Pb accumulation on the surface of low density polyethylene (LDPE) were discussed. Pb deposition onto LDPE as a function of time was modeled using the pseudo-1st-order equation, and an ozone based accelerated aging method for LDPE oxidation was developed. Greater Pb precipitation rates were found for

aged LDPE compared to new LDPE at both tested pH values. However, at pH 11 less Pb surface loading on aged LDPE was detected compared to Pb loadings at pH 7.8. The final chapter of this dissertation explains an investigation into the abundance of metal deposition onto 1-year old crosslinked polyethylene (PEX) plumbing system. Results showed that total metal loadings differed between hot and cold water line pipe segments and water temperature influenced surface scales. A bench scale experiment revealed that the polyethylene surface served as a nucleation site for Fe crystals. This dissertation work provides a foundation for continued exploration of contaminant fate in water infrastructure.

AUTHOR'S PREFACE & ATTRIBUTION

This dissertation contains four different manuscripts that are enclosed as Chapters and the research spans three major disciplines: water chemistry, polymer science and public health. The dissertation presents results from four different multidisciplinary projects. Within each individual manuscript, the scientific literature was reviewed and the current knowledge gap was described. The manuscript title, contributing authors, and an abstract are presented the beginning of each chapter.

Funding for this research was provided by several organizations. Work conducted for the completion of Chapter 1 was partially funded by the NASA (EPSCoR #NNX10AN26A), NSF (EPSCoR #1158862, CBET #1228615), and NIST. Funding for Chapters 2, 3 and 4 was provided by NSF (grant CBET-1228615) and US EPA (grant R836890). Partial funding for chapters 3 and 4 was provided by Purdue University Birck Nanotechnology Center.

Attribution

Several colleagues helped compile and analyze information contained in this dissertation. A concise description of the background and contributions of each person is included here. Maryam Salehi, Ph.D. (doctoral student) and Andrew Whelton, Ph.D. (Assistant Professor, Lyles School of Civil Engineering, Purdue Univ., the Advisor, and Committee Chair) contributed to every chapter in dissertation so their contributions will not be discussed in detail.

Aaron Forster, Ph.D., (National Institute of Standards and Technology) is a research scientist who contributed to **Chapter 1** by assisting with polymer composite characterization.

Kuang–Ting Hsiao, Ph.D., (Dept of Mechanical Engineering, Univ. of South Alabama) is a Professor who contributed to **Chapter 1** by synthesis the polymer composites.

Chad Jafvert, Ph.D., (Lyles School of Civil Engineering, Purdue Univ.) is a Professor who contributed to **Chapter 3** by helping with the design of polymer aging method and analyzing the metal adsorption data.

John Howarter, Ph.D., (School of Materials Engineering and Environmental and Ecological Engineering, Purdue Univ.) is an Assistant Professor who contributed to **Chapter 3** in terms of X-ray photoelectron spectroscopy (XPS) experimental design and data interpretation.

Zhi Zhou, Ph.D., (Lyles School of Civil Engineering and Environmental and Ecological Engineering, Purdue Univ.) is an Assistant Professor who contributed to **Chapter 2** by helping design the experimental plan and interpret the results for water quality microbial analysis.

Amir Pouyan Nejadhashemi, Ph.D., (Dept. of Biosystems and Agricultural Engineering; Dept. of Plant, Soil and Microbial Science, Michigan State Univ.) is an Associate Professor and Jade Mitchell, Ph.D., (Dept. of Biosystems & Agricultural Engineering) is an Assistant Professor who contributed to **Chapter 2** through discussion of water flow analysis approach.

Mohammad Abouali, Ph.D., (Dept. of Biosystems and Agricultural Engineering; Dept. of Plant, Michigan State Univ.) is a Post-doctoral Research Scientist who contributed to **Chapter 2** through analyzing the water flow data.

Mian Wang, (Lyles School of Civil Engineering, Purdue Univ.) is a Ph.D. student who contributed to **Chapter 2** in terms of conducting microbial experiments, analyzing and interpreting the results.

CHAPTER 1 : POLYESTER COMPOSITE WATER UPTAKE AND ORGANIC CONTAMINANT RELEASE AFFECTED BY CARBON NANOFIBER REINFORCEMENTS

Maryam Salehi, Ajay Krishnamurthy, Aaron M. Forster, Kuang–Ting Hsiao, Andrew J. Whelton

Published in *Journal of Applied Polymer Science* (2016), 133(30), 1-9

1.1 Abstract

The incorporation of carbon nanofiber (CNF) into glass fiber (GF) composites is a potential route to extend polymer composite service-life and enhance mechanical properties. Under non-static conditions, only limited information concerning water uptake and contaminant release properties of nanocomposite materials is currently available. Polyester composites containing glass fiber and oxidized carbon nanofiber were immersed in water for 30 days under nominal pressure at 23 °C, below the polymer's glass-transition temperature. Water was analyzed and changed every three days to simulate water chemistry regeneration similar to exposures in flowing systems. Composites with oxidized CNF had greater water sorption capacity and leaching rates than CNF-free composites. The total mass of organic contaminant released correlated with the amount of water sorbed by each composite ($r^2 = 0.91$), although CNF dispersion was found to vary greatly within composites. The greatest and least contaminant release rates were found for the polyester-CNF and the polyester-GF composites, respectively. While, volatile aromatic resin solvents and stabilizer compounds were detected, their concentrations declined over the 30 day exposure period. We hypothesize that the hydrophilic nature of the oxidized CNF increased the water sorption capacity of the polyester composites. Additional studies are warranted that examine the impact of this phenomenon on composite mechanical and long-term durability properties.

1.2 Introduction

As North American buried water infrastructure pipelines continue to deteriorate, inexpensive and corrosion resistant replacement materials are needed. Corrosion resistant fiber reinforced plastic (FRP) pipes have been used for more than 60 years for drinking water conveyance[1-3] and have a high strength to weight ratio. FRPs typically consist of a polymer matrix (i.e., polyester, epoxy, or nylon) reinforced with glass, carbon, graphite, or aramid fibers[4-10]. Incorporation of carbon nanofiber (CNF) into resins and fiber composites can further improve their mechanical properties[11]. CNF reinforcements are high aspect ratio nanofibers spanning a wide range of diameters (50 nm to 200 nm) and lengths (30 µm to 100 µm). Further, the hydrophilic nature of CNF surfaces reportedly enables easy dispersion into polar matrices. This combination of properties have been shown to improve FRP tensile strength, compression strength, Young's modulus, fracture toughness, and delamination resistance[12-16]. Many nanotechnology enhanced water infrastructure materials containing multi wall carbon nanotubes (MWCNT), TiO_2 and clay, have already received U.S. patents and some are being sold outside North America for potable water transport[17-21].

Despite scientific research associated with the performance of nanocomposites, such as CNF in FRP pipes, there is little to no information regarding its influence on water/polymer interactions. It is well-known that polyester composites uptake water when immersed in deionized, tap, brackish, and salt water solutions (**Table 1-1**)[22-25]. Composite water sorption is important because water can degrade the polymer/fiber interface, facilitate matrix oxidation or void formation, and lead to FRP mechanical performance reductions[26-32]. Investigators have observed that GF reduces water sorption compared to resin only materials[31, 33, 34], since glass fibers displace resin volume, do not absorb water, and may reduce the water diffusion coefficient through the composite[31]. Though the glass fibers do not absorb water, secondary degradation processes can be triggered by surface reactions in the presence of water, which degrades the fiber/matrix interface resulting in loss of mechanical performance. The presence of CNF can adversely affect moisture diffusion properties in an FRP but the extent of diffusion on damage tolerance is not sufficiently quantified in the literature.

A percolated, hydrophillic CNF network has the potential to adversely affect water quality. In the presence of water, contaminants normally confined within the polymer network can diffuse into the contact water. The diffusion rate is a function of the contaminant molecule size, polarity, concentration gradient, and temperature. The relationship between water transport through reinforced composites and the chemical leaching by the composites are a fairly well studied phenomenon[35-37]. As the composite achieves equilibrium with the surrounding water, the diffusion process can be modeled by applying one of three approaches: Fickian, Case II, and the two phase model[38]. Generally, the water uptake rate (immersion) and water loss rate (drying) are greatest (linear) during the initial exposure periods because the concentration gradients between contact water and composite are at a maximum.

Table 1-1 Impact of water exposure on FRP mechanical properties: literature summary

Polymer Matrix (Reinforcement Type)[Reference]	Aging Condition	Result Summary
u–Isophtalic polyester & vinyl ester resins (Glass fiber)[31]	DI (pH NR); 40 °C, 80 °C; 3 months	Glass fiber composites sorbed 45% to 82% less water than polyester resin only materials at 40 °C and roughly 20% less water at 80 °C. Water absorption was controlled by T_g and water temperature. Decrease in mechanical properties observed for both composites as a result of decrease in fiber-matrix interfacial adhesion.
u–Polyester resin (Glass fiber)[37]	TW (pH NR); 20 °C; 1, 000 hr	Water uptake measurements were conducted but not reported; Water immersion reduced creep strength by 60%.
u–Polyester resin (Glass fiber)[30]	DI (pH NR); 30 °C; (7, 14, 21) days	Water uptake measurements were not conducted; Water immersion caused delamination between fiber and matrix along with increasing bending strength, and a significant reduction in tensile strength.
Urethane &modified urethane resin (Glass fiber)[34]	Alkaline water (pH 13.4); temp NR; 6 months	Glass fiber inhibited water uptake. After 6 months aging, no reduction in tensile strength for unloaded composites was observed but tensile strength reduction was observed for the samples that were subjected to sustained load during the aging.
u–Polyester resin (Glass fiber)[38]	DI (pH NR); Room temp; 9 months	Glass fiber composite elastic modulus decreased by 2% to 5%; Water absorption data did not fit the Fickian diffusion model; The Lucas–Washburn capillary flow model was deemed more appropriate.
u–Polyester resin (Glass fiber)[27]	Artificial sea water (3.4 % to 3.5 % salinity) (pH NR); 30 °C; (10, 30, 60, 90, 120) days	Water uptake data were not reported; Water immersion decreased composite tensile strength and bending resistance; Material extraction was detected by an observed reduction in specimen mass during immersion.
Epoxy resin (Glass fiber, flax fiber)[33]	Water (pH NR); Room temp; (10, 20, 30, 40) days	The fiber–polymer interface was damaged due to water immersion for both reinforcement types; flax fiber reinforced composites sorbed 12 times more water than glass fiber composites.

u = unsaturated; DI = Distilled water; TW = Tap water; NR = Not reported; Not all studies reported water pH or the ionic quality of the test water.

From an application standpoint, the impact of a polymer composite on water quality is extremely significant, considering an estimated 60-100 year expected lifetime use of these pipelines[39]. However, on surveying water quality from 16 countries, there were only two published FRP investigations concerning water quality and both had little or no data on nanomaterial reinforced plastics. [40] FRP pipes are manufactured using three basic components namely, the resin (i.e., polyester, vinyl ester), the solvents (i.e., styrene, benzene, ethylbenzene), and the catalysts (i.e., methyl ethyl ketone peroxide (MEKP), dimethyaniline, cobalt naphthenate)[41]. It has been shown that the solvents and catalysts used for composite manufacture are often environment polluting and highly carcinogenic. In the 1990s, researchers in the U.K. discovered that polyester/glass fiber (P/GF) pipe released several carcinogenic and endocrine disrupting organic contaminants into distilled water during a 24 h leaching period[3]. Several organic contaminants with and without drinking water health standards were found and included: Phthalic acid ester (26 μg/L), dimethyl phthalate (21 μg/L), benzaldehyde (4 μg/L), acetophenone (3 μg/L), styrene (0.7 μg/L), and tris(2–carboxyethyl)phosphine (TCEP) (3 μg/L). Other contaminants detected but not quantified were dialkoxy phthalate ester, dioctylphthalate (DOP), benzoic acid, nonanol, and 2–ethyl hexanoic acid. This 24 h test was the most experimentally quantitative effort found in the literature. In another effort, researchers in the U.S. reported that FRP well casings leached "five different contaminants into distilled water," but neither the contaminants nor experimental conditions were described[42]. No other studies were found that described either FRP contaminant leaching, the role of CNF reinforcement on material leachability, or water quality impacts caused by CNF containing composites. As real world applications of nano-FRPs are being realized, understanding the influence of nanofillers on the type and concentration of contaminants released into contact waters would highly benefit municipalities installing these solutions, standards bodies developing test methods, safety regulators, and commercial composite pipe manufacturers.

The hypotheses for this work were that glass fiber reinforced FRP materials would uptake less water than a polyester material and CNF incorporation would not affect water uptake or leaching because of its low mass fraction in the composite. Specific objectives of these measurements were to: (1) quantify the impact of CNF on

water quality and composite mass during a 30 day aging period and subsequent desiccator drying, and (2) identify relationships between the contact solution quality and the composition of the composites. Several water quality characterization methods were applied to elucidate the magnitude of chemical release.

1.3 Experimental

1.3.1 Composite Fabrication

Four specimens were manufactured: Polyester only (P/O), and three composites including polyester/CNF (P/CNF), polyester/glass fiber (P/GF) and polyester/GF/CNF (P/GF/CNF). Unsaturated polyester resin (Cook Composites & Polymers, Product ID: CI–1001–25), 0.005 mass fraction methyl ethyl ketone peroxide (MEKP), eight layers of E–glass random fiber mats sized with an undisclosed silane coupling agent (Saint–Gobain Vetrotex America Inc., M113 random chopped strand mat) and 0.01 mass fraction of CNF (Pyrograf, PR–24 LHT, 150 nm average diameter, range of 70 nm to 200 nm diameter, 50 µm to 200 µm length, density of 1.9 g/mL) were used. Because of their high surface area, oxidized CNFs can be dispersed easily into polar polymer matrices such as epoxy, polyester and vinyl ester and show significant improvements in their mechanical properties[43]. In the present study, oxidized CNFs were mixed with polyester resin and sonicated in a cold water bath for 45 min. The mixture was then degassed for 10 min and MEKP was added. P/GF and P/GF/CNF panels were manufactured with the Vacuum Assisted Resin Transfer Molding (VARTM) process[15]. P/O and P/CNF panels were cast in an open mold and allowed to cure for 12 h at room temperature. Composite thicknesses were statistically not different from one another and the surface area of each composite subjected to water immersion was approximately 435 cm^2. Sample thickness ranged from 2.85 mm to 3.40 mm.

1.3.2 Water Immersion and Water Quality Testing

Synthetic water (pH 6.9, 47.2 mg/L as $CaCO_3$, 23 °C) was prepared using Type I Millipore® Milli–Q water, $NaHCO_3$, and HCl. Specimens were immersed in covered

glass jars filled with synthetic water (headspace free) for 30 days. Every three days, contact water was removed, characterized, and replaced with new synthetic water. The water exchanges simulated two conditions: water replenishment similar to a flowing system and water chemistry stabilization through solvated ion renewal. Water quality characterization was conducted using three replicates for each composite. The 30 day immersion period was selected to characterize short-term water quality changes caused by composite contact. The concentration gradient between the composite and contact water was reset every three days. Thus, the water uptake data does not represent a single equilibrium condition. This approach was necessary to obtain enough water sample to describe chemical leaching during the study period and the release of volatile organics. This concentration gradient "reset" approach is often used by the National Sanitation Foundation International, an organization that certifies potable water contact materials in the US[44]. While this approach enabled quantification of water quality impacts, standard water diffusion models were not applicable with the data collected in this study. Regardless, the contaminant concentration was expected to decrease over time and this trend was confirmed from our experiments.

Water quality monitoring techniques in accordance with standard methods[45] were applied to examine how the composites influenced the water chemistry. Alkalinity was determined with 0.025 N sulfuric acid and a titration end point of pH 4.5. Water pH was measured using an Accumet pH meter (Fisher Scientific; Pittsburg, PA) based on standard methods. Chemical oxygen demand (COD) concentration was measured by application of the U.S. Environmental Protection Agency (EPA) ultralow range reactor digestion method. COD represents the total amount of organic contaminants present that are biodegradable as well as nonbiodegradable. Total organic carbon (TOC) concentration was determined by applying the nonpurgeable organic carbon method with a Shimadzu TOC Analyzer. Contaminant biodegradability testing was carried-out according to methods described in the SI. UV absorbance at 254 nm (UV_{254}) wavelength was recorded using a HACH DR5000 UV–VIS spectrophotometer. UV_{254} measures the quantity of sp^2 hybridized carbon and is frequently applied to gauge the level of dissolved aromatic compounds in water. On day 3 and 30, contact waters were also characterized using solid–phase microextraction (SPME) gas chromatography–mass spectroscopy

(GCMS) to determine if volatile organic compounds (VOCs) were leached from the composites. A 85 µm polyacrylate coated SPME fiber was conditioned at 280 °C for 3h before initial application of the GC port. For sampling, the fiber was exposed to the sample headspace with a 10 min adsorption time at 55 °C. Desorption was conducted in the GC injector at 220 °C for 2 min. A SPME inlet liner (splitless, 0.75 mm I.D.) was used in the injection port. The GC carrier gas was helium at a flow rate 0.65 mL/min. The GC temperature program involved a ramp from 50 °C to 100 °C at 10 °C/min., and was maintained for 25 min. A split/splitless injector in the splitless mode was used and held isothermally at 220 °C.

1.3.3 Composite Characterization

Water absorption and desorption was characterized for each composite. Absorption was measured gravimetrically during the 30 day water immersion period. Desorption was calculated during 30 days desiccator drying at room temperature. Moisture uptake and mass loss were calculated (Equation 1-1):

$$\text{Mass Gain, Mass Loss} = \frac{M_0 - M_t}{M_0} \times 100 \qquad (1\text{-}1)$$

where M_o was the initial sample mass and M_t was the specimen mass at time of t.

Thermogravimetric (TGA) measurements were conducted with a Q500 instrument (TA Instruments) with an air purge flow. Three replicates were conducted to determine variability within the composites. Specimens were degraded utilizing a stepped isotherm process. In the first step, the sample was rapidly heated (< 10 min.) to 500 °C and held for 15 min. This action removed the majority of matrix polymer from the composite. The sample was then rapidly heated to 700 °C and held for 15 min. This process removed residual CNF material and left a residual glass in the TGA pan, for the case of glass containing composites. Thermal oxidation of raw carbon nanofibers exhibited a mass fraction loss of approximately (0.03 ± 0.01) mg/mg during the 500 °C isotherm and a final mass fraction of (0.045 ± 0.001) mg/mg (residual mass fraction) after heating to 700 °C. The presence of a stable char indicates there were non-combustible components left from the thermal degradation process. Since there is a residual char present in both the

combustion of the polyester and the CNF and the void fraction of the composite was not measured, it is not possible to calculate the exact composition of the original composite. The residual char in the composite is assumed to polyester decomposition in order to calculate the apparent mass fraction of resin in each composite. The glass transition temperature (T_g) of each composite was identified using TA Instrument Q2000 differential scanning calorimeter (DSC). Temperature was ramped from 40 °C to 150 °C at 10 °C/min., quickly cooled to 40 °C at 20 °C/min., then reheated to 150 °C at 10 °C/min. to confirm the observed T_g. Nitrogen (50 mL/min.) was the applied purge gas.

For scanning electron microscopy, fractured cross section surfaces of P/CNF and P/GF/CNF were mounted onto a stainless steel stub using a highly conductive, double coated carbon tape (Ted Pella ®) inside a JEOL®, JSM – 7600F (Schottky field emission), scanning electron microscope (SEM). The samples were imaged primarily using the GB-H (gentle beam) settings to counteract excessive surface charge. The SEM settings utilized are as follows; gun voltage: 0.7 – 2kV, substrate bias: 0.7 – 2kV, probe currents: 20 – 40pA; WD: 4 – 8mm. Exposed surfaces of the P/GF/CNF samples were imaged as provided to preserve the surface details on the specimens.

1.3.4 Data Interpretation and Analysis

Water quality data represent a series of 3-day leaching tests with the same composite over a 30 day period. Based on this approach, the 30 day results were analyzed by two-way analysis of variance (ANOVA) and 95% confidence interval. To interpret water quality results, each aqueous contaminant concentration (mg/L) was divided by the initial mass of resin in each composite (mg/L–mg resin), determined as the mass fraction loss at the end of the 500 °C isotherm. This enabled all water quality data to be compared on a “mg of contaminant / L of water – mg of resin” estimated basis. This method incorporates an inherent mass error of 0.01 mg/mg mass fraction in the resin. Water sorption data were converted to “mg of water sorbed/mg of resin” basis. All statistics were applied using a Type I error of 0.05. Regression analyses were conducted on each contaminant leaching data set. Regression slopes using 95 % confidence intervals were applied to elucidate whether or not contaminant release rates differed between the various composites.

1.4 Result and Discussion

1.4.1 Composite Composition

TGA showed the quantity of CNF was smaller than expected from processing (**Figure 1-1**). The instrument was able to resolve the decomposition of the CNF, but the standard deviation was 33% for the P/CNF and 57% for the P/CNF/GF. The magnitude of uncertainty is similar to the uncertainty in the residual mass fraction, which suggests the quantity of CNF in the composites is near the limit of measurement resolution or the distribution of CNF in the composites is heterogeneous. Scanning electron microscopy (SEM) was conducted on sample cross-sections to verify the distribution of CNF.

No difference was found between the glass-transition temperatures either before or after water adsorption/desorption testing. T_g values for the epoxy ranged between 64 °C and 72 °C (**Table 1-2**). SEM images of the fractured P/CNF composite revealed large agglomerates of CNFs with diameters of a few tens of microns (**Figure 1-2a,b**). These large agglomerates were found uniformly across the cross-section. Despite CNF's hydrophilic nature, the sonication process did not effectively disperse individual large aspect ratio CNFs (**Figure A1**). Similar SEM analysis on the P/GF/CNF samples found a bimodal CNF distribution where individual CNFs were sparsely visible in the cross-sectional regions between glass fiber layers (**Figure 1-2c**), while dense CNF agglomerates were found on the top surface of the VARTM processed composite (**Figure 1-2d**). The dimensions of the CNFs observed in both cases agreed with manufacturer specifications of diameters and fiber lengths.

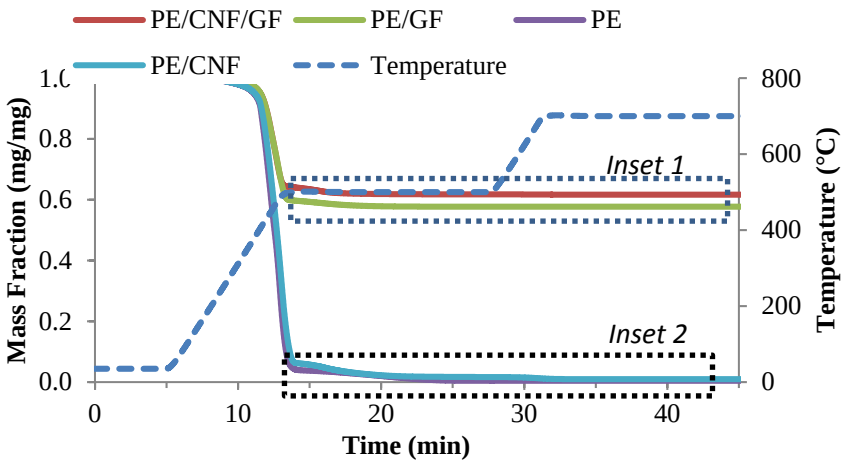

Inset 1

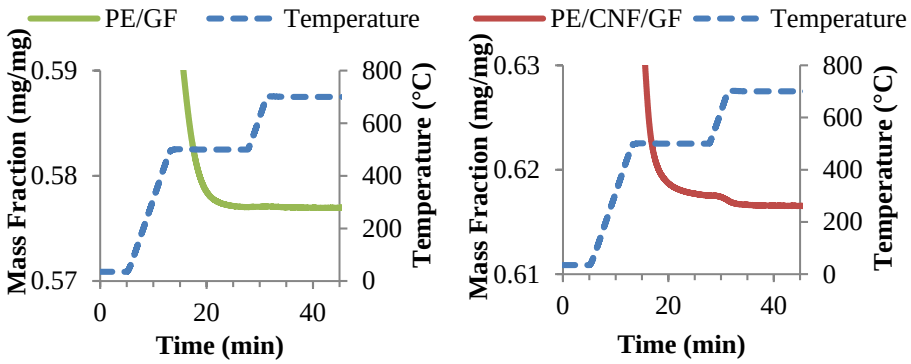

Inset 2

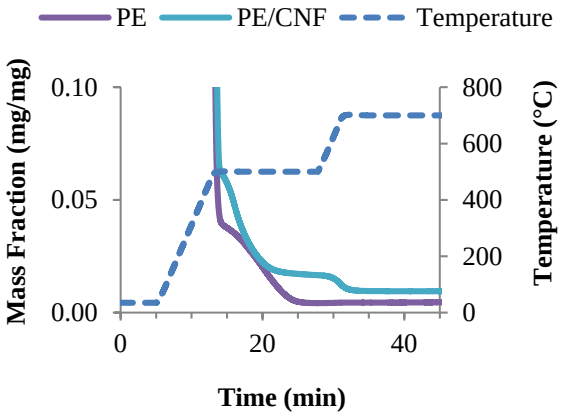

Figure 1-1 Thermogravimetric scans for P/O, P/CNF, P/GF and P/CNF/GF.

Inset 1, left shows the loss of mass during the ramp to 700˚°C for glass fiber composites. Inset 1, right shows the loss of mass during the ramp to 700˚°C for the glass

fiber composite containing CNF. Inset 2 shows the loss of mass during the ramp to 700 °C for the non-glass containing composite for matrix and nanocomposite.

These analytical techniques suggest an inhomogeneous dispersion and a unique mass fraction and distribution of CNFs within each composite type. The surface aggregation of CNF in the glass fiber composite likely results from the VARTM processing combined with the presence of large CNF agglomerates in the matrix. The VARTM process is a dynamic method that utilizes the flow of a low viscosity resin to fill the glass fiber. Since the CNFs were found to exist as large agglomerates in the P/CNF composite, it is likely these agglomerates were either filtered by the glass fibers or preferentially transported to the exterior surface of the composite, in particular, resin rich regions where the flow velocities are higher.

Table 1-2 Composite properties from gravimetric and thermal characterization

Composite	**Material Type**			
	Polyester	**Polyester/CNF**	**Polyester/GF**	**Polyester-GF/CNF**
Resin, mass fraction	0.988 $\pm$ 0.005	0.980 $\pm$ 0.005	0.400 $\pm$ 0.032	0.368 $\pm$ 0.014
GF, mass fraction	0	0	0.600 $\pm$ 0.032	0.631 $\pm$ 0.014
CNF, mass fraction	0	0.006 $\pm$ 0.002	0	0.0007 $\pm$ 0.0004
Residual, mass fraction	0.012 $\pm$ 0.005	0.014 $\pm$ 0.008	N/A	N/A
Measured T_g, °C	67.6 $\pm$ 2.9	65.3 $\pm$ 2.1	72.0 $\pm$ 0.9	68.1 $\pm$ 1.5

* The constituent components are based on the change in mass from TGA thermal degradation. T_g results represent mean and standard deviation values for two individual replicates on first heating. Residual for P/GF and P/GF/CNF composites at 700 °C could not be differentiated from GF.

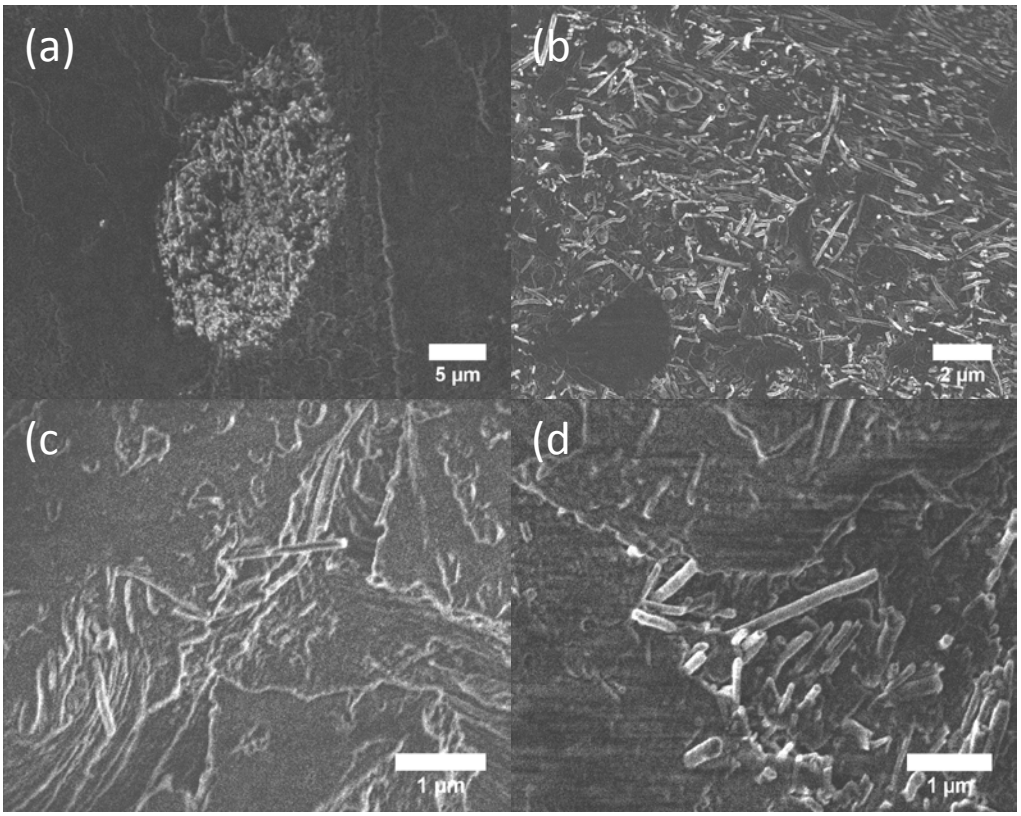

Figure 1-2 Representative SEM images of (a) large agglomerate of CNF in the P/CNF composite, (b) distribution of CNF within a CNF agglomerate in the P/CNF cross-section, (c) sparsely distributed CNF across the P/GF/CNF cross-section (arrows), (d) dense agglomerate of CNF on the top surface of P/GF/CNF composite. Supplemental contains low magnification images of the P/GF/CNF top surface.

Each material reached water saturation over the course of the 30 day exposure (**Figure 1-3**). All specimens exhibited a small mass loss of approximately 0.5 % for P/O, P/CNF and P/GF/CNF after desiccation (**Table A1**). Observed mass loss indicated that the water diffusion coefficient calculations could not be conducted.

Composites that contained oxidized CNF sorbed more water compared to the non-CNF containing materials (**Figure 1-3**). The GF composite absorbed the least amount of water and this result is similar to what has been observed in the literature, where polyester GF composites absorbed less water than its resin-only counterparts[31,33,34]. The inclusion of glass fiber reduced the volume of polyester resin available for water

absorption. Oxidized CNF also increased water absorption for the P/GF/CNF composite, but the change was not drastic as the polyester CNF composite. The hydrophilic nature of the oxidized CNFs likely contributed to the increased water sorption capacity of CNF containing materials. Other investigations indicate that incorporation of hydrophilic reinforcement fibers (i.e., vegetable, flax) increases polyester composite water sorption capacity by as much as 12 times[33,23]. When compared to the non-CNF containing materials, the initial rate of moisture uptake was greatest for the CNF materials in the present study.

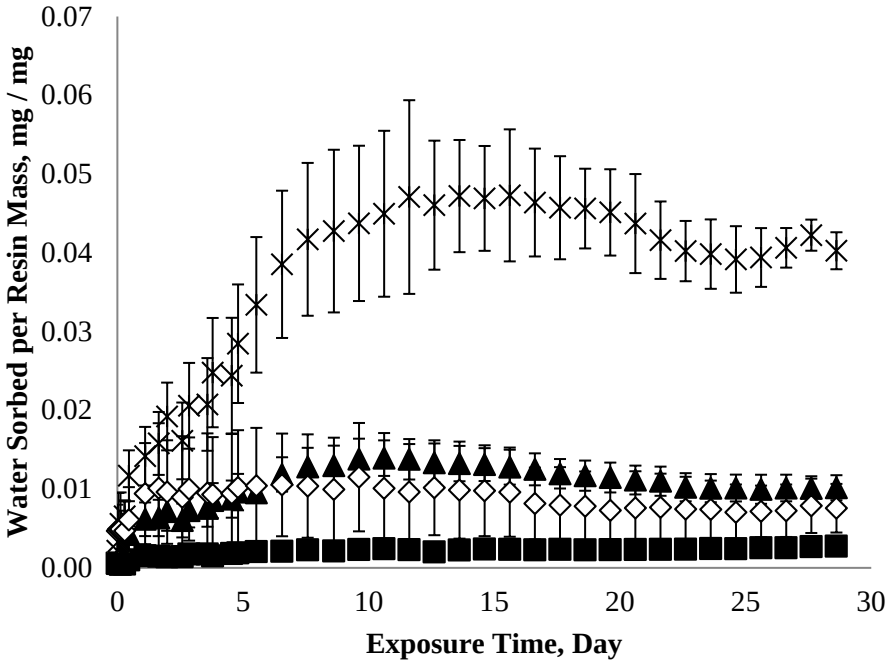

Figure 1-3 Moisture content of composites compared on a composite mass of resin basis. Symbols represent (▲) P/O, (■) P/GF, (✳) P/CNF, (◇) P/GF/CNF. The standard deviation of the measurement was ± 0.05 mg/mg.

1.4.2 Impact of Composites on Water Quality

All composites released organic contaminants during the entire 30-day study period. The expected exponential decay curve for contaminant release was not observed because the exposure period consisted of a series of 3-day exposure periods; the concentration gradient was constantly reset. As a result, a diffusion model was not fit to the leaching data. **Figure 1-4** shows the normalized leaching total organic contaminant

(TOC) and chemical oxygen demand (COD) concentrations for the four tested materials. Constituent abstraction from the polyester matrix followed a similar trend to the water absorption measurements. Contaminant concentration in the exposure water decreased monotonically after each 3-day water change. The greater mass fraction of polyester resin corresponded to a greater number of chemicals detected in the water. In both the resin and glass fiber composites, the presence of CNF increased the rate and quantity of contaminants released.

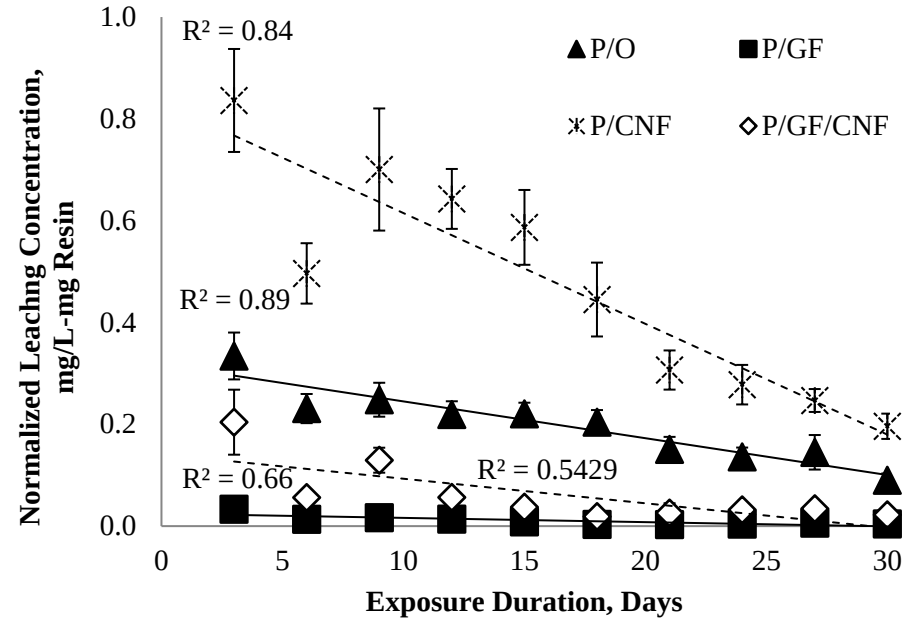

(a)

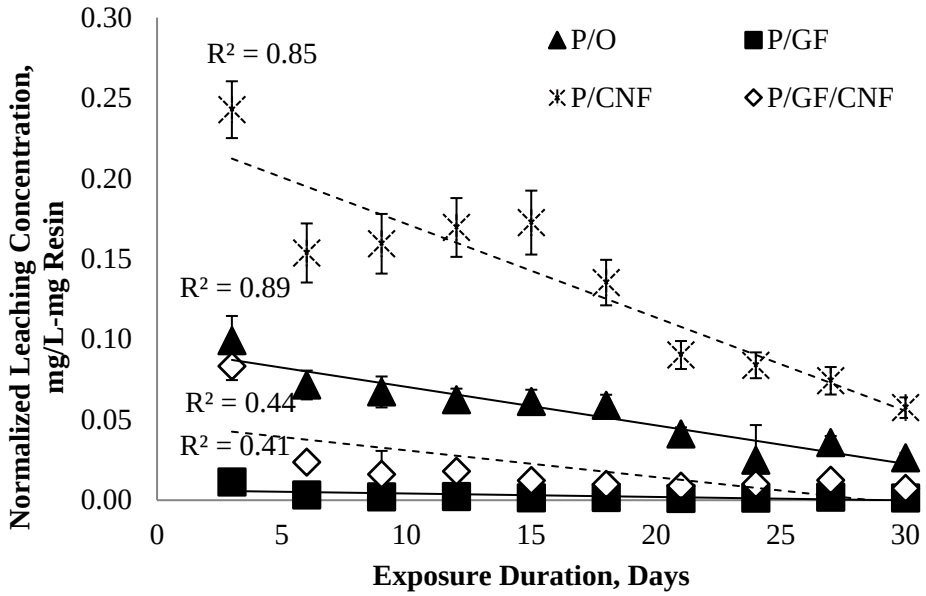

(b)

Figure 1-4 Water quality characteristics of immersion testing normalized leaching (a) COD, (b) TOC. Symbols represent (▲) P/O, (■) P/GF, (✳) P/CNF, (◇) P/GF/CNF. The standard deviation of the measurement was ± 0.02 mg/L-mg Resin. The dashed lines represent a guide for the eye.

TOC and COD leaching rates differed across composites as determined by linear regression analysis. All regression slopes were non-zero. The greatest contaminant release rate was found for P/CNF, while normalized leaching for P/O and P/GF/CNF composites were not different for COD or TOC results, similar to the moisture absorption results (**Table A2**). The P/GF composite had the lowest contaminant release rate. GF inhibited contaminant release but CNF inclusion into the P/GF composite caused that composite to perform similar to the polyester only material. UV_{254} absorbance results also showed inclusion of CNF into polymers increased contaminant release into the contact water. A small fraction of contaminants released from each material were biodegradable and this quantity was similar across the composites tested (**Table A3**).

Several VOCs were detected in composite contact waters that include aromatic resin solvents and stabilizer compounds (**Table 1-3**). These compounds were similar to those found by previous research on leachate from fiberglass resin circuit board composites[47]. None of the aqueous contaminants reported by others were found in the present work[3]. Possible reasons for this difference could be that the other study characterized the presence of semi-volatile organic contaminants and the polyester resin formulation differed. Inclusion of CNF into composites did not impact the number of VOCs released.

Table 1-3 Volatile organic contaminants detected in contact waters at day 3 and day 30.

Name of Compound (Purpose)	**Day 3**				**Day 30**			
Styrene (resin solvent)	O	CNF	GF	GF/CNF	O	CNF	GF	GF/CNF
Ethylbenzene (resin solvent)[b]	X	X	X	X	X	X	X	X
p–, *o*–Xylene (resin solvent)[b]	X	X	X	X	X			
1–Ethyl–toluene (resin solvent)[b]	X	X	X	X	X	X		
1,2,3–TMB (stabilizer)[c]	X	X	X	X				
1,3,5–TMB (stabilizer)[c]	X	X	X	X	X			

* "x" signifies the contaminant was detected as confirmed with a >93% library match; b. Suspected purpose of the contaminant; c. TMB = trimethylbenzene.

A linear relationship between organic contaminant release and the amount of water sorbed by each composite was detected ($r^2 = 0.96$) (**Figure 1-5**). Chemical release was likely facilitated by water diffusion into the material and subsequent contaminant extraction. The incorporation of a small quantity of oxidized CNFs into polyester composites (0.01 mass fraction) caused nanocomposites to become more susceptible to water aging than their CNF free counterparts.

A dynamic system existed during the experiment as evidenced by composite and water quality characterization results. It was shown that oxidized CNF caused composites to be more sensitive to water uptake compared to the CNF-free composites. Even a small magnitude of CNF in the GF composite caused a substantial change in composite water uptake. Because oxidized reinforcements are preferred to achieve better dispersion and bonding in hydrophilic matrices the impact of these materials on water sorption and mechanical properties deserve further study. Results also indicate that a nanocomposite design strategy that limits water uptake may also limit organic contaminant leaching.

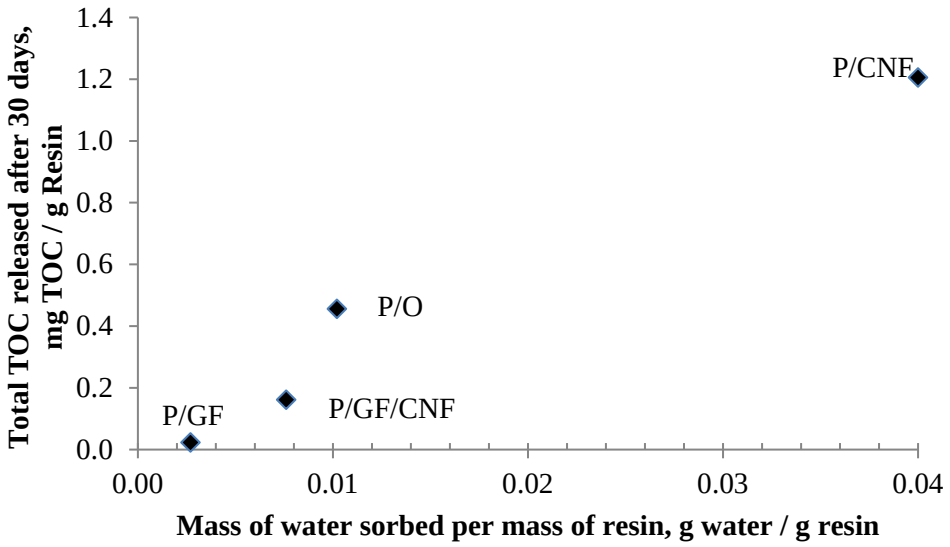

Figure 1-5 Relationship between total mass of organic carbon released by each material during the 30 day exposure period and maximum quantity of water sorbed into each material measured on Day 30.

The figure the shows the total mass of organic carbon released per composite during the total 30 day exposure period versus the initial mass of resin per composite. Simultaneous water sorption and organics extraction occurred. Error bars (not shown) are equivalent to measurements in **Figure 1-2** and **Figure 1-3**.

1.5 Conclusion

Results of this work have direct relevance to composite manufacturers and water infrastructure managers. Incorporation of a very small amount of oxidized CNF significantly altered water-composite interactions. Specifically, composites with CNFs sorbed more water and leached more organic contaminants than CNF-free composites. Even an addition of small oxidized CNF quantities in the GF composites caused the P/GF/CNF composites to absorb more water and release higher contaminants than the plain P/GF counterparts. While oxidized CNFs are preferred for hydrophilic matrices, results from the present study indicate composite manufacturers should also consider their impact on composite mechanical and long-term durability properties. Greater water sorption may expedite chemically induced degradation processes. Water infrastructure managers should also consider that greater VOC leaching may be a CNF composite performance challenge that current CNF-free materials do not encounter. In addition, the additional rate of leaching from CNF containing materials is important in the context of water quality standards used to return rehabilitated pipelines to service.

1.6 Acknowledgements

The authors thank Jesus Estaba, Eddy Colmenarez, Landon Wallace, and Basil Farah for their assistance. Special thanks are also extended to Ms. Laura Linn at Dauphin Island Sea Lab and Keven Kelley for water quality analyses. Partial project support was provided by the US NASA (EPSCoR #NNX10AN26A), US National Science Foundation (EPSCoR #1158862, CBET #1228615), and National Institute of Standards and Technology.

1.7 References

1. American National Standards Institute (ANSI)/AWWA. Standard C950–07 for Fiberglass Pressure Pipe. 2007. Denver, CO USA.

2. AWWA. M45 Fiberglass Pipe Design, Second Edition. 2005. Denver, CO USA.

3. Crathorne B, James C P, Norris M. Effect of distribution on organic contaminants in potable water. Final Report to the Department of Environment 1990. Water Research Centre (WRc), Birmingham, UK.

4. GangaRao H, Liang R. Advanced fiber reinforced polymer composites for sustainable civil infrastructures. Proceedings of the International Symposium on Innovation & Sustainability of Structures in Civil Engineering 2011. Xiamen University, China.

5. GangaRao H, Vijay PV. Feasibility review of FRP materials for structural applications. Report submitted to U.S. Army Corps of Engineers, Engineering Research & Development Center. 2010. Vicksburg, MS USA.

6. Ehsani M, Peña C. FRP Repair of Mile–Long Pipeline with Minimum Downtime, The Northern California Pipe User's Group. Proceedings of the 18th Annual Sharing Technologies Seminar. February 2010. Berkley, CA USA.

7. Varga CS, Miskolczi N, Bartha L, Lipoczi G. Improving the mechanical properties of glass–fibre–reinforced polyester composites by modification of fibre surface. *Materials and Design.* 2010. 31: 185–193.

8. Karbhari VM. Durability data for FRP rehabilitation systems, Final Report. Submitted to the California Department of Transportation. Contract No. 59A0309. February 2009. Sacramento, CA USA.

9. Gamstedt EK, Skrifvars M, Jacobsen TK, Pyrz R. Synthesis of unsaturated polyesters for improved interfacial strength in carbon fiber composites. *Composites: Part A.* 2002. 33: 1239–1252.

10. Salibi Z. Performance of reinforced thermosetting resin pipe systems in desalination applications: a long–term solution to corrosion — the Arabian Gulf example. *Desalination.* 2001. 138 (1–3): 379–384.

11. Khanna V, Bakshi BR. Carbon nanofiber polymer composites: Evaluation of life cycle energy use. *Environmental Science and Technology*. 2009. 43: 2078-2084.

12. Sahin ÖS, Akdemir A, Avci A, Gemi L. Fatigue crack growth behavior of filament wound composite pipes in corrosive environment. *Journal of Reinforced Plastics and Composites*. 2009. 28 (24): 2957–2970.

13. Li B, Wood W, Baker L, Sui G, Lee C, Zhong WH. Effectual dispersion of carbon nanofibers in polyetherimide composites and their mechanical and tribological properties. *Polymer Engineering and Science*. 2010. 50: 1914–1922.

14. Gou J, O'Braint S, Gu H, Song GJ. Damping augmentation of nanocomposites: Using carbon nanofiber nanopaper. *Journal of Nanomaterials*. 2006. 32803: 1–8.

15. Sadeghian R, Gangireddy S, Minaie B, Hsiao K–T. Manufacturing carbon nanofibers toughened polyester/glass fiber composites using vacuum assisted resin transfer molding for enhancing the mode–I delamination resistance. *Composites Part A*: Applied Science and Manufacturing. 2006. 37(10): 1787–1795.

16. Finegan IC, Tibbetts GG, Glasgow DG, Ting JM, Lake ML. Effect of carbon nanofiber–matrix adhesion on polymer nanocomposite properties II. *Journal of Material Science.* 2003. 38: 3485–3490.

17. McDonald E, Whelton AJ, Jefferson GA, Nguyen T. Significance of MWCNT and TiO_2 nanofillers on low–density polyethylene thermal & mechanical properties: Applicability for pipes used in water &energy systems. *American Society of Mechanical Engineers (ASME) Early Career Technical Journal.* 2011. 1–4.

18. Lee J, Mahendra S, Alvarez PJJ. 2010. Nanomaterials in the construction industry: A review of their applications and environmental health and safety considerations. *ACS Nano.* 4 (7): 3580–3590.

19. Whelton AJ, Duncan TV, Koontz J, Nguyen T. Nanoparticle release from polymer nanocomposites used for potable water infrastructure and food packaging: Current Progress &beyond. Proceedings of Nanotech Conference and Exposition. Session: Nanotechnology Environment, Health & Safety. Boston, MA USA2011. 3: 505–508.

20. Jarvenkyla, J., Plastic Pipe, US Patent No. 8470423 B2, Jun 25, 2013.

21. Jarvenkyla, J., Multilayer pipe, EP1708881 A2, Oct 11, 2006.

22. Dunphy Guzman KA, Taylor MR, Banfield JF. 2006. Environmental risks of nanotechnology: National Nanotechnology Initiative funding, 2000-2004.

23. Whelton AJ, Nguyen T. Contaminant migration from polymeric pipes used in buried potable water distribution systems: A review. *Critical Reviews in Environmental Science and Technology.* 2013. 43 (7): 679–751.

24. Zenko JR, Wicks W, Jones, N F, Peter Pappas S, Wicks D A. Organic Coatings: Science and Technology 3rd Edition. 2007. John Wiley and Sons, Inc. Hoboken, NJ USA.

25. Ranney TA, Parker LV. Susceptibility of ABS, FEP, FRE, FRP, PTFE, and PVC Well Casing to Degradation by Chemicals, Special Report 95–1. US Army Corp of Engineers, Cold Regions Research & Engineering Laboratory, January 1995. Hanover, NH USA.

26. Santhosh K, Muniraju M, Shivakumar N D, Munusamy R. Hygrothermal durability and failure modes of FRP for marine applications. *Journal of Composite Materials.* 2012. 46 (15): 1889–1896.

27. Gu H. Behaviours of glass fiber/unsaturated polyester composite under seawater environment. Materials and Design2009.30: 1337–1340.

28. Svetlik SL. An investigation in the hygrothermal degradation of an E–glass/vinyl–ester composite in humid and immersion environments. 2008. Dissertation. Department of Civil Engineering, University of California San Diego, CA USA.

29. Visco AM, Calabrese L, Cianciafara P. Modification of polyester resin based composites induced by seawater absorption. *Composites: Part A.* 2008. 39: 805–814.

30. Huang G, Sun H. Effect of water absorption on the mechanical properties of glass/polyester composites. *Materials and Design.* 2007. 28: 1647–1650.

31. Fraga AN, Alvarez VA, Vazquez A, Osa ODL. Relationship between dynamic mechanical properties and water absorption of unsaturated polyester and vinyl ester glass fiber composites. *Journal of Composite Materials.* 2003. 37: 1553–1574.

32. Chateauminois A, Chabert B, Soulier JP, Vincent L. Hygrothermal ageing effects on the static fatigue of glass/epoxy composites. *Composites.* 1993. 24 (7): 547–555.

33. Assarar M, Scida D, Mahi A EL, Poilâne C, Ayad R. Influence of water ageing on mechanical properties and damage events of two reinforced composite materials: Flax–fibers and glass–fibres. *Materials and Design.* 2011. 32: 788–795.

34. Cho EH, Mounts JL. Durability of glass–fiber–reinforced polymer composites in an alkaline environment. Journal of Vinyl and Additive Technology. 2007. 13 (4): 221–228.
35. Mezghani K. Long term environmental effects on physical properties of vinylester composite pipes. *Polymer Testing*. 2012. 31: 76–82.
36. Cruz VCA, Nobrega MMS, Silva WP, Carvalho LH, Lima AGB. An experimental study of water absorption in polyester composites reinforced with macambira natural fiber. *Material Science and Engineering Technology.* 2011. 42 (11): 979–984.
37. Farshad M, Necola A. Effect of aqueous environment on the long–term behavior of glass fiber–reinforced plastic pipes. *Polymer Testing*. 2004. 23: 163–167.
38. Czel G, Czigany T. A study of water absorption and mechanical properties of Glass Fiber/Polyester Composite Pipes–Effect of Specimen geometry and preparation. *Journal of Composite Materials*. 2008.42(26): 2815–2827.
39. Ghani MAA, Salleh Z, Hyie KM, Berhan MN, Taib YMD, Bakri MAI. Mechanical Properties of Kenaf/Fiberglass Polyester Hybrid Composite. *Procedia Engineering*. 2012. 41: 1654 –1659.
40. Dhakal HN, Zhang ZY, Richardson MOW. Effect of water absorption on the mechanical properties of hemp fibre reinforced unsaturated polyester composites**.** *Composites Science and Technology.* 2007. 67: 1674–1683.
41. Zhang J–H, Mao–Sheng Z. Visual Experiments for Water Absorbing Process of Fiber–reinforced Composites. *Journal of Composite Materials*. 2004. 38 (9): 779–790.
42. Crank J, Park JS. Diffusion in Polymers.1968. Academic Press, Inc. London UK.
43. Lafdi K, Fox W, Matzek M, Yildiz E. Effect of carbon nanofiber-matrix adhesion on polymeric nanocomposite properties-Part II. *Journal of Nanomaterials*. 2008. (5), 1-8.
44. National Sanitation Foundation International Standard/American National Standards Institute. Drinking Water Treatment Units, Ann Arbor, Michigan, USA. 2007.
45. American Public Health Association (APHA), Water Environment Federation (WEF), and American Water Works Association (AWWA)2012. Standard Methods for the Examination of Water and Wastewater, 20th Edition. Washington, DC USA.
46. Hodzic A, Kim JK, Lowe AE, Stachurski ZH. The effects of water aging on the interphase region and interlaminar fracture toughness in polymer–glass composites. *Composites Science and Technology*. 2004. 64: 2185–2195.

47. Chatterjee AP. Percolation thresholds for rod-like particles: polydispersity effects. *Journal of Physics: Condensed Matter*. 2008. 20: 250-255.

48. Pfeifer S, Park SH, Bandaru PR. Analysis of electrical percolation thresholds in carbon nanotube networks using the Weibull probability distribution. *Journal of Applied Physics.* 2010. 108.

49. Guo J, Jiang Y, Hu X, Xu Z. Volatile organic compounds and metal leaching from composite products made from fiberglass–resin portion of printed circuit board waste. *Environmental Science and Technology*. 2012. 46 (2):1028–1034.

50. Henze H. Biological Wastewater Treatment: Principles, Modeling and Design. 2008. Cambridge University Press, Inc. London, UK.

51. Whelton AJ, Salehi M, Tabor M, Donaldson, B, Estaba J. Impact of infrastructure coatings on stormwater quality: A review and experimental study. *Journal of Environmental Engineering*. 2013. 139 (5): 746–756.

CHAPTER 2 : LINK BETWEEN FIXTURE WATER USE AND DRINKING WATER QUALITY IN A NEW RESIDENTIAL GREEN BUILDING

Maryam Salehi, Mohammad Abouali, Mian Wang, Zhi Zhou, Amir Pouyan Nejadhashemi, Jade Mitchell, Stephen Caskey, Andrew J. Whelton

2.1 Abstract

Low-flows in building plumbing present an emerging human health concern. This study's aim was to understand the link between fixture water use and drinking water quality in a newly plumbed residential green building. Water use and quality were monitored at four in-building locations from September 2015 through December 2015. Once the home was fully inhabited average water stagnation periods were shortest for the 2nd floor fixture for hot water (0.23 hr to 0.5 hr). The maximum water stagnation time found was 72.0 hr. Bacteria and organic carbon levels were greater inside the plumbing system compared to the municipal tap water entering the building. A positive correlation between organic carbon and bacterial concentration at select locations was observed. A greater amount of bacteria was detected in hot water samples compared to cold water. This suggested that hot water plumbing promoted greater microbial growth. At some fixtures metal plumbing components caused Zn, Cu and Pb levels to increase above the levels measured at the water treatment plant. At the basement fixture, where the least amount of water use events occurred, greater organic carbon, bacteria, and heavy metal concentration were detected. Different fixture use patterns resulted in disparate drinking water quality within the same residential building.

2.2 Introduction

Residential plumbing is critical for the health and safety of populations worldwide. In the U.S., potable water is distributed through an estimated five to ten million miles of plumbing pipe[1] and through approximately 24.55 billion square meters of residential buildings[2]. In recent years' potable water plumbing design and operations have transitioned towards energy and water saving, low-flow devices[3-6]. Low-flow faucets have resulted in flow reductions of 30%[5,7]. When not coupled with plumbing pipe size reductions, the resulting low-flows can increase water age[8], enable contaminant leaching from plumbing components[9], contribute to disinfectant residual loss[10], microorganism proliferation[10, 11], and sometimes waterborne disease outbreaks[12-14]. Analysis of U.S. building plumbing design methods has revealed 'excessive over-design' of water use and incorrect assumptions with fixture use in single family residential buildings[5]. With the frequency of disease outbreaks and degraded aesthetic drinking quality incidents increasing[15], there is a growing need to understand the impact of plumbing design, material, operation and water usage patterns on drinking water quality. To the best of our knowledge, no study has linked the water usage pattern and drinking water quality for a new residential plumbing system.

A variety of bench- and pilot-scale studies have documented water quality deterioration in building plumbing[16-19], but a limited number of studies described water quality within full-scale residential buildings (**Table 2-1**)[20-30]. Full-scale investigations have focused on buildings that have been in operation for six months or an unreported amount of time. Building water sampling has involved a very limited number of samples for each study period (1 to 21). Drinking water has been monitored for microbiological, metal, volatile organic compound (VOC), semi-volatile organic compound (SVOC), total organic carbon (TOC), disinfectant by products (DBP) concentrations, heterotrophic plate counts (HPC), and aesthetic properties. However, a challenge arises when comparing past studies using the exact plumbing material type/brand, condition of the plumbing, and composition, as well as water quality, temperature, residence time, and flow fluctuations.

Table 2-1 Water quality monitored at the residential buildings

Location and Type of Buildings (Number)	**Parameter Monitored**	**Pipe Type / Plumbing Age (years)**	**Summary of Results**
USA	DBPs, TOC, pH, chlorine	nr[#]/nr	No changes in DPBs level for on demand heating system; DBPs concentrations increased in hot water system with long storage time; TOC (cold & hot): 0.89 & 1.01 mg/L; pH (cold & hot): 7.56 & 7.55, chlorine (cold): 0.23 to 0.53 mg/L as Cl_2; Chlorine (hot): BDL[Δ]-0.43 mg/L as Cl_2[25]
SFRBs[*] (18)			
NZE[φ] SFRB (1)	VOCs, sVOCs	PEX-a/ 0.5	Several PEX pipe's antioxidants, degradation products and resin solvents were detected PEX-a plumbing[23]
NZE SFRB & SFRB (2)	Temp, ammonia, nitrate, pH, chlorine, *Legionella*, *L. pneumophila* gene), *V. vermiformis*, *M. avium*, & total bacteria	Cu, PEX[o]/nr	Chlorine and chloramine residuals were decaying up to 144 times faster in building plumbing with high water age compare to conventional buildings; NZE chlorine (hot & cold): 0.04 & 0.02 mg/L as Cl_2; Conventional house chlorine (hot & cold): 0.71 & 0.06 mg/L as Cl_2[8]
SFRB (3)	TOC, TON, UV_{254}, VOC & sVOC	PEX-a, PEX-b/0.5-2	Several regulated and unregulated VOCs and SVOCs detected in water collected from PEX plumbing systems[21]
Households[ϕ] (nr)	Cu, Pb, Ni, Zn	Cu, plastic[3]/nr	The concentrations of Cu, Pb, Ni and Zn, four indicator elements of brass corrosion, were greater in the all-plastic-plumbed houses[24]
Canada	Cu, Zn, Pb, Sn, Fe, Mn	Cu, plastic[3]/ <5, >10, >40	No significant effect of plumbing age or type on the extent of metal leaching. Plumbing type had a marked effect on the lead and iron levels in drinking water. Metal leaching into stagnant water was mostly from kitchen faucets[27]
SFRBs & Apartments (nr)			

SFRBs (6)	DBPs	nr/nr	Greater level of DBPs for water stagnant in cold water pipes and water that resided longer in water heater tanks. Water use frequency identified as significant factor on DBP level[22]
Italy SFRBs (nr)	*Legionella* & *Pseudomonas* , hardness, chlorine, Ca, Mg, Fe, Mn, Cu, Zn	Metal, plastic[3]/nr	Water heater type, tank distance and capacity, water treatment plant age, and mineral content influenced the level of bacteria present in the water; Ca 85 mg/L, Mg 17.6 mg/L, Fe: 15 µg/L, Mn: 2.4 µg/L, Cu: 11.5 µg/L, Zn: 62.6 µg/L, Cl_2: 9.2 µg/L[20]
Switzerland Households[ϕ] (10)	Temp, nitrate, pH, TOC, conductivity, ATP[υ], HPC[β]	nr/nr	Considerable microbiological changes found due to water stagnation. Microbial level increased with water stagnation and reduced after flushing. pH:7.9 ± 0.2 and TOC: 0.8 ± 0.0 mg/L[11]
Germany Households[ϕ] (1,674)	pH, conductivity, hardness, SO_4^{2-}, Cu	Cu/0.5-5	Mean Cu concentration of 0.18 mg/L in stagnant samples and 0.11 mg/L in the flowing water samples. Average pH :7.83, hardness :11.76 °dH, SO_4^{2-}: 57.01 mg/L[29]
Households[ϕ] (1,485)	Pb, SO_4^{2-}, hardness	nr/nr	For stagnant water samples, 3.1% had Pb level greater than the WHO limit and 0.6% had level above German drinking water regulation (0.04 mg/L). For flowing water samples were 2.1% above 0.01 mg/L and 0.2% greater than 0.04 mg/L[28]
SFRBs (nr)	*Legionella*, Cu	Cu, plastic[3], galvanized steel/nr	High temperature influenced *Legionella* occurrence; copper plumbing was more contaminated with *Legionella* compare to plastic and steel plumbing[26]
SFRBs (4)	Cu, Zn, Pb, Ni, Cd, nitrate, pH, oxygen consumption, hardness	Cu/nr	Ni was released by terminal taps into the water, Zn was released by brass corrosion. Pb containing installation parts were the source of Pb. Cu (79-499 µg/L), Zn (88-946 µg/L), Pb (<1-1.6 µg/L), Ni (2.4-12.8 µg/L), Cd (<0.0 µg/L)[30]

* SFRB: Single family residential building; [#] nr: Not reported; [Δ] BDL: below detection limit; [φ] NZE: Net zero energy; [e] Type of PEX was not mentioned; [ϕ] Type of residential building was not mentioned; [ʒ] Type of plastic was not mentioned; [υ]ATP: adenosine tri-phosphate; [β]HPC: heterotrophic plate counts

Drinking water contaminated with heavy metals can pose acute and chronic risks to human health. Heavy metals in tap water; can originate from ground and surface waters (i.e., As, Co, Mn), are added during water treatment (i.e., Al, Mn, Fe), and can be released from water distribution and building pipes, scales, and plumbing fixtures (i.e., Cr, Cu, Fe, Pb, Zn, Sn)[31-33]. Hence, some water utilities and building owners are choosing to replace lead service lines and indoor plumbing with plastic pipes in order to reduce heavy metal levels in tap water.

In the U.S., cross-linked polyethylene (PEX) pipes are being installed in 75% of new building construction and up to 54% of renovations[34]. While more than 70 PEX pipe brands have been certified for potable water use in the U.S., their water quality impact test results are not publicly disclosed. A few U.S., PEX pipe, water quality investigations where data are publicly available have been conducted[21, 35-37]. Results from these studies showed that the chemical and odor impacts of eight PEX brands studied over a one-month period varied significantly: TOC concentration from 0.26 to 6.38 mg/L and threshold odor number (TON) 2 to 102. Bench-scale testing also showed some PEX pipes caused odor and odor intensity was unchanged by the presence of chlorine disinfectants.[38] Researchers have found that PEX pipes leached organic carbon and water temperature can influence bacterial growth[38-40]. A few U.S. full-scale PEX plumbing building investigations have been conducted and odors have been found[21, 23, 35]. The cleaning method applied to newly installed PEX pipe can also affect its short-term chemical leaching[23]. European researchers have found PEX pipes contributed 0.001-22 mg/L TOC to drinking water at room temperature[41-44], and TON values varied between 16 to greater than 128 after 72 hr exposure at 23 ºC[41].

This study was designed to better understand the link between water use and drinking water organic, inorganic, and odor levels during the first three months of a newly installed plumbing system while inhabited. The objectives were to: (1) Examine water use patterns at four fixtures (hot/cold) in the PEX plumbing system; (2) Monitor pH, free chlorine, TOC, specific ultraviolet absorbance (SUVA), bacterial concentrations, and TON levels at four different in-building locations; and (3) Examine the linkage between fixture use and water quality.

2.3 Material and Methods

2.3.1 Plumbing Design, Water Source, and Onsite Sampling

Tap water sampling was conducted at a newly renovated, low-energy and low-water use, residential building in West Lafayette, Indiana USA from September 25th 2015 to December 24th 2015. The structure was a 266 m^2, four bedroom, two bath home initially constructed in the 1920s and renovated in 2014[45, 46]. The building was a joint collaboration between Whirlpool Corporation and Purdue University. The building contained new 1.9 cm and 1.3 cm diameter PEX type A pipe with a modified trunk-and-branch design (**Table B1**). Building tap water was received from a local drinking water supplier that relied on a groundwater source. Groundwater underwent $KMnO_4$ oxidation, unilever filtration, and the addition of free chlorine secondary disinfectant and polyphosphate corrosion inhibitor. Water quality entering the municipal water distribution system varied: pH 7.0 to 7.5, free chlorine 0.8 to 1.1 mg/L as Cl_2, hardness 280 to 440 mg/L as $CaCO_3$ (metal concentrations shown in **Table B2**). Tap water traveled through polyvinylchloride (PVC) and ductile iron water distribution pipes before reaching the building service line. A Hersey 420 composite water meter with copper service line was connected to the plastic building plumbing. All water entering the house, first passed through a whole-house water softener (Whirlpool model WHES33 LE33) before entering the rest of the plumbing. After plumbing installation, the system (hot and cold water lines, and tanks) was shock chlorinated in accordance methods in **B.1.1**.

Flow and water sampling was conducted at several building sampling locations (**Figure 1**). The hot water system included a recirculation pump. Design fixture flow rates with aerators were: kitchen faucet (6.8 LPM [1.8 GPM]) and bathroom sinks (4.5 LPM [1.2 GPM]). Three 409 L [108 G] glass lined hot water storage tanks in series were installed. Also, a fourth, electrically-driven, water heater (151 L [40 G] capacity) was also installed. The large in-building water storage volume was primarily designed to support the rooftop solar, thermal-photovoltaic systems, but also used for domestic hot water demand. Water sampling was conducted for four fixtures on day 3, 15, 30, 60 and 90. The building was not occupied on day 0 or 3, was partially occupied at day 15, and became fully occupied on day 30. At the water softener sampling point, water was

flushed for approximately 3 min before a water sample was taken. This action was taken to obtain fresh municipal water. More building plumbing system details are described in **B.1.2**.

All other in-building water samples were immediately collected, no water flushing was conducted. Tap water was characterized onsite for pH, temperature, and free chlorine concentration. Next, water samples were transported to the laboratory, dechlorinated using $Na_2S_2O_3$, analyzed immediately for alkalinity, TOC, UV_{254}, SUVA (**B.1.3**).

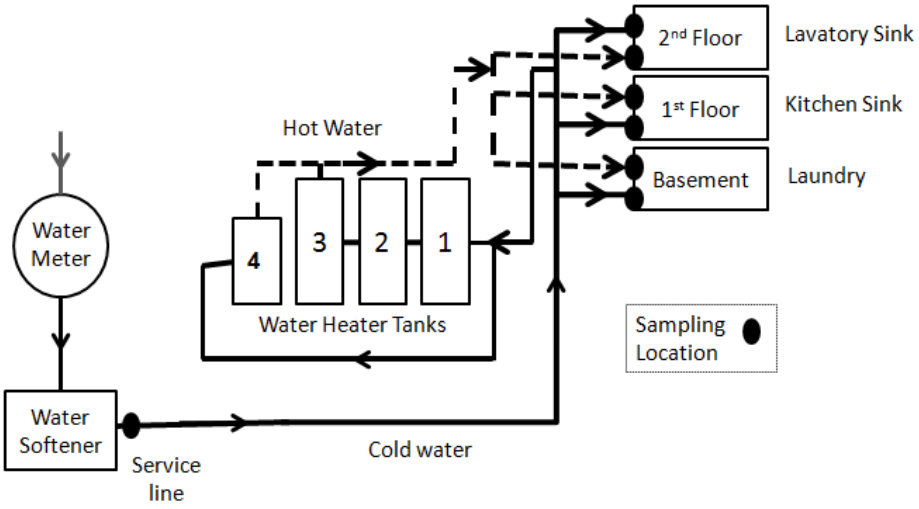

Figure 2-1 Plumbing system outline and sampling locations

2.3.2 Flow Monitoring

Automated impeller flowmeters (Omega, FPR300 series) were installed on each hot and cold water supply line with 0.4 LPM accuracy. The devices continuously recorded the flow rate at each fixture with a one second temporal resolution. All data were collected using a LABVIEW system. High temporal resolution enabled the tracking of both short and long events. An event was defined as the continuous portion of the time where the flow rate was non-zero. Prior to any analysis, the data were checked for missing records. If there was a single record missing (one second duration), the record was recovered by averaging the two, immediate records, before and after the missing

record. However, if two or more records were missing continuously, they were marked as missing and an artificial event was assigned to them – a missing record event (**Figure B1**).

Monitoring was conducted to ascertain flow and water quality at the service line and three fixtures: Basement (cold/hot), 1st floor kitchen sink (cold/hot), and 2nd floor bathroom sink (cold/hot). The basement fixture was brass needle valve which is not certified for potable water uses. To examine the water usage pattern through this building, flow data points were recorded and analyzed every second of every day from September 1st to December 31st at these three fixtures and the service line. Due to a few computer data acquisition system challenges, some flow records were not collected during September (27.0%), October (6.3%), November (6.0%), and December (9.3%), and thus were not included in this analysis. Total volume of water used (L), number of fixture use events, average event duration (s), average water flow rate (LPM), average elapsed time since last event (hr), and maximum elapsed time since last event (hr) were calculated based on flow monitoring data. The basis for these calculations is described in **B.1.4** and also shown in **Figure B1**.

2.3.3 Water Quality Monitoring

Free chlorine concentration, water pH, alkalinity concentration, TOC concentration, and UV_{254} absorbance were analyzed in accordance with methods described in B.1.3. For bacteria enumeration, culture-based HPC and culture-independent quantitative real-time PCR (qPCR) methods were used. HPC was performed by using the membrane filter method on m-HPC agar.48 Five dilutions (500 mL, 100 mL, 10 mL, 1 mL, 0.1 mL) were prepared using tap water samples and incubated at 37 ºC for 48 hr in triplicate. Two liters of water samples were filtered through 0.22 µm pore size mixed cellulose ester membrane filters (Millipore, Billerica, MA) to prepare for DNA extraction. More details are described in SI-1.3. The limit of detection (LOD) for all qPCR assays ranged from 78 gene copies/reaction to 2,220 gene copies/reaction, and the limit of quantification (LOQ) ranged from 89 gene copies/reaction to 3,711 gene copies/reaction. All standard curves had a coefficient of determination 0.95, and an efficiency of 91% to 108%.

2.3.4 Statistical Analysis

SPSS 22 was used to perform statistical analysis. Three factor analysis of variance (ANOVA) with two order interactions was applied to study the significant influence of pipe location and water temperature for building water sampling data. A type I error of 0.05 was selected as the significance level for all data. Geometric means for TON data are reported in accordance with the standard method.[47] All other results are reported as arithmetic mean and standard deviation. Principal component analysis (PCA) was applied to reduce the dimension of data to identify patterns in data. OriginPro 9.3 (Northampton, MA) was used for PCA analysis. All the water quality parameters, i.e., 13 metals, pH, chlorine, water volume, odor, alkalinity, and TOC, were included in PCA analysis and the results were plotted in principal component PC1 and PC2, which explained most of the variability of the data. The Pearson correlation coefficient was calculated pairwise for TOC and bacterial concentration.

To calculate the correlation between water quality and water usage parameters, three water usage parameters were defined (i) number of events, (ii) total volume and (iii) average elapsed time between the sampling intervals. Water was sampled six times during the study period (day 0, day 3, day 15, day 30, day 60 and day 90), thus, there were five intervals between each sampling for the water fixtures studied. Total organic carbon and bacterial concentration (gene copy number) were measured in each sampling sessions at each of the fixtures. Linear or rank correlation (Pearson type) was calculated for all the possible combinations.

2.4 Results and Discussion

2.4.1 Water Use as the Building Became Occupied

The water usage pattern was examined by recording and analyzing 64,891,484 water flow data points from September 1st to December 31st. For all fixtures monitored, September usage significantly differed from the October, November, and December usage. Service line flow data showed the total volume of water used in the building from September 1st to September 17th was only 0.1 m^3, and from September 18 to September 30th was 19.0 m^3. Because 27.0% of September flow monitoring data were not collected

by the data acquisition system, it is possible additional water use occurred. The total volume of water used in September (19.1 m^3) was substantially greater than the total monthly volume of water used during October to December (5.1 to 7.6 m^3). Water use in September was associated with plumbing construction and the building was not inhabited. The plumbing system and two external rainwater collection tanks were installed September 21 (working volume 5.4 m^3 per tank). On September 21, the plumbing and rainwater tanks were filled with superchlorinated municipal tap water and allowed to stagnate for 18 hr, on September 22, this water was flushed out and plumbing was filled with fresh municipal water. Between September 22 and September 23, 12.6 m^3 of water passed through the service line. This water was associated with plumbing flushing and rainwater tank disinfection. After this event, only 2.8 m^3 of water passed through the service line during the last week in September while indoor construction activities were being completed. From September 18th to September 30th only 14.7% of total water used at the basement, 1st floor, 2nd floor fixtures that were subsequently monitored in the present study.

The house was partially occupied during the second week in October (2 people) and became fully occupied (3 people) during the last week in October. As **Table 2-2** shows once the house was occupied, water use increased at the three fixtures where water sampling was conducted. Water at these three fixtures represented a growing portion of the total water used in the building per month (27.9% October, 31.9% November, 39.0% December). When full occupancy occurred, the basement fixture was the least used (number of events at cold: 60 to 105, hot: 21 to 69) compared to the other fixtures in the building (number of events at cold: 145 to 856, hot: 326 to 2,230). During October to December the most frequently used fixture was the 2nd floor hot water (bathroom sink, number of events per month 2,230). In prior a study, lower water use frequency was reported for bathroom sinks compared to kitchen faucets[48], but in the present study the maximum water use frequency was greatest at 2nd floor bathroom sink compared to the kitchen faucet.

From October to December, the average stagnation period was the greatest at the 2nd floor cold (1.12-2.00 hr) compared to the two other monitored fixtures in the house (0.23-1.32 hr). In October and December average water stagnation periods was shortest

in duration at 2nd floor hot fixtures (0.23 hr and 0.50 hr). During the entire study period the maximum water stagnation time was found for all fixtures to be 72.0 hr (3 days) in December. Due to an unexpected data acquisition system error, water use events on Day 90 (December 24) were not recorded. As a result, in December the maximum fixture stagnation time could have been longer than 72.0 hr because following the data acquisition error fixtures were not used.

Table 2-2 Residential home water usage data, September 18 to December 31, 2015

Parameter	Total Volume Used (m^3)	Number of Events	Average Duration (s)	Average Flow Rate (L/min)	Average Elapsed Time (hr)	Maximum Elapsed Time (hr)
Fixture	September 18th to 30th					
	October; November; December					
Service Line	19.00	791	115	12.5	0.12	19.61
	7.59, 5.08, 5.19	4498,4271, 3535	19, 16, 20	5.4, 4.4, 4.4	0.12, 0.12, 0.12	42.19, 49.71,
Basement-Cold	0.38	133	20	8.8	0.51	22.06
	0.39, 0.24, 0.37	105, 66, 60	31, 31, 54	7.3, 7.0, 6.9	0.45, 0.89, 0.53	51.34, 53.52,
Basement-Hot	1.91	127	77	11.6	0.50	22.06
	0.10, 0.17, 0.04	69, 44, 21	18, 16, 41	4.9, 4.4, 2.9	0.89, 1.32, 0.70	51.34, 53.52,
1st Floor-Cold	0.15	163	21	2.7	0.62	19.61
	0.41, 0.57, 0.33	667, 856, 619	13, 15, 14	2.8, 2.7, 2.4	0.61, 0.55, 0.59	48.98, 50.08,
1st Floor-Hot	0.08	200	15	1.5	0.55	19.61
	0.16, 0.27, 0.20	326, 485, 389	14, 16, 15	2.1, 2.1, 2.2	0.96, 0.91, 0.88	48.98, 49.71,
2nd Floor-Cold	0.11	140	19	2.5	0.37	21.61
	0.17, 0.09, 0.05	325, 206, 145	13, 11, 10	2.4, 2.3, 2.3	1.12, 2.30, 2.00	51.34, 50.65,
2nd Floor-Hot	0.16	288	12	2.9	0.38	19.61
	0.89, 0.40, 1.02	2230, 707, 825	7, 9, 12	3.4, 3.7, 6.3	0.23, 0.70, 0.50	42.20, 50.45,

Important dates of building commissioning and the inhabitants: Building partial occupation October 10, 2015 and full occupation October 25, 2015; October 12-13 Fall break; November 25-28 Thanksgiving break; December 19, 2015 fall semester ended; Drinking water sampling began September 25, 2015.

2.4.2 Plumbing Water Quality during the First Three Months

2.4.2.1 Differences in Water Quality within the Building and with Time

Municipal tap water quality that entered the home varied: pH 7.3 to 7.9; alkalinity of 270 to 285 mg/L $CaCO_3$; free chlorine 0.4 to 1.6 mg/L as Cl_2; TOC 0.73 to 1.68 mg/L (**Tables B7-B9**). Water quality characteristics before and after superchlorination were described in **B.2.1**. For all sampling periods except day 3, the greatest free chlorine concentration was found at the service line water sample and lower concentrations of free chlorine were found inside the building. The lowest water pH recorded was 7.1 at the basement hot water sampling point. Free chlorine concentration was less than 0.5 mg/L as Cl_2 for 20 out of the 35 total water samples collected. Two samples collected from basement hot and cold lines at day 15 had no detectable free chlorine. This loss of disinfection residual could be due to the longer water stagnation time in the basement fixture compared to the other fixtures inside the building.

Organic contaminants were detected in the building water. TOC concentration significantly differed over the exposure period (**Table B10**). Tap water TOC concentration exiting the water softener increased from 0.73 mg/L to 1.68 mg/L between day 3 to day 90 and results were typical of water distribution systems (0.5 mg/L to 6 mg/L)[49]. TOC concentration was greater inside the building across all fixtures during the entire study period except 1st floor (cold) and 2nd floor (hot and cold) water samples on day 30 compared to the water entering the building (**Figure 2-2**). TOC concentration increased from day 3 to day 15 at the basement and 1st floor fixtures. The finding is counter to prior bench-scale TOC monitoring results for PEX pipe where TOC levels decreased during 30 days of simulated use[21,23]. Results indicate that organic carbon detected could be due to contributions from municipal tap water, plastic pipe chemical release, microbial growth within the plumbing system, and organics release from biofilms[3,50,51].

SUVA values differed based on fixture (0.5 to 5.3 L-mg/M) and implied differences in disinfectant byproduct formation potential (DBPFP) at each fixture. SUVA exceeded 4 L-mg/M on occasion (**Table B11**) and was positively correlated with free

chlorine concentration (p=0.026) (**Table B12**), which indicated the potential to form disinfectant byproducts[52,53]. According to the USEPA (2012), SUVA values < 2 represent low DBPFP; Between 2 and 4 represent potential to increase DBPFP; > 4 represent high DBPFP[52]. It is known when less cold water is used or hot water storage times are long, greater DBP levels can occur[25].

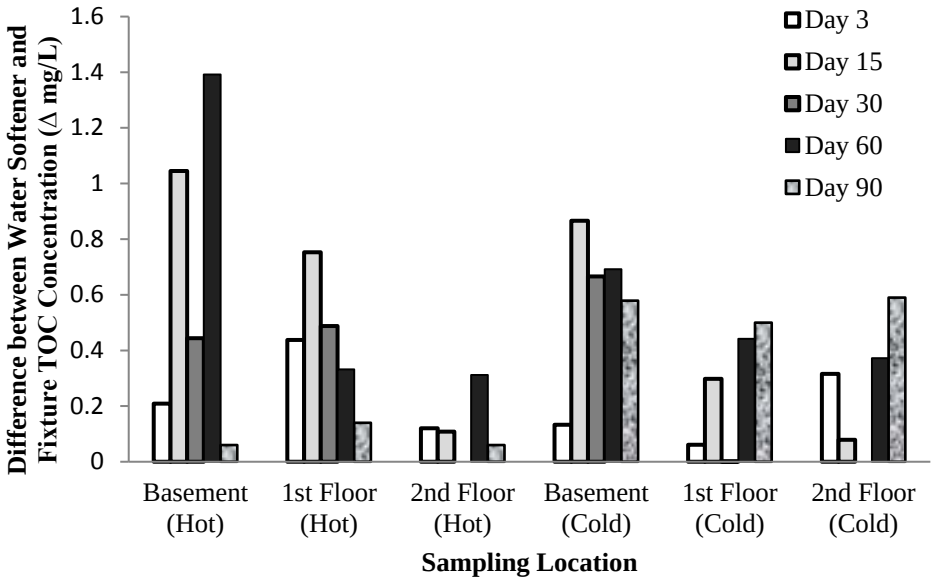

Figure 2-2 Differences between TOC concentrations at the fixture compared to water entering the building for cold and hot water samples at various exposure periods.

During the entire study period, TON values ranged from 0 to 22, and were sometimes greater inside the house compared to tap water exiting the water softener (**Figure B2**), but no trends were detected. The USEPA 3 TON odor tap water SMCL was only exceeded at the water softener on day 3, while at all other fixtures this level was exceeded for a total 18 times. Cold water samples from the basement sampling point exceeded the SMCL during the entire study duration, and this location was the least frequently used. A drinking water's TON value for similar brand of PEX at residential building in Maryland (2 year old) and Colorado (0.8 year old) was reported as an average of 6, albeit under different disinfectant conditions[21]. Drinking water odors can be caused by: contaminants released from PEX pipe, compounds generated when free chlorine reacts with those chemicals released, chemicals released by pipe biofilms, and chlorine potentially masking underlying odors present[21,23,37,51,54].

Several metals with drinking water health and aesthetic limits were detected and their abundances were significantly correlated ($p<0.05$), such as Zn and Fe (R=0.78, $p=3.11*10^{-8}$) (**Figure 2-3**, **Table B12**). On nearly every sampling date, higher Cu levels were detected inside the building than at the water softener in all but for 3 of the 30 water samples collected. No Cu concentrations exceeded the USEPA SMCL of 1,000 µg/L, but one building water sample exceeded the Zn USEPA SMCL of 5,000 µg/L. Zn concentration increased through the building plumbing which could be due to leaching by brass fittings[55]. Pb was also detected exiting the water softener and in additional building water samples (0.5 µg/L to 23.5 µg/L). The greatest drinking water Pb levels were found at the basement sampling point cold water line: 23.5 µg/L on day 15, which exceeded the USEPA action level (15 µg/L)[56]. The basement sampling point was a brass, needle valve and may have contributed to the high level of Pb and Zn detected at this fixture. Inkinen et al. (2014) also found that Pb and Cu increased from an office building service line (Pb: 1.5 µg/L, Cu: 12 µg/L) through PEX building plumbing (Pb: 34.7 µg/L, Cu: 35 µg/L) during its first year operation[57]. Zn, Pb and Cu variation across fixtures could be due to the ball valves, brass barb tees, brass elbows, copper fittings and faucets[36,58,59], and water chemistry fluctuations[60]. Sometimes Cu, Zn, Pb and Ni levels were greater than levels reported for other buildings with all plastic plumbing[29], but the type of plastic piping system/components and appurtenances studied by others was not mentioned[35].

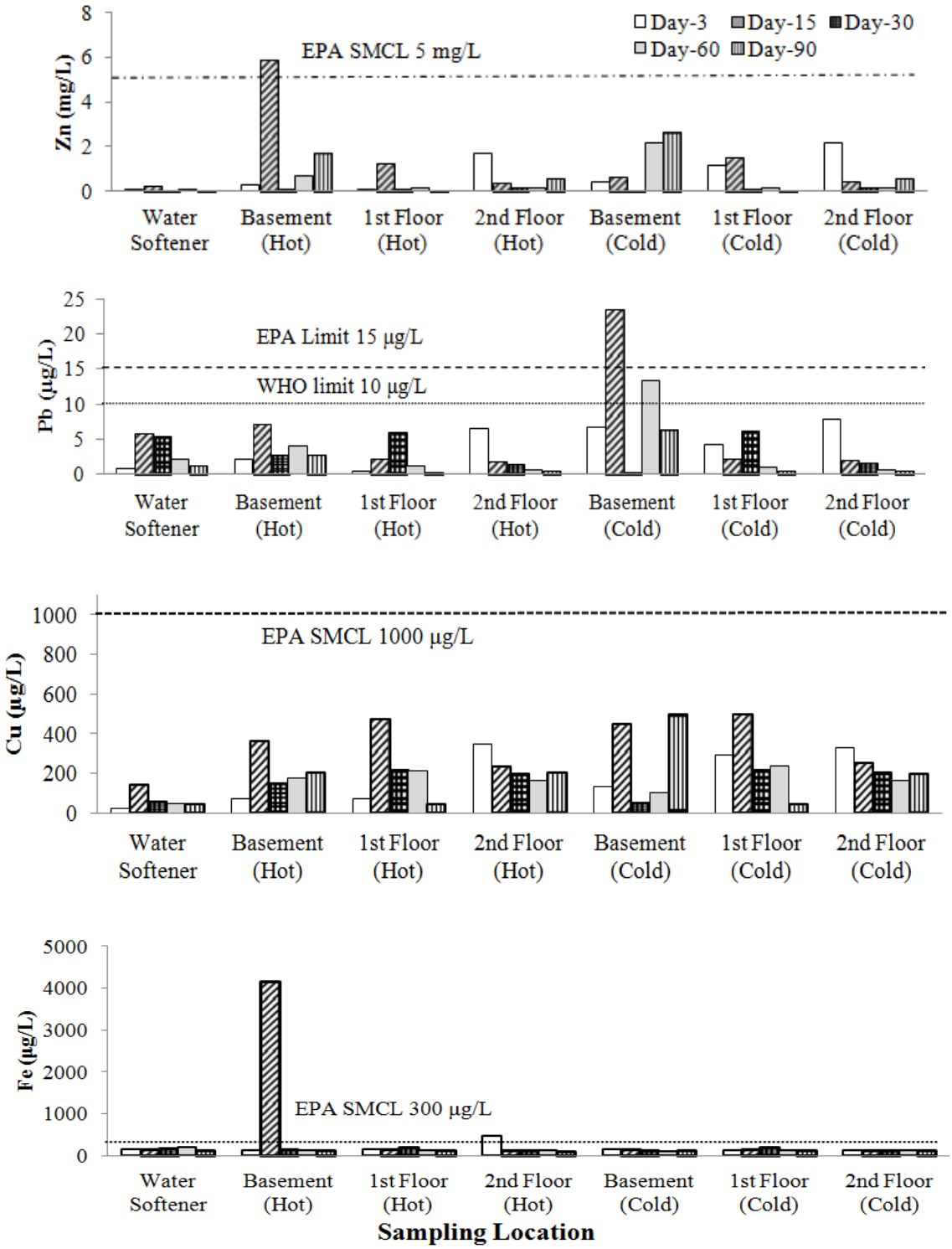

Figure 2-3 Drinking water Zn, Pb, Fe and Cu concentrations in the cold and hot water samples. Results shown represent one water sample.

Fe drinking water levels were nearly always similar throughout the house, and only twice, on day 3 and 15, exceeded the 300 µg/L USEPA SMCL. The high Fe concentration on day 15 in basement hot water sample could be due to Fe release by water heater tank carbon-steel heat exchangers[61] or Fe contaminated drinking water that entered the plumbing system during water main use and flushing activities[62]. Heat exchangers were exposed to superchlorinated water during plumbing system disinfection. Mn exceeded its 50 µg/L USEPA SMCL in the basement hot water on day 15 only and could have originated from the $KMnO_4$ water treatment plant process or water distribution system scales (**Table B13**). Tap water Al, Ca, Cr, Mg, Na, and Se levels were unremarkable (**Tables B14, B15**)[63].

2.4.2.2 Microbial Growth, Organic Carbon, and Water Temperature

During the entire three month study, both HPC and bacteria gene copy numbers increased at the 1st floor and 2nd floor fixtures (hot/cold). However, only for the first two months, HPC and bacteria gene copy numbers increased at the water softener and basement fixtures (hot/cold) (**Table B16**). At these fixtures on day 90, both HPC and gene copy number were reduced. The greatest HPC level (856.7 CFU/mL) was detected in basement hot water at the end of the study. This value was 3,440-fold and 2,298-fold greater than those levels measured in water exiting the water softener and basement cold water, respectively. Bacteria gene copy numbers showed a similar increasing trend at all seven locations similar to HPC results (**Table B16**) although, the bacteria concentrations found by the HPC method were only 0.63% of those detected by qPCR. At the end of the study, the greatest bacterial gene copy number detected by qPCR (2.25×10^4 gene copies/mL) was present in basement hot water. This value was 711-fold and 222-fold greater than bacteria gene copy numbers found in water exiting the softener and basement cold water sampling point, respectively. Although the bacteria population from another green building[8] were greater than the present study and included PEX piping (but no pipe type or age description was found), plumbing and water quality characteristics differed significantly. The other building included a manifold PEX plumbing design and this likely contributed to longer stagnation times as individual pipe segments convey water from a single manifold to each fixture in the house. In the present study, PEX pipe was

installed with the trunk-and-branch design thereby limiting water stagnation in common trunk plumbing pipes.

Statistical analysis indicated that organic carbon affected bacterial growth. Pearson correlation analyses were conducted among the water quality parameters at the different sampling locations. The positive correlations (R=0.812 to 0.833, p=0.080 to 0.095) between TOC levels and bacterial gene copy numbers were observed at four locations (water softener, 1st floor (cold), 2nd floor (cold/hot) across the five time points together (**Figure B3**). But the correlations were not significant ($0.05<p<0.1$) **(Table B17)**. Further Pearson correlation analysis indicated that TOC levels and bacterial gene copy numbers were significantly correlated (p=0.041), but in individual locations they were not significantly correlated. No significant correlation was observed between TOC levels and heterotrophic bacteria number quantified by culture-based method (p=0.5248), which may be attributed to the inadequacy of detecting total microbial community using the HPC method.

Greater bacteria levels were detected in hot water samples collected from the basement (day 3 to 90), 1st floor (day 3 and 90) and 2nd floor (day 15 to 90) (**Figure 2-4**). This finding implied that hot water plumbing (32°C to 50°C) was more conducive to bacteria metabolism and growth. It is important to note that hot water cooled in the plumbing pipes when fixtures were not in use. Hot water at the basement fixture had the greatest organic carbon concentration (TOC up to 4.4 mg/L) and bacteria gene copy number (up to 74,002 gene copy number/mL). Hot water in the basement was the least frequently used fixture. A relationship may exist between organic carbon and bacteria level (**Table B15**, **Table B23**, and **Figure B3**). Future work should consider measuring the total amount of carbon available for bacteria growth.

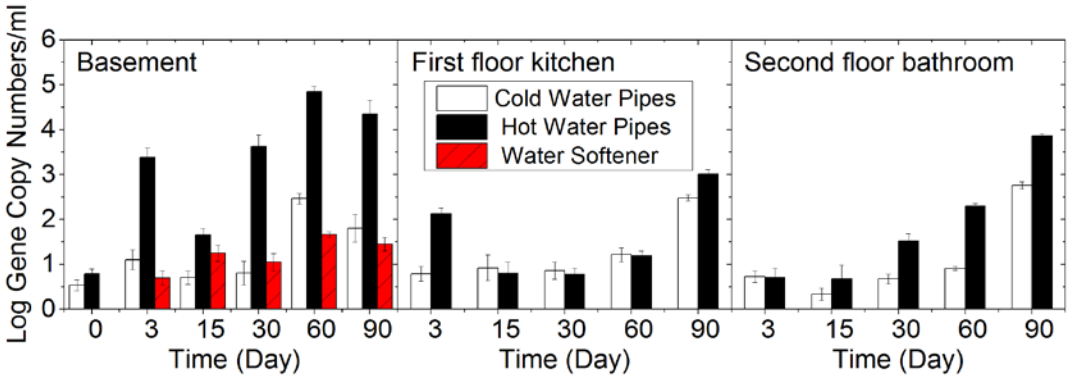

Figure 2-4 Gene copy numbers per milliliter in cold water pipes and hot water pipes at water softener, basement, first floor kitchen, and second floor bathroom.

2.4.3 Principal Component Analysis of Plumbing Water Quality Parameters

Principal component analysis (PCA) was conducted to identify variability and patterns of measured plumbing water quality data. Results of this analysis (**Figure B4**) showed clusters of data for the five sampling dates (day 3, 15, 30, 60, 90). The data indicated that TOC and pH were the two most important parameters that strongly affected water quality during the study. On day 3 and day 15 PCA results were rather dispersed and not correlated with specific water quality parameters. It is interesting that data at day 30 were clustered together and their standard deviations on PC1 and PC2 were 53.7% and 46.1% lower than those at day 3, respectively. However, no clear correlation was identified between day 30 data and any of the chemical and biological parameters. Water quality on day 60 and day 90 shifted to the top left region **Figure B4** and showed a strong correlation with TOC, pH, 16S rRNA gene, and heterotrophic bacteria. Although the correlation between Se and day 90 data was observed, Se concentrations did not change significantly (92 to 101% in hot or 101% to 115% cold water) and instead Se concentrations were significantly correlated with pH (p=0.005) and water volume (p=5.64*10^{-6}) (**Table B12**).

2.4.4 Link between Fixture Use and Water Quality

Different fixture use patterns resulted in disparate drinking water quality within single family home. Results show infrequently used fixtures such as bathrooms and sinks

could have markedly different chemical and microbiological quality than more frequently used fixtures located in a building. The greatest changes to drinking water quality were detected at the basement fixture, which had the least number of water use events, and was determined to be a hot spot for degraded water quality. At this location, the least amount of disinfectant residual was found (not detected to 0.6 mg/L as Cl_2) compared to other fixtures (0.1 to 1.6 mg/L as Cl_2). The greatest difference in TOC concentration compared to the service line was detected at the basement fixture (Δ=1.4 mg/L, hot water, day 60). Also, basement hot water samples contained the greatest bacteria concentration in the building on days 3, 30, 60 and 90 (2,707, 4,469, 74,002, 22,509 gene copy number/mL) (**Figure 2-4**). The basement hot water sample HPC on day 90 was the greatest in the building (857 CFU/mL) but HPC was less than 1 at other fixtures during the entire study. The basement hot water sample exceeded Zn and Fe USEPA SMCLs, and the basement cold water sample exceeded USEPA action level for Pb (**Figure 2-3**).

Water use significantly influenced chemical and microbiological levels at each fixture. The number of fixture use events, total water volume used, and average elapsed time at each fixture sometimes correlated with TOC and bacteria concentration (**Table B18**). During the study period, as the number of fixture use events increased, the TOC concentration increased (positive correlation). Also, it was found that as the total volume of water used at each fixture increased, TOC concentration increased at each fixture, except for the basement fixture. With a longer stagnation period, TOC concentration increased at all fixtures (positive correlation) except for the 2nd floor fixture hot water condition. At the water softener, a strong correlation (0.97) was detected between bacterial concentration (gene copy number) and number of water softener use events. In addition, bacterial concentration increased with the total water volume that passed through the water softener.

2.5 Implications and Limitations

Chemical and microbiological drinking water quality variations found within the single family residential plumbing mimicked the complexity of drinking water quality exhibited by large water distribution systems. Like water distribution systems, the fixture's distance from the service line resulted in greater water age, lower disinfectant

residual, greater microbiological characteristics, and was exacerbated at fixtures with low water use. The higher surface area to water volume ratio of plumbing pipes compared to larger diameter water distribution pipes likely amplified the observed drinking water quality impacts. In plumbing, a smaller volume of water was exposed to a greater surface area of biofilm, chemical leaching, and microbiological contamination. To better understand the carbon source in building drinking water assimilable organic carbon and biodegradable dissolved organic carbon analysis should be considered. Adsorption of organics, metals, and bacteria onto and release from plumbing materials under different water chemistry, temperature, and flow conditions may also have influenced study results and should be investigated. The plumbing product testing protocol used for the PEX piping that was installed currently considers 16 hr and 24 hr stagnation periods[64] but should be revised to account for worst-case more realistic stagnation periods identified in the present work (72 hr).

While water flow was measured with a one-second resolution, much fewer drinking water chemical and bacteria measurements were conducted. To better identify the relationships between fixture use and water quality more frequent water chemical and microbiological analysis would be required. The authors propose conducting more frequent water sampling over a short duration (1 week) and couple these results with service line pressure and fixture flow monitoring for the development of integrated water quality-hydraulic plumbing models. This process has been implemented to better design water distribution systems and should be considered for building plumbing.

In the U.S., residential building plumbing is designed to deliver a certain volume of water to fixtures based on number of building inhabitants. Factors such as drinking water chemical and microbiological levels are not explicitly considered in plumbing design. Future work should consider how different design characteristics (i.e., plumbing designs for multi-story vs. long single story buildings) influence drinking water quality. Identification and examination of plumbing branches to include residence time, disinfectant decay, chemical leaching, and microbiological growth kinetics should be considered. This information will be useful to better avoid lower-flow, hot spots of degraded drinking water quality.

2.6 Acknowledgement

Funding was provided by National Science Foundation grant CBET-1228615 and Environmental Protection Agency grant R836890. Special thanks to Whirlpool Corporation including Eric Bowler and Ronald Vogelwede for providing technical assistance and hosting the test site at the ReNEWW house project. The authors thank Drs. Chloe De Perre for assisting in ICP-MS analysis, Celeste Bronson and Jesse Li for helping with water sampling and the TON panelists. American Water is also thanked for providing municipal water source and treatment plant testing data. All opinions are those of the authors, not any organization that provided funding, technical assistance, or data support.

2.7 References

1. Loganathan GV, Lee J. Decision tool for optimal replacement of plumbing systems. *Civil Engineering and Environmental Systems.* 2005. 22(4): 189-204.

2. Navigant Research. Total Single-Family Residential Building Stock in the United States Will Shrink by 4 Billion Square Feet by 2021. https://www.navigantresearch.com/newsroom/total-single-family-residential-building-stock-in-the-united-states-will-shrink-by-4-billion-square-feet-by-2021 (July 14, 2016), accessed on May 22nd 2017.

3. Brazeau RH, Edwards MA. A Review of the Sustainability of Residential Hot Water Infrastructure: Public Health, Environmental Impacts and Consumer Drivers. *Journal of Green Building.* 2011, 6(4): 77-95.

4. Brazeau RH, Edwards MA. Water and Energy Savings from On-Demand and Hot Water Recirculating Systems. *Journal of Green Building* 2013, 8(1): 75-89.

5. Buchberger S, Omaghomi T, Wolfe T, Hewitt J, Cole D. Peak Water Demand Study: Probability Estimates for Efficient Fixtures in Single and Multi-family Residential Buildings. 2015. https://www.aspe.org/sites/default/files/Peak_Water_Demand_Study_Draft_for%20_Peer_Review.pdf , accessed on May 24th 2017.

6. US Green Building Council, LEED Water Efficiency Credits. http://www.usgbc.org/credits/healthcare/v4/water-efficiency (March 1, 2016). Accessed on May 24th 2017.

7. EPA WaterSense: An EPA Partnership Program. https://www3.epa.gov/watersense/products/bathroom_sink_faucets.html, accessed on May 24th 2017.

8. Rhoads WJ, Pruden A, Edwards MA. Survey of green building water systems reveals elevated water age and water quality concerns. *Environmental Science: Water Research & Technology.* 2016, 2(1), 164-173.

9. Sarver E, Edwards M. Effects of flow, brass location, tube materials and temperature on corrosion of brass plumbing devices. *Corrosion Science* 2011, 53(5), 1813-1824.

10. Nguyen C, Elfland C, Edwards M. Impact of advanced water conservation features and new copper pipe on rapid chloramine decay and microbial regrowth. *Water Res.* 2012, 46(3), 611-21.

11. Lautenschlager K, Boon N, Wang Y, Egli T, Hammes F. Overnight stagnation of drinking water in household taps induces microbial growth and changes in community composition. *Water Res.* 2010, 44(17), 4868-77.

12. Falkinham, JO. Common features of opportunistic premise plumbing pathogens. *Int J Environ Res Public Health* 2015, 12(5), 4533-4545.

13. Falkinham JO, Pruden A, Edwards M. Opportunistic Premise Plumbing Pathogens: Increasingly Important Pathogens in Drinking Water. *Pathogens.* 2015, 4 (2), 373-86.

14. Kusnetsov J, Torvinen E, Perola O, Nousiainen T, Katila ML. Colonization of hospital water systems by legionellae, mycobacteria and other heterotrophic bacteria potentially hazardous to risk group patients. APMIS. 2003, 111(5), 546-56.

15. Gunther F, Craun JMB, Yoder JS, Roberts VA, Carpenter J, Wade T, Calderon RL, Roberts JM, Beach MJ, Roy SL. Causes of Outbreaks Associated with Drinking Water in the United States from 1971 to 2006. *Clinical Microbiology Reviews,* 2010, 23(3), 507–528.

16. Boulay N, Edwards M. Role of temperature, chlorine, and organic matter in copper corrosion by-product release in soft water. *Water Res.* 2001, *35*(3), 683-90.

17. Heim TH, Dietrich AM. Sensory aspects and water quality impacts of chlorinated and chloraminated drinking water in contact with HDPE and cPVC pipe. *Water Res.* 2007, 41(4), 757-64.

18. Ji P, Parks J, Edwards MA, Pruden A. Impact of Water Chemistry, Pipe Material and Stagnation on the Building Plumbing Microbiome. *PLoS One.* 2015. 10(10), e0141087.

19. Waines PL, Moate R, Moody A J, Allen M, Bradley G. The effect of material choice on biofilm formation in a model warm water distribution system. *Biofouling* 2011, 27(10), 1161-74.

20. Borella P, Montagna M T, Romano-Spica V, Stampi S, Stancanelli G, Triassi M, Neglia R, Marchesi I, Fantuzzi G, Tato D, Napoli C, Quaranta G, Laurenti P, Leoni E, De Luca G, Ossi C, Moro M, Ribera D'Alcala G. Legionella infection risk from domestic hot water. *Emerg Infect Dis* 2004, 10(3), 457-64.

21. Connell M, Stenson A, Weinrich L, LeChevallier M, Boyd SL, Ghosal RR, Dey R, Whelton AJ. PEX and PP Water Pipes: Assimilable Carbon, Chemicals, and Odors. *Journal of American Water Works Association* 2016, 108(4), 192-204.

22. Dion-Fortier A, Rodriguez MJ, Serodes J, Proulx F. Impact of water stagnation in residential cold and hot water plumbing on concentrations of trihalomethanes and haloacetic acids. *Water Res.* 2009, 43(12), 3057-3066.

23. Kelley KM, Stenson AC, Dey R, Whelton A J. Release of drinking water contaminants and odor impacts caused by green building cross-linked polyethylene (PEX) plumbing systems. *Water Res.* 2014, *67*, 19-32.

24. Kimbrough DE. Brass Corrosion as a Source of Lead and Copper in Traditional and All-plastic Distribution Systems. *Journal of American Water Works Association.* 2007, 99(8), 70-76.

25. Liu B, Reckhow DA. Impact of Water Heaters on the Formation of Disinfection By-products. *Journal of American Water Works Association.* 2015, 107(6), 328-338.

26. Mathys W, Stanke J, Harmuth M, Junge-Mathys E. Occurrence of Legionella in hot water systems of single-family residences in suburbs of two German cities with special reference to solar and district heating. *Int J Hyg Environ Health.* 2008, 211(1-2), 179-85.

27. Viraraghavan T, Subramanian KS, Rao BV, Drinking water at the tap: Impact of plumbing materials on water quality. *Journal of Environmental Science and Health. Part A: Environmental Science and Engineering and Toxicology.* 1996, 31(8), 2005-2016.

28. Zietz B, de Vergara JD, Kevekordes S, Dunkelberg H. Lead contamination in tap water of households with children in Lower Saxony, Germany. *Sci Total Environ.* 2001, 275(1-3), 19-26.

29. Zietz BP, de Vergara JD, Dunkelberg H. Copper concentrations in tap water and possible effects on infant's health--results of a study in Lower Saxony, Germany. *Environ Res* 2003, *92*, (2), 129-38.

30. Zietz BP, Richter K, Laß J, Suchenwirth R, Huppmann R. Release of Metals from Different Sections of Domestic Drinking Water Installations. *Water Quality, Exposure and Health.* 2015, 7(2), 193-204.

31. Cerrato JM, Alvaradob CN, Dietrich AM. Effect of PVC and iron materials on Mn(II) deposition in drinking water distribution systems. *Water Res*. 2006, *40*, 2720-2726.

32. Malassa H, Al-Qutab M, Al-Khatib M, Al-Rimawi F, Determination of Different Trace Heavy Metals in Ground Water of South West Bank/Palestine by ICP/MS. *Journal of Environmental Protection.* 2013, 4, 818-827.

33. McNeil L, Edwards M. Iron Pipe Corrosion in Water Distributin System. Journal of *American Water Work Association.* 2001, 93(7), 88-100.

34. Lee J, Kleczyk E, Bosch DJ, Dietrich AM, Lohani VK, Loganathan GV. Homeowners' decision-making in a premise plumbing failure-prone area. *Journal of American Water Works Association.* 2013, 105(5), 236-241.

35. Chemaxx Inc. Cross-Linked Polyethylene Tubing and Water Contamination. http://www.chemaxx.com/polytube1.htm accessed on July 28, 2016.

36. California Plumbing Code Chapter 6 Water Supply and Distribution. http://www.iapmo.org/California%20Plumbing%20Code/Chapter%2006.pdf accessed on May 25, 2017.

37. Durand ML, Dietrich AM. Contributions of silane cross-linked PEX pipe to chemical/solvent odours in drinking water. *Water Sci Technol.* 2007, 55(5), 153-60.

38. Van der Kooij D, Veenendaal HR, Scheffer WJ. Biofilm formation and multiplication of Legionella in a model warm water system with pipes of copper, stainless steel and cross-linked polyethylene. *Water Res.* 2005, 39(13), 2789-98.

39. Kerneïs A, Nakache F, Deguin A, Feinberg M. The effects of water residence time on the biological quality in a distribution network. *Water Res.* 1995, 29(7), 1719-1727.

40. Niquette P, Servais P, Savoir R. Impacts of pipe materials on densities of fixed bacterial biomass in a drinking water distribution system. *Water Res.* 2000, 34(6), 1952-1956.

41. Koch A. *Gas Chromatographic Methods for Detecting the Release of Organic Compounds from Polymeric Materials in Contact with Drinking Water*. Hygiene-Inst. des Ruhrgebiets: Ruhr, Germany, 2004; p 176.

42. Lund V, Anderson-Glenna M, Skjevrak I, Steffensen IL. Long-term study of migration of volatile organic compounds from cross-linked polyethylene (PEX) pipes and effects on drinking water quality. *J Water Health.* 2011, 9 (3), 483-97.

43. Skjevrak I, Due A, Gjerstad KO, Herikstad H. Volatile organic components migrating from plastic pipes (HDPE, PEX and PVC) into drinking water. *Water Res.* 2003, 37(8), 1912-20.

44. Loschner D, Rapp T, Schlosser, FU, Schuster R, Stottmeister E, Zander S. Experience with the application of the draft European Standard prEN 15768 to the identification of leachable organic substances from materials in contact with drinking water by GC-MS. *Analytical Methods.* 2011, 3(11), 2547-2556.

45. Venere, E. Whirlpool Corporation, Purdue turning house into 'net-zero' home.

46. K. Hawes, E. Conkling, K. Casteloes, R. H. Brazeau, M. Salehi, A. J. Whelton, Predicting Contaminated Water Removal from Residential Water Heaters under Various Flushing Scenarios. In Press. *Journal of American Water Work Association*, 109(8), 2017

47. American Public Health Association, AWWA and Water Environment Federation, *Standard Methods for the Examination of Water and Wastewater*. Washington D.C., USA, 1995.

48. Burr-Rosenthal K. Avoiding Water Waste with Convenience. *City of San Diego.* 2005. *Instant Hot Water Delivery System Pilot Project* 2005. San Diego, CA.

49. Van der Wielen P, Van der Kooij D. *Microbial Growth in Drinking-Water Supplies. Problems, Causes, Control and Research Needs*. IWA Publishing, 2013.

50. Rhoads WJ, Ji P, Pruden A, Edwards MA. Water heater temperature set point and water use patterns influence Legionella pneumophila and associated microorganisms at the tap. *Microbiome.* 2015. 3(1), 1-13.

51. Skjevrak I, Lund V, Ormerod K, Herikstad H. Volatile organic compounds in natural biofilm in polyethylene pipes supplied with lake water and treated water from the distribution network. *Water Res.* 2005, 39(17), 4133-41.

52. USEPA, Drinking Water Guidance on Disinfection By-Products Advice Note No. 4. Version 2. 2012.

53. Hua G, Reckhow DA, Abusallout I. Correlation between SUVA and DBP formation during chlorination and chloramination of NOM fractions from different sources. *Chemosphere.* 2015, 130, 82-89.

54. Worley JL, Dietrich AM, Hoehn RC. Dechlorination techniques to improve sensory odor testing of geosmin and 2-MIB. *Journal of American Water Works Association.* 2003, *95*(3), 109-116.

55. Zhang Y. Dezincification and Brass Lead Leaching in Premise Plumbing Systems : Effects of Alloy, Physical Conditions and Water Chemistry Dezincification and Brass Lead Leaching in Premise Plumbing Systems : Effects of Alloy, Physical Conditions and Water Chemistry. Master Thesis, 2009. Virginia Polythechnique Institute and State University, Blacksburg, VA.

56. US EPA, National Primary Drinking Water Regulation, 2010.

57. Inkinen J, Kaunisto T, Pursiainen A, Miettinen IT, Kusnetsov J, Riihinen K, Keinanen-Toivola MM. Drinking water quality and formation of biofilms in an office building during its first year of operation, a full scale study. *Water Res.* 2014, *49*, 83-91.

58. Gardels MC, Sorg TJ. A Laboratory Study of the Leaching of Lead from Water Faucets. *Journal of American Water Works Association.* 1989, 81(7), 101-113.

59. Samuels ER, Méranger JC. Preliminary studies on the leaching of some trace metals from kitchen faucets. *Water Research.* 1984, 18(1), 75-80.

60. Ang, R. Up the Pipe: A literature review of the leaching of copper and zinc from household plumbing systems. http://www.cawthron.org.nz/media_new/publications/pdf/2015_08/Up_the_Pipe_-_A_literature_review_of_the_leaching_of_copper_and_zinc_from_household_plumbing_systems_FINAL.pdf accessed on July 25th 2016.

61. STIBEL Electron. Engineering Specification Sheet of SBB Indirectly Fired Water Heater Tanks. http://www.stiebel-eltron-usa.com/sites/default/files/pdf/specification-sheet-sbb.pdf accessed on July 25 2016.

62. Peng CY, Korshin GV, Valentine RL, Hill AS, Friedman MJ, Reiber SH. Characterization of elemental and structural composition of corrosion scales and deposits formed in drinking water distribution systems. *Water Res.* 2010, 44(15), 4570-4580.

63. Azoulay A, Garzon P, Eisenberg MJ. Comparison of the mineral content of tap water and bottled waters. *J Gen Intern Med.* 2001, 16(3), 168-75.

64. NSF International/ ANSI 61, Drinking water systems components- health effects. 2013, Michigan, USA.

CHAPTER 3 : INVESTIGATION OF THE FACTORS THAT INFLUENCE LEAD ACCUMULATION ONTO POLYETHYLENE: IMPLICATION FOR POTABLE WATER PLUMBING PIPES

Maryam Salehi, Chad T Jafvert, John A Howarter, Andrew J Whelton

3.1 Abstract

The influence of polymer aging, water chemistry, and aqueous Pb concentration on Pb deposition onto low density polyethylene (LDPE) was investigated. LDPE pellets were aged by ozonation at 85 °C. Attenuated total reflectance Fourier transform infrared spectroscopy (ATR-FTIR) analysis, water contact angle measurements, and Field Emission-Scanning Electron Microscopy (FE-SEM) imaging were conducted to identify surface chemistry and morphology changes due to polymer aging. The influence of water pH on Pb precipitation rates was determined for new and aged (oxidized) LDPE. The type and amount of Pb species present on these surfaces was evaluated using X-ray photoelectron spectroscopy (XPS). The influence of exposure duration on Pb deposition onto LDPE was modeled using the pseudo-first-order equation. Results showed that the accelerated aging of LDPE surfaces caused carbonyl (>C=O) and ether (>C-O<) bonds to form. Distribution ratio calculations showed Pb precipitates had greater affinity for the surface of aged (oxidized) LDPE compared to new LDPE. Aged LDPE had less Pb surface loading at pH 11 compared to loading at pH 7.8. Pb surface loading for aged LDPE changed linearly with aging duration (from 0.5 to 7.5 h). Pb surface loading on both new and aged LDPE increased linearly with increasing Pb initial concentration. Greater Pb precipitation rates were found for aged LDPE compared to new LDPE at both tested pH values. XPS analysis revealed that aging caused the formation of a variety of polar functional groups (>C-O<, >C=O, >COO) on LDPE's surface. These functional groups likely provided more nucleation sites for $Pb(OH)_2$ deposition compared to new LDPE, which did not have these oxygen-containing functional groups.

3.2 Introduction

Lead (Pb) exposure through tap water is a global concern due to the contaminant's acute and chronic health impacts. Exposure can delay children's mental development, cause behavior disorders, Anemia, renal dysfunction, impaired hearing and postnatal growth[1–4]. In the U.S., lead in tap water remains a serious health risk, with large-scale lead drinking water poisonings occurring most recently in Washington, D.C. in 2004 (at up to 7,500 μg/L)[2] and in Flint Michigan in 2015 (at up to 13,200 μg/L)[5,6].

Lead in building tap water can originate from the corrosion of plumbing materials such as lead service lines or lead containing brass appurtenances, solders, and fixtures[7–11]. Pb also can enter buildings from the water distribution piping network and then deposit and release from the surface of metal plumbing components (i.e., galvanized steel)[12]. Pb can either be in particulate or dissolved form and the concentration of each form can be influenced by water conditions (i.e., pH, hardness), as well as network operational conditions (i.e., residence time, temperature, corrosion inhibitor, flow rate)[11,13–18]. Pb levels in U.S. buildings have been reported to range from 0.2 to 13,000 μg/L in first draw water samples, and 0.2 to 7,400 μg/L in flushed (30 s) water samples[19–22]. If water quality or operational conditions are altered, excessive metal leaching from piping components and pipe scales can occur as evidenced by Pb poisonings in Washington D.C.[2] and Flint Michigan[5,6]. Due to the complex interactions of hydraulics, temperature, stagnation times, materials, and water chemistry, the fate of Pb in building plumbing is not well understood.

To reduce tap water metal drinking water levels some water utilities and building owners are choosing to replace lead service lines and indoor plumbing with plastic pipes. Popular U.S. buried water distribution and service line plastic pipes are composed of high-density polyethylene (HDPE) or polyvinylchloride (PVC). Crosslinked polyethylene (PEX, 54% of replumbed households) and chlorinated polyvinylchloride (cPVC, 7% of replumbed households) pipes are also being installed primarily for water service connections and within premise plumbing instead of copper (9% of replumbed households)[23]. Among these materials, it is well-known that PVC and cPVC pipes can

leach metal heat stabilizers[24–27], while polyethylene pipes do not leach heavy metals. Ginige et al (2017) reported Fe and Mn deposition onto HDPE pipe[28].

The limited examination of in-service plastic pipes however, has revealed heavy metals (including Pb) can accumulate on plastic pipe surfaces (**Table 3-1**). For example, on a PVC pipe, the scale on the inner pipe surface was 6% Mn by weight and was easily dislodged by flowing water[29]. In a survey of 15 U.S. water utilities, very high loadings of As (1,416 to 13,650 µg/g) and Pb (210 to 9,681 µg/g) were detected on PVC drinking water distribution pipes (**Table 3-1**)[30–32]. Pb adsorption has been detected on drinking well PVC casings, and less Pb adsorption was found at lower pH values, but no adsorption differences were found between 50 µg/L and 100 µg/L Pb concentrations[26]. The role of plastic pipe surface aging on heavy metal sorption has gone unstudied, as most literature has focused on new (unaged) plastic materials, or plastic pipes in-service, where aging history is unknown and uncontrolled. Plastics pipes are known to undergo oxidative attack and degradation caused by drinking water chlorine disinfectants. Several oxidized functional groups including >C=O, >OH, and >C-O-C< have been detected on polymer surfaces exposed to chlorine water[33–36]. These polar functional groups may influence heavy metal interactions with the plastic surface, and hence deserve scrutiny.

The plastic pollution literature contains a great amount of studies regarding heavy metal adsorption to plastic materials. Metal ion adsorption to new polyethylene resin pellets has been described using Langmuir and Freundlich isotherms[37]. Aged polyethylene pellets removed from a beach were found to have a greater absorption capacity for Cd, Co, Cr, Cu, Ni, and Pb adsorption than new pellets[37]. As water pH increased, adsorption of Cd, Co, and Ni increased, Cr adsorption decreased, and Cu adsorption was unaffected (2014)[38]. The influence of water pH on Pb adsorption with the plastic pellets was studied by others as well. Although, no significant effect was found for the Pb loadings as increased river water pH increased from 7.5 to 10.5 at Pb concentration of 5 µg/L[38].

No studies were found that identified why aged plastics adsorbed a greater mass of heavy metals than new plastics. Prior studies also did not fully explore the condition of the plastics examined. The working hypotheses in the literature are that: (1) metal cations (e.g., Pb^{2+}, Ni^{2+}) or oxy-anions (e.g., $HCrO_4^-$ and CrO_4^{2-}) directly adsorb onto oppositely

charge sites or neutral regions of the polymer surface[39–42] and (2) co-precipitation with or adsorption onto Fe and Mn hydrous oxides occur. However, no testing of these hypotheses was found.

Because plastic pipes are increasingly being used for potable water distribution and the literature indicates some plastics can adsorb from and release metals into the drinking water, this study was conducted. The goal of this study was to investigate drinking water quality and polymer surface characteristics that influence Pb deposition on and adsorption to LDPE. LDPE is not used for drinking water piping in the U.S., but it was previously used for pipe manufacture in Europe[43], and is widely used for domestic and commercial irrigation[44]. LDPE is a model material for investigating the factors that control contaminant-plastic interactions. Specific objectives of the work were to: (1) Determine the role of LDPE aging on Pb surface loadings; (2) examine the influence of water pH on Pb precipitation over the time for new and aged LDPE; (3) determine the precipitation rates for new and aged LDPE at pH values of 7.8 and 11; and (4) identify the type and amount of Pb species present on new and aged LDPE surface.

Table 3-1 Studies found in the literature that reported detecting heavy metals on plastic potable water pipes

Metal	Water Main						Service Line		
	nr	PVC	PVC	PVC	PVC	HDPE	PB	HDP	HDP
	Mass Found								
	(µg/g solid scale)						*(mg/cm² pipe surface*		
As	1,230	13,650	1,416	7,842	nr	49.9	0.097 *	0.010 *	0.041 *
Ba	nr	nr	nr	nr	nr	446			
Cd	0.3	<4.8	36	375	nr	34.1			
Cr	nr	nr	nr	nr	nr	0.82			
Ni	18	6	110	137	nr	330			
Pb	114	210	4,667	9,681	0.96 w%	25.1			
U	nr	nr	nr	nr	nr	113			
V	nr	nr	nr	nr	nr	137			
Al	4,955	1,906	1,025	2,329	19.72	641			
Ca	57,79	22,939	28,859	4,455	1.29 w%	2,856			
Mg	21,15	1,492	1,736	442	0.1 w%	2,435			
Fe	144,2	442,52	77,030	237,293	1.42 w%	5.5 w%			
Mn	882	5,142	290	1,267	6.12 w%	2,324			
P	10,00	15,410	850	1,410	nr	728			
Zn	206	8,915	535,783	541,564	0.35 w%	1,846			
Ref	30				29	31	32		

nr = not reported; All data reported “as is” from cited studies; *Total mass of scale on inner pipe wall

3.3 Methods

3.3.1 Materials

Low density polyethylene (LDPE) pellets and films (0.1 mm thickness) were purchased from Sigma Aldrich, and LDPE sheets (3.1 mm thickness) were purchased from McMaster-Carr. LDPE plastic sheets and films were cut in 1×1 cm^2 prior to experiments. LDPE films were used for XPS analysis, and LDPE sheets were used for water contact angle measurements, for all other experiments LDPE pellets were used. LDPE powder (diameter: 500 µm) were purchased from Alfa Aesar and were used for surface area measurement (BET). Pb ICP-MS standard (1000 mg/L) was purchased from RICCA

Chemical Company. As mentioned by produced company, the Pb ICP-MS standard was produced by dissolving Pb metal in HNO_3. Ultrapure Milli-Q™ (18 MΩ*cm) system treated the water used for all experiments conducted in this study. It should be noted that different forms of LDPE used in this study may not have exactly the similar compositions.

3.3.2 LDPE Aging with Ozone

A Pacific Ozone Technology Lab 11 ozone generator was used to generate ozone (O_3) from pure (99.5%) oxygen (O_2). LDPE samples were placed in glass containers with water and connected to a condenser (**Figure C1**). Polymer aging was conducted at 85 °C. Ozone was sparged into the solution using a glass gas washing dispenser. LDPE plastic pellets were aged from 30 min to 10 h. The ozone mass flow rate was measured at 3.84 mg/min using the method described by Blatchley et al. (2007)[45].

3.3.3 LDPE Pellet Conditioning

In order to remove residual organics from new and aged LDPE pellets, pellets were conditioned before Pb exposure and carbon leaching experiments. For conditioning, 15 g of pellets were initially rinsed three times with water, then they were stirred with 250 mL water for 24 h, then rinsed again three times with water, and finally dried at room temperature.

3.3.4 Organic Carbon Release Experiment

The release of organic carbon from new and aged LDPE, measured as total organic carbon (TOC) concentration, was monitored after 2, 6, 12, 24, and 48 h and at 5 days of exposure in water at pH 6, 7.8 and 11. Surface area to volume ratio S/V was selected as 0.85 cm^2/mL for the pellets. To obtain this S/V ratio, 40 LDPE pellets were added to 26 mL water at the desired pH in 40 mL amber glass vials. Next, the samples were mechanically stirred during each exposure period at room temperature. Water pH was adjusted using HCl or NaOH. Water pH was measured using an Orion Star A329 portable pH meter (Thermo Scientific).

3.3.5 Pb Exposure Procedure

To limit the type of Pb species present in aqueous solution, Pb exposure experiments were conducted in an oxygen-free environment. To remove the oxygen from the water, high purity N_2 (99.995%) was sparged into the water for 45 min within a glove box. The appropriate amount of Pb (ICP-MS standard) was added to 300 mL water in a 1L PTFE bottle to make a stock aqueous solution. Then the pH was adjusted using HCl or NaOH. Under N_2 (in the glove box) 13 mL of the Pb stock solution was added to 20 pellets in 50 mL PTFE bottles (S/V ratio of 0.85 cm^2/mL).

3.3.6 Five Day Pb Exposure Experiments

Experiments were conducted at pH values of 7.8 and 11 for new and 10 h aged LDPE pellets during 5 day exposure period. In these experiments the initial aqueous Pb concentration was 300 µg/L. During each experiment, three replicates were removed at each exposure period. To quantify Pb on the pellets, the pellets were removed from the water and digested with 2% HNO_3 for 24 h.

3.3.7 Influence of Aging Duration, Organics Content and Pb Initial Concentration on Pb Deposition

The role of polymer oxidation on Pb surface loading was examined. LDPE pellets were aged for 0.5, 2.5, 5, 7.5, and 10 h and exposed to Pb aqueous solution (300 µg/L) for 48 h. The water pH was adjusted at 7.8. A solution of residual organic matter leached from the pellets was prepared. This solution was used to examine the effect of organics leached from the aged LDPE on Pb surface deposition. To prepare this solution, 10 h aged LDPE pellets were exposed to water at pH 11 for 5 days. Then the aqueous solution was removed and TOC was measured as 47 mg/L. This solution (TOC as 47 mg/L) was diluted to achieve 28 mg/L and 13 mg/L TOC levels. Then Pb (300 µg/L) was added to all these three solutions. The water pH was adjusted at 7.8. Then 10 h aged LDPE pellets were exposed to these solutions in triplicates for 48 h. The impact of initial Pb concentration on Pb surface deposition was also tested. New and 10 h aged LDPE pellets

were exposed to an initial Pb concentration of 100 µg/L, 600 µg/L, 1,000 µg/L, 3,000 µg/L and 5,000 µg/L. For each condition, water pH was adjusted at 7.8 and 11.

3.3.8 Pb Exposure of LDPE Films Prior to XPS Analysis

New and aged LDPE plastic films (5 h and 10 h aged) were exposed to Pb concentration of 5,000 µg/L for 48 h. The water pH was adjusted at 7.8. These plastic films were not conditioned before the experiment. S/V ratio was selected as 1 cm^2/mL. After the exposure period the films were removed from the solution. They were dried in the glove box with slow purging N_2. After drying, the films were transferred to the XPS facility in the N_2 filled bottles.

3.3.9 ATR-FTIR Analysis

To identify the plastic surface functional groups after the aging process Attenuated Total Reflectance Fourier Transform Infrared (ATR-FTIR) spectroscopy was applied on LDPE pellets, sheets and films. Spectra were recorded on a Perkin-Elmer Spectrum 100 FT-IR Spectrometer from 4000 to 650 cm^{-1}. A 2 cm^{-1} resolution was applied. Carbonyl bond intensity has previously been used to examine polymer oxidation[46–49]. In this study the degree of polymer oxidation (carbonyl index) was estimated by comparing the ratio of the carbonyl peak intensity (1710 cm^{-1}) and reference peak intensity at 720 cm^{-1} [50].

3.3.10 Water Contact Angle Measurement

The surface wettability changes were examined by application of static water contact angle titration. New and 10 h aged LDPE sheets were studied. Water contact angle measurements were carried out by averaging 20 readings of three replicates using Ramé-hart contact angle goniometer and tensiometer: Model 500. Buffer solutions (pH 2 to 12) were prepared by addition HCl and NaOH to Ultrapure Milli-Q™ water. The pH has been adjusted with 0.01 accuracy. These measurements were conducted on new and 10 h aged LDPE sheets. Two independent student t-tests were used to elucidate the difference between new and aged LDPE sample water contact angles.

3.3.11 BET Surface Area Measurement

LDPE powder was aged for 10 h, was dried at the room temperature and was used surface area measurement. The Brunauer, Emmet and Teller (BET) model was applied to the N_2-adsorption data in order to evaluate the surface area changes due to the LDPE aging. The surface area was measured using a Micromeritics (Tristar 3000) analyzer.

3.3.12 TOC Measurement and Pb Quantification

TOC concentration was measured using a Shimadzu TOC-L CPH/CPN in accordance with USEPA method 415.1. Standard calibration curve was conducted on instrument from 0 to 100 mg TOC/L (r^2=0.995) using potassium acid phthalate[51].

For Pb surface loading quantification the plastic (LDPE) pellets were removed from aqueous solution. Then they acidified for 24 h in 2% HNO_3 solution in 15 mL polypropylene tubes. After that they removed from the acidified solution, and Pb concentration was determined in acidified solution. The residual floc was defined as the amount of Pb that was not deposited on LDPE pellets or container wall and left in the solution. To quantify the residual floc, after removing the LDPE pellets from PTFE bottles, the solution was transferred to 15 mL polypropylene tubes and acidified with 2% HNO_3. The residual floc also was monitored for the control samples (contained only Pb solution and no LDPE pellets) in triplicates. If needed the acidified solutions were diluted using UMQW treated water then they analyzed with a Perkin Elmer Elan-DRCE II Inductively Coupled Plasma Mass Spectrometer (ICP-MS). Pb standards for ICP-MS analysis were prepared in 5 µg/L, 25 µg/L, 50 µg/L, 100 µg/L, 200 µg/L and 300 µg/L concentrations.

3.3.13 FE-SEM and XPS Analysis

Field emission scanning electron microscopy (FE-SEM) imaging was conducted to examine the polymer surface morphology changes. New and 10 h aged LDPE sheets were used for FE-SEM imaging. FE-SEM instrument was FEI Nova Dual Beam with an Oxford 80 EDX detector. Before analysis, sheets were coated with gold and palladium under vacuum conditions. X-ray photoelectron spectroscopy (XPS) measurements were

conducted using a Kratos Axis Ultra DLD spectrometer with monochromatic Al Kα radiation (hυ=1486.6 eV). High-resolution spectra were collected at constant pass energy with a PE of 20 eV and survey spectra at PE of 160 eV. A charge neutralizer was used to achieve better resolution. Binding energy value refers to the Fermi edge and the energy scale was calibrated using Au 4f7/2 at 84.0 eV and Cu 2p3/2 at 932.67 eV. The data were converted into the VAMAS file format (*.vms) and imported into the CasaXPS software package for manipulation and curve-fitting. A Shirley background was subtracted from each region before quantification. All C 1s peaks were adjusted so that the peak maximum appeared at a binding energy of 284.8 eV and all binding energies (BEs) are measured relative to this C 1s (hydrocarbon) reference.

3.4 Results and Discussion

3.4.1 Low Density Polyethylene (LDPE) Degradation

3.4.1.1 ATR-FTIR Analysis

For new LDPE pellets absorption bands at 2914 cm^{-1} and 2848 cm^{-1} were detected. These can be attributed to sp^3 >C-H asymmetric and symmetric stretching. Absorption bands at 1464 cm^{-1} and 715 cm^{-1} were also found for new LDPE and are assigned to >C-H bending. Several oxidized surface functional groups were also identified on aged LDPE (**Figure 3-1a**). The 1710 cm^{-1} carbonyl functional group revealed the LDPE pellets were oxidized. This functional group has been previously found on aged HDPE water pipes exposed to disinfected drinking water[52]. For LDPE samples aged 2.5 h to 10 h, a wide peak was observed at 938 cm^{-1}. This wide peak was attributed to >C-O-C< and was not found on new LDPE[33]. Several other peaks were observed for 2.5 h to 10 h aged LDPE that could be attributed to >C-O-C< functional groups (1096, 1154, 1411, 1214, and 1291 cm^{-1})[33]. Formation of the >C-O-C< bond was also detected on polyethylene water pipes exposed to hot chlorinated and nonchlorinated waters[33,53]. With increased aging duration (from 0 h to 10 h), the degree of oxidation increased linearly (r^2=0.97) (**Figure 3-1b).**

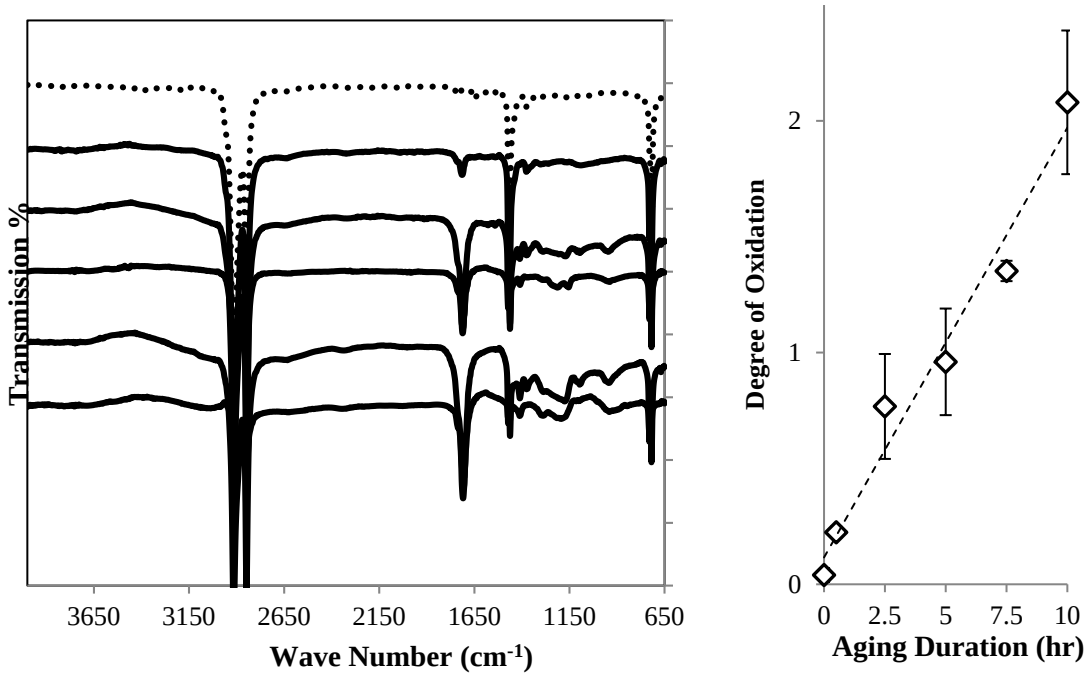

(a) (b)

Figure 3-1 (a) ATR-FTIR spectra of new and aged LDPE, (b) Degree of oxidation over the aging duration (error bars represent standard deviation for three samples)

Similar surface functional groups were found for 10 h aged LDPE sheets, films and pellets (**Figure C2**). The absorption intensity of >C=O and >C-O-C< functional group peaks for aged LDPE sheets and films were lower than aged LDPE pellets. The LDPE sheet (carbonyl index: 1.34 ± 0.09) and the LDPE film (carbonyl index: 1.35 ± 0.2) were slightly less oxidized compared to LDPE pellets (carbonyl index: 2.08 ± 0.31). Aged LDPE pellets (10 h) were selected for Pb exposure experiments because they provided greater surface area available for Pb sorption compared to LDPE sheets and films. The aged LDPE pellet surface functional groups were similar to polyethylene pipes aged by chlorinated water[33].

3.4.1.2 Influence of Polymer Aging on Surface Wettability, Morphology and Surface Area

Water contact angle measurement showed significantly lower water contact angles (*p-value* <0.01) for aged LDPE (98.6º ± 1.6º) compared to the new LDPE (104.6º ± 2.8º). This finding is likely due to the aged LDPE's surface being more hydrophilic, caused by the chemical oxidation. It is well-known that water adsorbs to polar polymer surfaces and oxidation can increase wettability[54]. Water pH (2 to 12) did not consistently influence water contact angle for aged LDPE (*p-value* 0.076). Water contact angles were greater for new LDPE at pH values 8, 9, and 10 (*p-value* 0.006), but not at any other pH condition (**Figure C3**). No surface morphology differences were observed for new and aged LDPE by FE-SEM **(Figure C4)**. BET surface area was greater for 10 h aged LDPE powder (0.12 ± 0.0 m^2/g) compare to new LDPE powder (0.03 ± 0.0 m^2/g).

3.4.1.3 Organic Carbon Release by New and Aged LDPE

Organic carbon release by LDPE pellets was significant over the five day experiment, but aged LDPE released the greatest amount of carbon compounds. Also, the observed TOC concentration by aged LDPE was a function of water pH. Organic carbon released by aged LDPE was significantly greater at pH 11 (> 48 mg/L) than pH 6 (< 3 mg/L) (**Figure 3-2**). For new LDPE, organic carbon release was low (< 1.7 mg/L at all pH conditions). The finding that water pH influenced organic carbon release from aged LDPE is important. The release of these compounds is likely altering the polymer nanostructure and could influence heavy metal fate and interaction with the plastic surface. LDPE can hydrolyze at room temperature[55]. Also, by increasing water pH from 5.0 to 8.1 polycarbonate hydrolysis resulted in greater chemical leaching[56]. Very little information was found regarding the impact of water pH on organic carbon release from plastic pellets, sheets, and pipes. Greater carbon release could be due to LDPE degradation at high water pH. Excess OH^- ion could attack vulnerable bonds created from chemical oxidation of polymer chains. Oxidized carbon functional groups formed on polymeric chain after ozone aging made the polymer vulnerable. As a result electron withdrawing by oxygen caused the positive charge for adjacent carbon atom. This positively charged

carbon atom can be attacked by OH^- ion present in water[57,58]. High reactivity of the radicals formed due to OH^- attack could initiate unsaturated bond formation[59]. In the present study exposure of aged LDPE to pH 11 water caused the vinyl bond formation (>C=C<). This bond was not detected after polymer exposure to either pH 6.0 or 7.8 (**Figure C5**).

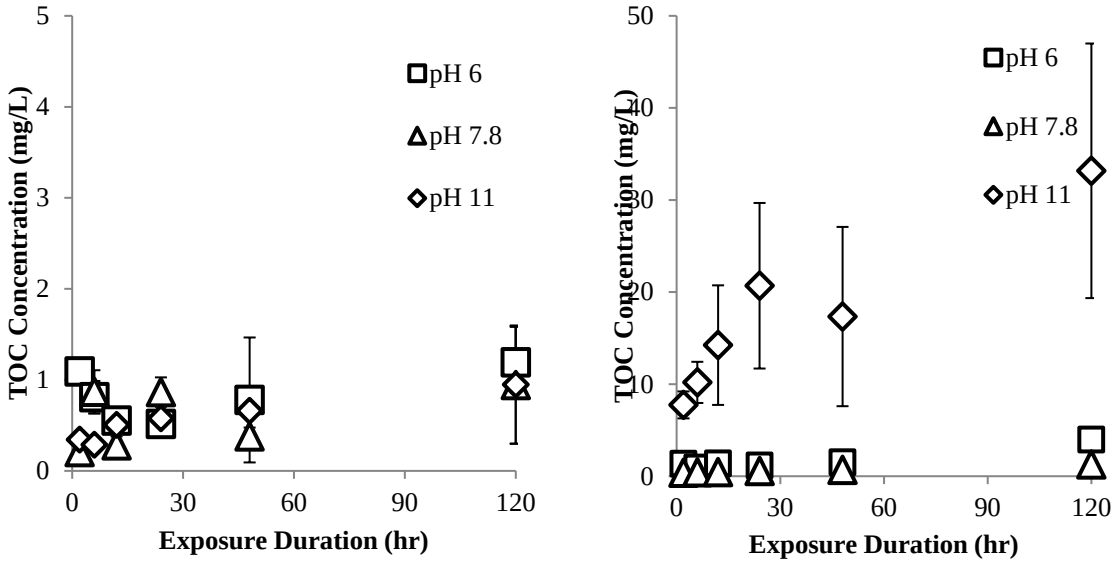

(a) (b)

Figure 3-2 Organic release over the time for (a) New and (b) 10 h aged LDPE (Mean ± std)

3.4.4 Pb Precipitation on New and Aged LDPE

3.4.4.1 Pb Speciation in DI Water

Pb chemical speciation in DI water when no oxygen was present, was determined through solving Pb hydroxyl complexation and solubility equations (**Table C1).** Results showed that Pb was precipitated onto new and aged LDPE, as the major portion of Pb species in the solutions was solid. Only very small amount of diluted HCl was used for pH adjustment, and based on the chemical equilibriums the concentrations of chloride complexes in the system were negligible. As a result, it was assumed that only Pb^{2+}, $Pb(OH)^+$, $Pb(OH)_{2\,(aq)}$, $Pb(OH)_{2\,(s)}$, $Pb(OH)_3^-$ and $Pb(OH)_4^{2-}$ were present in the water. **Figure C6** shows Pb speciation based on these complexation equations (pH 2 to 12). For

5 day Pb exposure $[Pb]_t$ was selected as 300 µg/L. This Pb concentration simulated the condition when new and aged plastic premise plumbing exposed to Pb level more than US Environmental Protection Agency (USEPA) action level (15 µg/L). Precipitation rates were determined for new and aged LDPE exposed to Pb (100 µg/L to 5,000 µg/L) to understand the magnitude of Pb deposition onto plastic plumbing system after exposure to excessive level of Pb at different water chemistry conditions. Based on Pb hydroxyl complexation and solubility equations, the concentration of soluble Pb species was 19.0 µg/L at all tested Pb initial concentrations (100 µg/L to 5,000 µg/L) at pH 7.8. It was almost 0.0 for all tested Pb initial concentrations (100 µg/L to 5,000 µg/L) at pH 11 (**Figure C7**). This soluble Pb level was neglected compare to total Pb concentration (100 µg/L to 5,000 µg/L).

3.4.4.2 Pb Precipitation on LDPE over 5-day Exposure Period

Pb precipitation on new and aged LDPE during the 5 day exposure period was examined using pseudo-first-order model (Equation 3-1 and 3-2). In this study we considered Pb precipitation onto LDPE as a mass transfer process, since pb species only transferred from solution to LDPE surface and no chemical reaction occurred.

$$\frac{dq}{dt} = -K(q - q_{eq}) \qquad (3\text{-}1)$$

$$q = q_{eq}(1 - e^{-Kt}) \qquad (3\text{-}2)$$

$$t_{1/2} = \frac{ln\,2}{k} \qquad (3\text{-}3)$$

Where q and q_{eq} are the Pb surface loading on LDPE (µg/m^2) at the time t (h) and at the equilibrium. The first-order mass transfer constant was shown by K (h^{-1}), and it was determined using the experimental data. The half-life ($t_{1/2}$) represents the time required for polymer to uptake half of equilibrium Pb surface loading and calculated using Equation (3-3).

In this study the authors defined the distribution ratio (*D*) as shown in Equation 3-4. The distribution ratio shows Pb distribution between LDPE surface and aqueous solution. The Pb distribution between LDPE surface and aqueous solution was estimated by determining the distribution ratio.

$$D\ (\text{mm}) = \frac{Pb\ Surface\ loading\ (\frac{\mu g}{m^2})}{Pb\ floc\ left\ in\ solution\ (\frac{\mu g}{L})} \quad (3\text{-}4)$$

3.4.4.2.1 Effect of Polymer Aging on Pb Precipitation Over the Time

Aged LDPE had a greater Pb surface loading than new LDPE and loading was a function of exposure duration (2 h to 5 days) (**Figure 3-3a**). Pb loading on aged LDPE was greater than new LDPE during all exposure periods. Aged LDPE achieved 45% of its surface loading equilibrium during the first 2 h exposure. But for new LDPE only 1.7% of equilibrium was obtained in the first 2 h. As **Table 3-2** shows the half-life ($t_{1/2}$) determined for new LDPE (46.21 hr) was greater than aged LDPE (33.00 h). At pH 7.8, Pb surface loading increased sharply for both new and aged LDPE during the first 12 h exposure period, and gradually approached equilibrium. Pb surface loading was quantified for LDPE pellets aged from 30 min to 10 h, after 48 h exposure to Pb aqueous solution. Pb surface loading increased linearly (r^2=0.966) with increased aging duration up to 7.5 h, then it became constant (**Figure 3-3b**). Polar functional groups on the aged LDPE (>C=O, >C-O, >C-O-C<) could be responsible for greater Pb surface loading compared to new LDPE. Other researchers have reported detecting greater Pb mass loading on aged polyethylene pellets compared to the new polyethylene pellets[37,38].

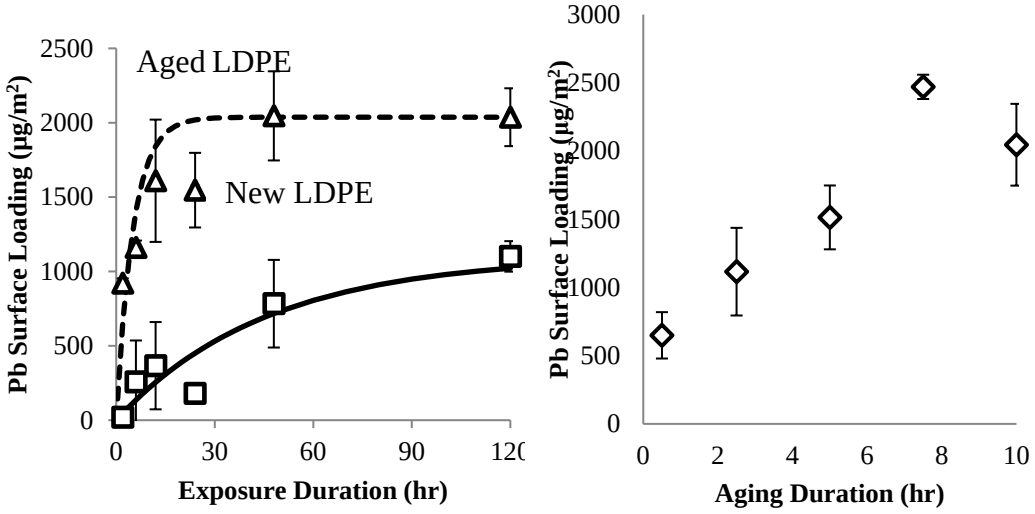

Figure 3-3 (a) Pb surface loading on new and aged LDPE over the time at pH 7.8, (b) Influence of LDPE aging duration on Pb surface loading, Error bars are standard deviation for three replicates

3.4.4.2.2 Effect of Water pH on Pb Precipitation Over the Time

As **Figure 3-4** shows less Pb surface loading was found on both new and aged LDPE at pH 11 compared to pH 7.8. Despite Pb surface loading great changes due to the pH increase from 7.8 to 11 much lesser changes occurred in Pb speciation. At pH 7.8, 93.7% of the lead was present as $[Pb(OH)_2]_{(s)}$ and at pH 11, the lead was 100% $[Pb(OH)_2]_{(s)}$ (**Figure C6**). Pb surface loading on both new and aged LDPE was time dependent. While the pH 11 condition was outside recommended U.S. drinking water pH standard (6.0 to 8.5), in some cases long water stagnation periods in iron pipes cause pH increase up two units and approach pH 11[60,61].

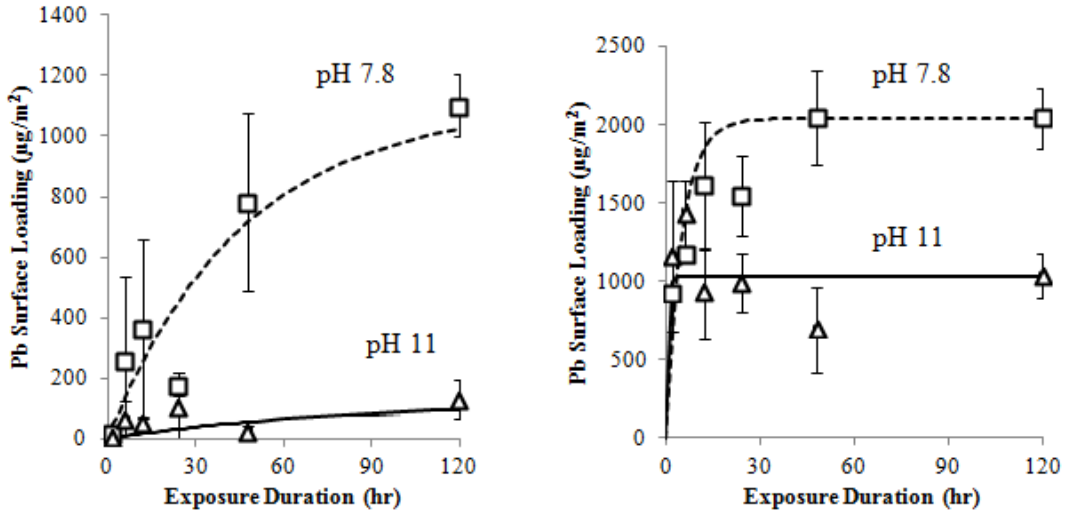

(a) (b)

Figure 3-4 Pb surface loading on (a) new and (b) aged LDPE over the time at pH 7.8 and 11 (Mean ± std)

The new LDPE first-order mass transfer constant was 2-fold greater at pH 7.8 compare to pH 11 (**Table 3-2**). In contrast, *K* for aged LDPE was more than 8-fold greater at the high pH condition. For aged LDPE the half-life ($t_{1/2}$) was significantly less at pH 11 (24 min) compare to pH 7.8 (3.55 h). According to distribution ratio (*D*), Pb precipitates demonstrated a greater affinity toward aged LDPE compared to new LDPE. At the high pH condition, the distribution ratio (*D*) was 50-fold lower than at pH 7.8 for new LDPE, and it was 19-fold lower for aged LDPE.

Table 3-2 The behavior of Pb precipitation over the time on new and aged LDPE at pH 7.8 and 11

LDPE	Water pH	Pseudo first order model			Distribution Ratio (mm)
		K (h^{-1})	R^2	t ½ (h)	
New	7.8	0.022	0.999	31.65	69.26
	11	0.011	0.980	60.27	1.37
Aged	7.8	0.195	0.996	3.55	251.50
	11	1.700	0.999	0.40	12.97

Pb surface loading was significantly reduced due to the increased pH after 48 h for new LDPE and after 24 h for aged LDPE. As mentioned earlier, a great amount of organic carbon was released from aged LDPE due to the exposure at pH 11. The influence of these organic chemicals on aged LDPE Pb surface loading was examined. The results showed that the presence of organic material leached by aged LDPE pellets reduced aged LDPE Pb surface loading (**Figure C8**).

3.4.4.3 Influence of Pb Concentration on its Precipitation on LDPE

At all Pb concentrations, greater Pb surface loading was detected for aged LDPE compare to new LDPE. Pb mass on polymer surface was graphed versus the residual Pb mass remaining in aqueous solution, where the pellet surface area was 1108 mm^2 and aqueous solution volume was 13 mL (**Figure 3-5**). Less Pb surface loading at higher pH, could not be related to the Pb species very small change due to pH changes. The high organic material release for aged LDPE at pH 11 may have caused lower Pb surface loading. No study was found that has investigated the influence of organic materials, released from plastics, on Pb adsorption. In other studies, the the type of organic material present, their concentration, contact time, and metal concentration can influence Pb adsorption to soil[62].

As described earlier with increased TOC level, less Pb surface loading was found for aged LDPE (**Figure C8**). By applying a linear model for the results, the slope was defined as the precipitation mass rate. This mass rate was greater for aged LDPE at both pH values (at pH 7.8 as 4.58 and at pH 11 as 0.54) compared to mass rates observed for new LDPE (at pH 7.8 as 0.05 and at pH 11 as 0.33). For aged LDPE, the precipitation mass rate reduced with increased water pH from 7.8 to 11. However, with increased pH from 7.8 to 11, the mass rate increased for new LDPE pellets. Increased Pb surface loading with increased aging duration supports this hypothesis (**Figure 3-3b**).

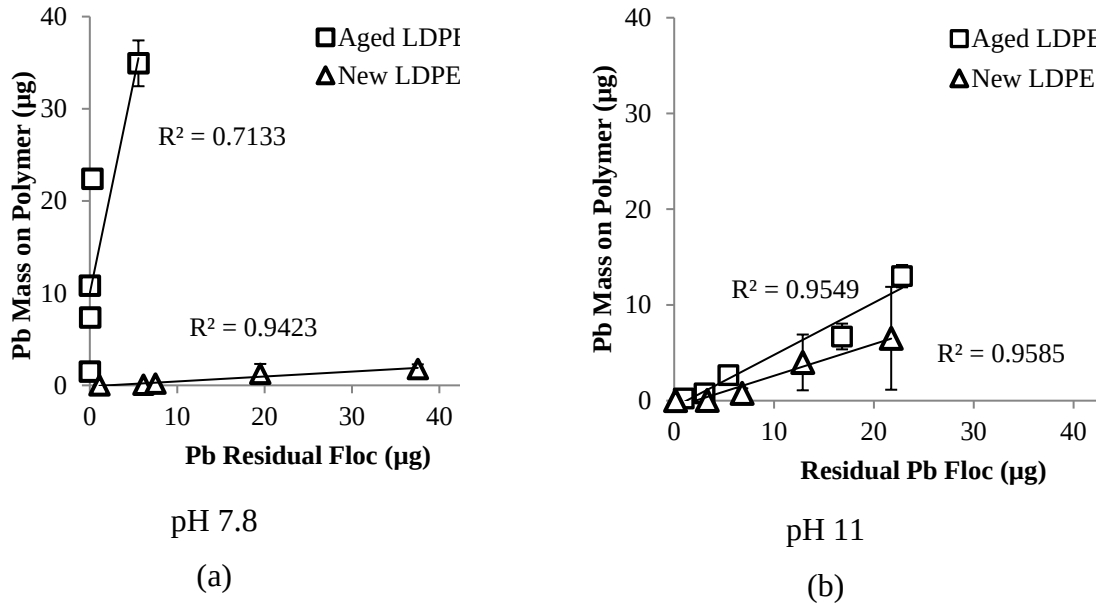

Figure 3-5 Pb mass loading on LDPE versus Pb residual mass in the solution at pH 7.8 and 11(error bars are standard deviations for three replicates)

The surface of both new and aged LDPE pellets served as nucleation sites for Pb precipitation and crystal growth. Different Pb mass loadings for new and aged LDPE could be due to the different number of nucleation sites present on each polymer. The aged LDPE oxidized surface provided more nucleation sites for Pb precipitation compared to new LDPE. For aged LDPE at pH 11, a high mass of organic compounds were released into the contact water. It is possible these organic compounds decreased Pb surface loading by (1) making non-adsorbable complexes with Pb, and (2) competed with Pb for available surface sites[63]. Both phenomena could have resulted in less Pb precipitated on the polymer surface. The influence of water pH on Pb adsorption with the plastic pellets was studied by others as well.

3.4.5 Polymer Surface Chemistry Analysis Using XPS

XPS analysis was conducted on LDPE films to understand the influence of polymer aging on Pb precipitation. As **Figure 3-6** shows the C1s peak at 284.8 eV[64,65] is the dominant feature associated with the LDPE structure. A weak O1s peak at 531.9 eV[66] was observed for new LDPE and its intensity was greater for aged LDPE indicating chemical oxidation had occurred. The weak O1s peak for the new LDPE sample was

probably due to intrinsic surface oxidation. All new, 5 h and 10 h aged LDPE samples were exposed to Pb aqueous solution (5,000 µg/L), but Pb 4d and 4f peaks in survey spectra were only detectable on aged LDPE samples. This finding indicates a persistent Pb residue resulting from LDPE aging/oxidation.

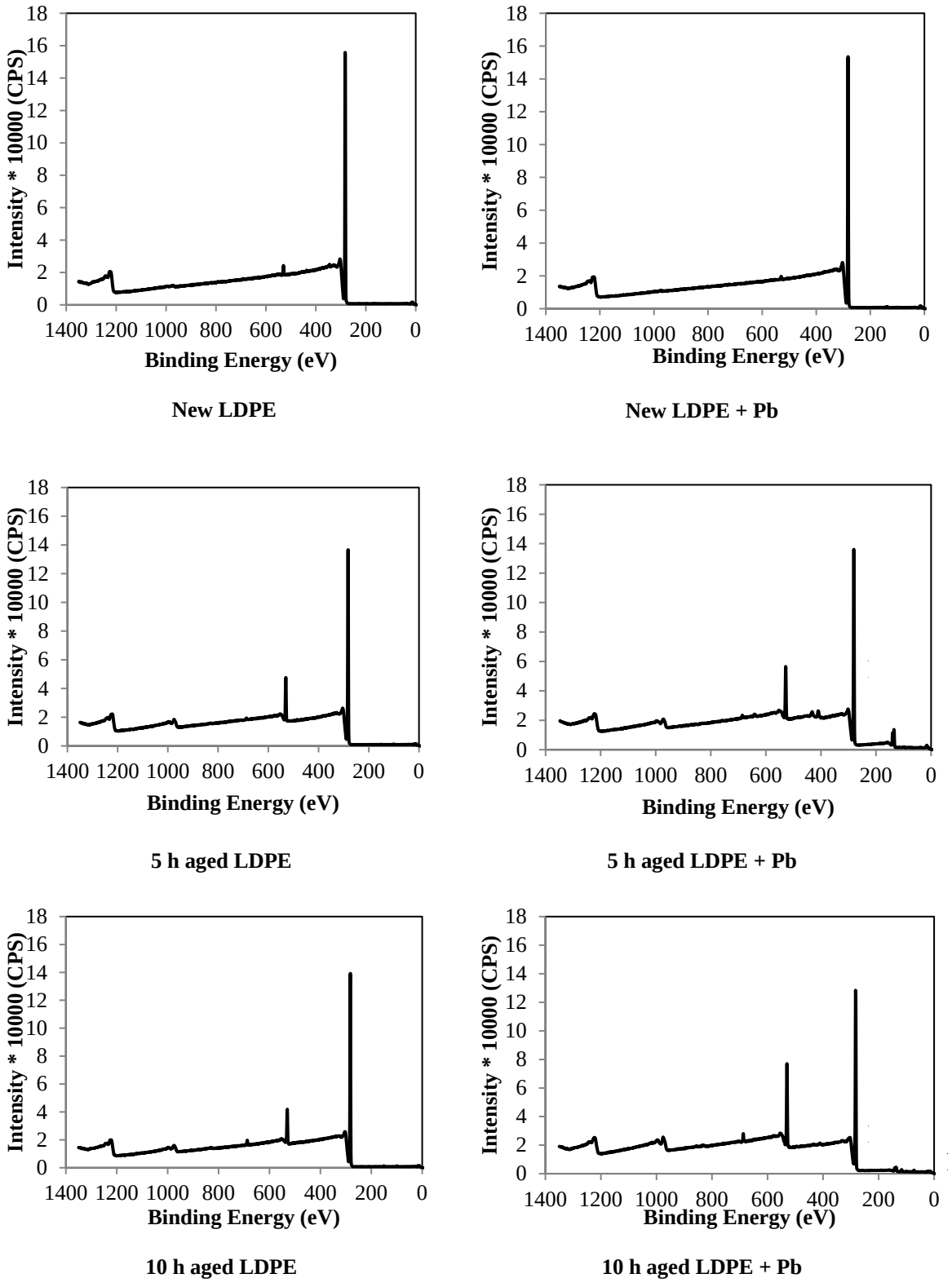

Figure 3-6 XPS survey spectra for LDPE samples before and after exposure to Pb

The atomic % of C, O, Pb were determined based on the peak area from XPS analysis (**Table 3-3)**. The measurement uncertainty was estimated to be 0.1%. Aged LDPE samples had a greater percentage of oxygen present on their surface than new LDPE (**Table 3-3**). As ICP-MS results show, a greater amount of Pb was deposited onto aged LDPE compared to the new LDPE.

Table 3-3 Elemental atomic concentration % in sample of LDPE

Sample Name	**C 1s**				**O 1s**	**Pb 4f**
	C-C	**C-O**	**C=O**	**O-C=O**		
New LDPE	98.3				1.7	0.0
	98.4	1.6	0.0	0.0		
New LDPE + Pb	99.3				0.7	0.0
	99.1	0.9	0.0	0.0		
5 h aged LDPE	90.6				9.4	0.0
	91.5	3.7	2.7	2.1		
5 h aged LDPE + Pb	89.0				10.6	0.5
	91.6	3.4	3.0	2.0		
10 h aged LDPE	92.1				7.9	0.0
	92.2	4.1	2.0	1.7		
10 h aged LDPE+ Pb	83.8				16.0	0.1
	86.1	4.9	4.1	4.9		

To verify that the observed oxygen percentage increase for aged samples was due to polymer oxidation, high-resolution C1s spectra was measured. Carbon atom chemical state was also studied. Analysis of C1s spectra for aged LDPE samples revealed four different peaks at 284.7 eV (>C-C<), 286.4 eV (>C–O), 287.7 eV (>C=O) and 289.2 eV (>O-C=O) (**Table 3-3, Figure C9**) similar to the peaks found by Briggs et al., (2003) who analyzed oxidized LDPE[67]. No differences were found between the surface oxidation of 5 h and 10 h aged LDPE. As the 10 hour LDPE may have experienced additional aging relative to the 5 hour sample, but the oxidation region measured by XPS was saturated after 5 hour aging. ATR-FTIR analysis revealed greater degree of oxidation for 10 h aged LDPE film compare to 5 h aged LDPE film (**Figure C10**). ATR-FTIR analysis depth is around 0.5 to 5μm however, XPS is only sensitive to the outermost 8 to 10 nm of material.

There was no change in the carbon envelop for new LDPE before and after the Pb solution treatment. From this result, the Pb solution treatment did not itself impact the LDPE. XPS analysis, coupled with the ATR FTIR results, indicates that deposited Pb is

likely electrostatically bound to the oxidized carbon. The doublets characteristic of lead derived from spin-orbit split appeared respectively, at 139 eV (assigned to Pb 4f7/2) and at 143.9 eV (assigned to Pb 4f5/2) after exposure of 5 h aged LDPE sample to Pb aqueous solution (**Figure C10**). The peak observed at 139 eV agrees with the 138.6 eV value reported for $Pb(OH)_2$[68,69]. The binding energies of C and O were also not changed by Pb(II) adsorption. This indicated no significant electron transfer occurred between unoxidized LDPE and Pb(II). As XPS and ATR-FTIR results demonstrated, the aging process clearly oxidized the LDPE, creating electrostatic dipoles at the surface. Results from this study indicate that Pb precipitation on LDPE was due to the electrostatic interaction between polymer charged surface and $Pb(OH)_2$. Aged LDPE with variety of polar groups (>C-O<, >C=O, >COO) on its surface provided more nucleation sites for $Pb(OH)_2$ deposition than new LDPE.

3.5 Conclusion

The influence of polymer aging, water chemistry and Pb initial concentration on Pb deposition onto LDPE was examined. Pb precipitation over 5 day exposure period for new and aged LDPE was determined at pH 7.8 and 11. The type and amount of Pb species and carbon functional groups present on new and aged LDPE surface were determined through XPS. Both ATR-FTIR and XPS analysis of aged LDPE showed that several oxidized carbon functional groups formed on the polymer surface. Greater Pb surface loading was found for aged LDPE compare to the new LDPE at both water pH conditions. Pb surface loading increased linearly (r^2=0.966) with longer aging duration, up to 7.5 h. Polar functional groups formed due to the aging could be responsible for greater Pb surface loading on aged LDPE compared to the new LDPE. Modeling Pb transfer from solution to LDPE surface with pseudo-first-order equation showed a greater rate of Pb deposition onto aged LDPE compared to new LDPE. Less Pb surface loading on both new and aged LDPE was found after 5 days at pH 11 compared to pH 7.8. The Pb precipitation rate was greater for aged LDPE compared to new LDPE at both water pH conditions. XPS analysis detected Pb only on aged polymer surface. Pb precipitation on LDPE was due to the electrostatic interaction between polymer charged surface and $Pb(OH)_2$. XPS analysis revealed several oxidized functional groups were formed on aged

LDPE, these functional groups likely provided better nucleation sites for $Pb(OH)_2$ deposition compared to new LDPE.

3.6 Acknowledgement

The authors thank the National Science Foundation (NSF) for funding this research under grant CBET-1228615. The authors thank Dr. Chloe De Perre for assisting in ICP-MS analysis, Dr. Rosa Diaz for assisting in FE-SEM imaging, Jessica Yaputri and Xianzhen Li for helping with metal adsorption and organic release experiments. Additional thanks is extended to the surface science analysis staff at Birck Nanotechnology center, Dr. Stephen Beaudoin, and Dr. Lia Stanciu at Purdue University.

3.7 References

1. De Burbure C, Buchet JP, Leroyer A, et al. Renal and neurologic effects of cadmium, lead, mercury, and arsenic in children: Evidence of early effects and multiple interactions at environmental exposure levels. *Environ Health Perspect*. 2006,114(4), 584-590.

2. Edwards M, Triantafyllidou S, Best D. Elevated blood lead in young children due to lead-contaminated drinking water: Washington, DC, 2001-2004. *Environ Sci Technol*. 2009, 43(5), 1618-1623.

3. Jain NB, Laden F, Guller U, Shankar A, Kasani S, Garshick E. Relation between blood lead levels and childhood anemia in India. *Am J Epidemiol*. 2005,161(10), 968-973.

4. Ngueta G, Abdous B, Tardif R, St-Laurent J, Levallois P. Use of a cumulative exposure index to estimate the impact of tap water lead concentration on blood lead levels in 1- to 5-year-old children (Montral, Canada). *Environ Health Perspect*. 2016, 124(3), 388-395.

5. Pieper KJ, Tang M, Edwards MA. Flint Water Crisis Caused By Interrupted Corrosion Control: Investigating "Ground Zero" Home. *Environ Sci Technol*. 2017, 51(4), 2007-2014.

6. Hanna-Attisha M, LaChance J, Sadler RC, Schnepp AC. Elevated blood lead levels in children associated with the flint drinking water crisis: A spatial analysis of risk and public health response. *Am J Public Health*. 2016, 106(2), 283-290.

7. Gulson BL, James M, Giblin AM, Sheehan A, Mitchell P. Maintenance of elevated lead levels in drinking water from occasional use and potential impact on blood leads in children. *Sci Total Environ*. 1997, 205(2-3), 271-275.

8. Jean Brown M, Raymond J, Homa D, Kennedy C, Sinks T. Association between children's blood lead levels, lead service lines, and water disinfection, Washington, DC, 1998-2006. *Environ Res*. 2011, 111(1), 67-74.

9. Triantafyllidou S, Raetz M, Parks J, Edwards MA. Understanding how brass ball valves passing certification testing can cause elevated lead in water when installed. *Water Res*. 2012, 46(10), 3240-3250.

10. Wang Y, Jing H, Mehta V, Welter GJ, Giammar DE. Impact of galvanic corrosion on lead release from aged lead service lines. *Water Research*. 2012, 46(16), 5049-5060.

11. Cartier C, Arnold RB, Triantafyllidou S, Prévost M, Edwards M. Effect of Flow Rate and Lead/Copper Pipe Sequence on Lead Release from Service Lines. *Water Res*. 2012, 46(13), 4142-4152.

12. Report to the President Science and Technology to Ensure the Safety of the Nation ' s Drinking Water. President's Council of Advisors on Science and Technology (PCAST), Dec 2016, Washington DC.

13. Imran S, Dietz JD, Mutoti G, Xiao W, Taylor JS, Desai V. Optimizing source water blends for corrosion and residual control in distribution systems. *Journal of American Water Work Association*. 2006, 98(5), 107-115.

14. Edwards M, Dudi A. Role of chlorine and chloramine in corrosion of lead-bearing plumbing materials. *Journal of American Water Work Association*. 2004, 96(10), 69-81.

15. Maas RP, Patch SC, Christian AM, Coplan MJ. Effects of fluoridation and disinfection agent combinations on lead leaching from leaded-brass parts. *Neurotoxicology*. 2007, 28(5), 1023-1031.

16. Masters S, Parks J, Atassi A, Edwards MA. Distribution system water age can create premise plumbing corrosion hotspots. *Environ Monit Assess*. 2015, 187(9), 559.

17. Zhang Y, Edwards M a, Boardman GD, Marr LC. Dezincification and Brass Lead Leaching in Premise Plumbing Systems : Effects of Alloy , Physical Conditions and Water Chemistry Dezincification and Brass Lead Leaching in Premise Plumbing Systems : Effects of Alloy , Physical Conditions and Water Chemist. Virginia Polythechnique Institute and State University, Blacksburg, Virginia, 2009.

18. Xie Y, Wang Y, Singhal V, Giammar DE. Effects of pH and carbonate concentration on dissolution rates of the lead corrosion product PbO_2. *Environ Sci Technol*. 2010, 44(3), 1093-1099.

19. Triantafyllidou S, Le T, Gallagher D, Edwards M. Reduced risk estmation after remediation of lead (Pb) in drinking water at tw US school districts. *Sci Total Environ*. 2014, 466(467), 1011-1021.

20. Bryant SD. Lead-contaminated drinking waters in the public schools of Philadelphia. *J Toxicol Toxicol*. 2004,42(3), 287-294.

21. Lambrinidou Y, Triantafyllidou S, Edwards M. Failing our children: lead in U.S.

school drinking water. *New Solut*. 2010, 20(1), 25-47.

22. Sathyanarayana S, Beaudet N, Omri K, Karr C. Predicting Children's Blood Lead Levels From Exposure to School Drinking Water in Seattle, Washington, USA. *Ambul Pediatr*. 2006, 6(5), 288-292.

23. Lee J, Kleczyk E, Bosch DJ, Dietrich a M, Lohani VK, Loganathan G V. Homeowners' decision-making in a premise plumbing failure-prone area. *Journal of American Water Work Association.* 2013, 105(5), 53-54.

24. Wong MK, Gan LM, Koh LL. Temperature Effects on the Leaching from Unplasticized Poly (Vinyl Chloride) Pipes. *Water Res*. 1988, 22(11), 1399-1403.

25. Ranney TA, Parker LV. Comparison of Fiberglass and Other Polymeric Well Casings, Part III. Sorption and Leaching of Trace-Level Metals. *Gr Water Monit Remediat*. 1998, 18(3), 127-133.

26. Parker LV, Hewitt AD, Jenkins TF. Influence of Casing Materials on Trace-Level Chemicals in Well Water. *Gr Water Monit Remediat*. 1990, 10(2), 146-156.

27. Hewitt AD. Potential of Common Well Casing Materials to Influence Aqueous Metal Concentrations. *Gr Water Monit Remediat*. 1992, 12(2), 131-136.

28. Ginige MP, Garbin S, Wylie J, Krishna KCB. Effectiveness of Devices to Monitor Biofouling and Metals Deposition on Plumbing Materials Exposed to a Full-Scale Drinking Water Distribution System. *PLoS One*. 2017, 12(1):e0169140.

29. Cerrato JM, Reyes LP, Alvarado CN, Dietrich AM. Effect of PVC and iron materials on Mn(II) deposition in drinking water distribution systems. *Water Res*. 2006, 40(14), 2720-2726.

30. Lytle D, Sorg TJ, Frietch C. Accumulation of arsenic in drinking water distribution systems. *Environ Sci Technol*. 2004, 38(20), 5365-5372.

31. Friedman, M. J., Hill, A. S., Reiber, S. H., Valentine, R. L., Larsen, G., Young, A., Korshin, G. V., Peng, C. Y. *Assessment of Inorganics Accumulation in Drinking Water System Scales and Sediments WRF #3118.* 2010. Water Research Foundation. Denver, CO USA.

32. Campbell, C. E., Whelton, A. J., Polera, R., Dietrich, A. M. (2008). The Characteristics and Chemical Performance of Polyethylene and Poly (1-Butene) Pipes Removed from a Water Distribution System. *VWRRC Special Report SR43-2008,* 1-13. Blacksburg, VA USA.

33. Castillo Montes J, Cadoux D, Creus J, Touzain S, Gaudichet-Maurin E, Correc O. Ageing of polyethylene at raised temperature in contact with chlorinated sanitary hot water. Part I - Chemical aspects. *Polym Degrad Stab*. 2012, 97(2), 149-157.

34. Devilliers C, Fayolle B, Laiarinandrasana L, Oberti S, Gaudichet-Maurin E. Kinetics of chlorine-induced polyethylene degradation in water pipes. *Polym Degrad Stab*. 2011, 96(7), 1361-1368.

35. Whelton AJ, Dietrich AM, Gallagher DL. Impact of Chlorinated Water Exposure on Contaminant Transport and Surface and Bulk Properties of High-Density Polyethylene and Cross-Linked Polyethylene Potable Water Pipes. *J Environ Eng*. 2011, 137, 559-568.

36. Whelton AJ, Dietrich AM. Critical considerations for the accelerated ageing of high-density polyethylene potable water materials. *Polym Degrad Stab*. 2009, 94(7), 1163-1175.

37. Holmes L, Turner A, Thompson RC. Adsorption of trace metals to plastic resin pellets in the marine environment. *Environ Pollut*. 2012, 160(1), 42-48.

38. Holmes L, Turner A, Thompson RC. Interactions between trace metals and plastic production pellets under estuarine conditions. *Mar Chem*. 2014, 167, 25-32.

39. Ashton K, Holmes L, Turner A. Association of metals with plastic production pellets in the marine environment. *Mar Pollut Bull*. 2010, 60(11), 2050-2055.

40. Cobelo-Garcia A, Turner A, Millward GE, Couceiro F. Behaviour of palladium(II), platinum(IV), and rhodium(III) in artificial and natural waters: Influence of reactor surface and geochemistry on metal recovery. *Anal Chim Acta*. 2007, 585(2), 202-210.

41. Fischer AC, Kroon JJ, Verburg TG, Teunissen T, Wolterbeek HT. On the relevance of iron adsorption to container materials in small-volume experiments on iron marine chemistry: 55Fe-aided assessment of capacity, affinity and kinetics. *Mar Chem*. 2007, 107(4), 533-546.

42. Giusti L, Taylor JH, Davison W, Hewitt CN. Artefacts in sorption experiments with trace metals. *Sci Total Environ*. 1994, 152(3), 227-238.

43. Brocca D, Arvin E, Mosbæk H. Identification of organic compounds migrating from polyethylene pipelines into drinking water. *Water Res*. 2002, 36(15), 3675-3680.
44. Ollick, A M., Al-Amir AM. Weathering Effects on Mechanical Properties of Low Density Polyethylene (LDPE) and High Density Polyethylene (HDPE) Pipes Used in Irrigation Networks. *Alexandria Eng J*. 2003, 42(6), 659-667.
45. Blatchley E, Weng S, Afifi MZ, Chiu H, Reichlin DB. Ozone and UV_{254} Radiation for Municipal Wastewater Disinfection. *Water Environ Res*. 2012, 84(11), 2017-27.
46. Barbeş L, Rădulescu C, Stihi C. ATR-FTIR spectrometry characterisation of polymeric materials. *Rom Reports Phys*. 2014, 66(3),765-777.
47. Corrales T, Catalina F, Peinado C, Allen NS, Fontan E. Photooxidative and thermal degradation of polyethylenes: Interrelationship by chemiluminescence, thermal gravimetric analysis and FTIR data. *J Photochem Photobiol A Chem*. 2002, 147(3), 213-224.
48. Ojeda T, Freitas A, Birck K, et al. Degradability of linear polyolefins under natural weathering. *Polym Degrad Stab*. 2011, 96(4), 703-707.
49. Yousif E, Haddad R. Photodegradation and photostabilization of polymers, especially polystyrene: review. *Springerplus*. 2013, 2(1), 398.
50. Popov AA, Blinov NN, Krisyuk BE, Karpova SG, Peverov AN, Zaikov GY. Oxidative Degradation of Polymers Under Load. Ozone-Oxygen Action on Oriented Polyethylene. *Polym Sci*. 1982, 23(7), 1666-1674.
51. USEPA. *Total Organic Carbon in Water EPA Method 415.1*. Vol 1. 1999.
52. Frank A, Pinter G, Lang RW. Prediction of the remaining lifetime of polyethylene pipes after up to 30 years in use. *Polym Test*. 2009, 28(7), 737-745.
53. Viebke J, Elble E, Ifwarson M, Gedde UW. Degradation of unstabilized medium-density polyethylene pipes in hot-water applications. *Polym Eng Sci*. 1994, 34(17), 1354-1361.
54. Holmes-Farley SR, Bain D, Whitesides GM. Wetting of Functionalized Polyethylene Film Having Ionizable Organic Acids and Bases at the Polymer-Water fnterface: Relations between Functional Group Polarity, Extent of lonization, and Contact Angle with Waterl. *Langmuir*. 1988, 4(10), 921-937.

55. Massey S, Adnot A, Rjeb A, Roy D. Action of water in the degradation of low-density polyethylene studied by X-ray photoelectron spectroscopy. *Express Polym Lett.* 2007, 1(8), 506-511.

56. Biedermann-Brem S, Grob K. Release of bisphenol A from polycarbonate baby bottles: Water hardness as the most relevant factor. *Eur Food Res Technol*. 2009, 228(5), 679-684.

57. Johnson EL. The effects of reaction temperature and hydrolysis on polyamic acids and polyimides. *J Appl Polym Sci*. 1971, 15(11), 2825-2839.

58. Lyu S, Untereker D. Degradability of polymers for implantable biomedical devices. *Int J Mol Sci*. 2009, 10(9), 4033-4065.

59. Colom X, Cañavate J, Suñol JJ, Pagès P, Saurina J, Carrasco F. Natural and artificial aging of polypropylene-polyethylene copolymers. *J Appl Polym Sci*. 2002, 87(10), 1685-1692.

60. Sarin P, Snoeyink VL, Bebee J, Jim KK, Beckett MA, Kriven WM, Clement JA. Iron release from corroded iron pipes in drinking water distribution systems: Effect of dissolved oxygen. *Water Res*. 2004, 38(5), 1259-1269.

61. McNeill LS, Edwards M. Phosphate inhibitors and red water in stagnant iron pipes. *J Environ Eng*. 2000, 126(12), 1096-1102.

62. Ahmed IM, Helal AA, El Aziz N A, Gamal R, Shaker NO, Helal AA. Influence of some organic ligands on the adsorption of lead by agricultural soil. *Arab J Chem*. 2015. In Press.

63. Lai CH, Chen CY. Removal of metal ions and humic acid from water by iron-coated filter media. *Chemosphere*. 2001, 44(5), 1177-1184.

64. Shofner ML, Khabashesku VN, Barrera E V. Processing and mechanical properties of fluorinated single-wall carbon nanotube-polyethylene composites. *Chem Mater*. 2006, 18(4), 906-913.

65. Wang Z, Hu K, Hu Y, Gui Z. Thermal degradation of flame-retarded polyethylene/magnesium hydroxide/poly(ethylene-co-propylene) elastomer composites. *Polym Int*. 2003, 52(6), 1016-1020.

66. Katsumata H, Tachi Y, Suzuki T, Kaneco S. Z-scheme photocatalytic hydrogen production over WO_3/g-C_3N_4 composite photocatalysts. *RSC Adv*. 2014, 4, 21405-21409.

67. Briggs D, Brewis DM, Dahm RH, Fletcher IW. Analysis of the surface chemistry of oxidized polyethylene: Comparison of XPS and ToF-SIMS. *Surf Interface Anal*. 2003, 35(2), 156-167.

68. Cant DJH, Syres KL, Lunt PJB, Radtke H, Treacy J, Thomas PJ, Lewis EA, Haigh SJ, O'Brien P, Schulte K, Bondino F, Magnano E, Flavell WR. Surface properties of nanocrystalline PbS films deposited at the water-oil interface: A study of atmospheric aging. *Langmuir*. 2015, 31(4), 1445-1453.

69. Koplík J, Kalina L, Másilko J, Šoukal F. The characterization of fixation of Ba, Pb, and Cu in alkali-activated fly ash/blast furnace slag matrix. *Materials*. 2016, 9(7), 533.

CHAPTER 4 : METAL ACCUMULATION IN REPRESENTATIVE PLASTIC DRINKING WATER PLUMBING SYSTEMS

Maryam Salehi, Xianzhen Li, Andrew J Whelton

4.1 Abstract

Metal abundance and scale morphology for crosslinked polyethylene (PEX) plastic pipes, and pipe oxidative condition was examined in a one year old residential plumbing system. Experiments were also conducted to determine if plastic pipe surfaces can influence scale formation. Within a single plumbing system, significant differences were found for scale morphology, the amount of metals present on pipe inner walls, and pipe aging condition. Metals found on the plastic pipes (Al, Ca, Co, Cu, Fe, Mg, Mn, Ni, Pb, Se, Zn) were corrosion products from water distribution and plumbing materials, and were present in the source water. Iron was the most abundant contaminant. Bench-scale experiments revealed that plastic served as a nucleation site for iron crystal growth and expedited crystal formation. Plastic plumbing pipes can adsorb metals that have health and aesthetic drinking water limits and additional work is needed to understand the conditions that affect metal accumulation and release.

KEYWORDS: PEX; Heavy Metal; Plastic Pipe; Drinking Water; Scale

4.2 Introduction

Heavy metals can pose acute and chronic human health risks and understanding their source and fate in drinking water infrastructure is important. Metals in tap water can originate from ground and surface waters (i.e., Ca, As, Co, Mn)[1], are added during water treatment (i.e., Al, Mn, Fe)[2], and can leach from water distribution, service lines, and building pipes, scales, and plumbing fixtures (i.e., Cr, Cu, Fe, Pb, Zn, Sn)[3,4]. Drinking water taste, color, and clarity problems can also be caused by Al, Cu, Fe, Mn, Ag, and Zn[5]. In recent years, very high heavy metal concentrations have been caused by water chemistry changes and backflow accidents: 7,500 µg Pb/L in Washington D.C.[6], 13,200 µg Pb/L in Flint Michigan[7,8], 41 mg Cu/L in Connecticut[9], 70 mg Cu/L in Wisconsin[10], and 50 mg Cr/L in Massachusetts[11]. For these incidents, it is unknown how much metal accumulated in plumbing infrastructure because no testing results were found.

In the U.S., plastic pipes such as high-density polyethylene (HDPE), polyvinylchloride (PVC), crosslinked polyethylene (PEX) and chlorinated polyvinylchloride (cPVC) are being installed to reduce tap water metal content[12-16]. PVC and cPVC pipes contain metal heat stabilizers and release microgram amounts of heavy metals[17]. No studies were found regarding heavy metals present in HDPE and PEX piping. A growing amount of evidence shows that plastic water distribution pipes can accumulate heavy metal scales (**Figure 4-1**)[2, 18-21], but no investigations were found that examined plastic building plumbing. In a survey of 15 U.S. water utilities, a wide range loadings of As (1,416 to 13,650 µg/g), Ca (4,455 to 57,790 µg/g), Fe (14,420 to 77,030 µg/g), and Pb (210 to 9,681 µg/g) were detected on PVC water distribution pipes[18]. High calcium (2,856 µg/g), Mg (2,435 µg/g), Mn (2,324 µg/g), and Zn (1,846 µg/g), were also detected on HDPE water mains[20]. A PVC water main from Honduras contained Mn at approximately 6 wt% of the pipe's scale[2]. Different metal loading reporting approaches inhibit a more detailed comparison of studies.

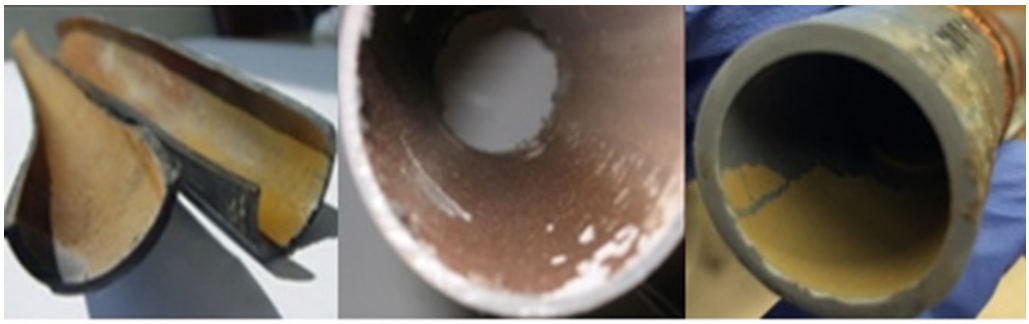

(a) (b) (c)

Figure 4-1 Scale visible on inner wall of drinking water (a) High-density polyethylene service line pipe, Florida, USA, (b) Polyvinylchloride water distribution pipe, Tegucigalpa, Honduras, and (c) Polybutylene service line pipe Alabama, USA. Image (b) represented by permission and courtesy of Dr. Jose M Cerrato, University of New Mexico.

Metal adsorption to plastics can be influenced by water chemistry, water flow, exposure duration, plastic type and the plastic's condition. PVC pipe scale formation was influenced by water hardness, water pressure, and water velocity for test water created using $CaCl_2$, $MgCl_2$, and $MgSO_4$[22]. Water chemistry variations have influenced As, Cd, Mn, Ca, Mg, Fe, and Ni accumulation and release from PVC and HDPE water distribution pipe scales[18, 21, 23]. Plastic pollution studies have also revealed metals can adsorb to plastics (**Table 4-1**). For example, as water pH increased, Cd, Co, Ni and Pb adsorption for polyethylene (type unreported) increased, but Cr adsorption decreased, and Cu adsorption was unaffected[24]. No information was found about metal loading on building plumbing plastic pipes.

Table 4-1 Metal adsorption onto various polymeric materials

Polymers Examined	Metals Studied	Application	Description of Results
PVC, PTFE, FEP, FRE	Cd, Cr, Cu, Pb, As	Well Casing	None of plastics tested adsorbed (Cr, As), but all adsorbed Cu, Cd, Pb[25]
PVC, PTFE	Cd, Cr, Cu, Pb, Fe, Ni	Well Casing	Less metals sorbed to PTFE compare to PVC[26]
PVC	Pb	Well Casing	Approximately 10% of the Pb in solution sorbed to the PVC surface[27]
PE (nr)	Zn, U, Co, R, Ag, I, Cs, Sb, Sr, Rb, Sc, In	Plastic Pollution	Lower pH prevented metal adsorption to plastic[28]
HDPE, PMMA, PTFE	Fe	Plastic Pollution	Fe^{+3} adsorbed onto a new HDPE polymer bottle while Fe^{+2} did not; 40% of iron remained in solution[29]
PE (nr)	Cr, Co, Ni, Cu, Zn, Cd, Pb	Plastic Pollution	Metal uptake on beached aged pellets was greater than on new pellets placed in an ocean [30]
PE(nr)	Fe, Al, Mn, Pb, Cu, Zn, Ag	Plastic Pollution	Accumulation was Fe>Al>Mn>Pb>Cu, Zn>Ag[31]
PET, HDPE, PVC, LDPE, PP	Al, Cd, Co, Cr, Mn, Fe, Ni, Pb, Zn)	Plastic Pollution	HDPE typically accumulated lesser metal loading than the other polymers tested. Equilibrium was reached for some polymers over the 12 month study period[32]
PE (nr)	Cd, Co, Cr, Cu, Ni, Pb	Plastic Pollution	In estuarine conditions metal adsorption was influenced by pH, salinity, and whether or not the plastic was "aged" [24]
Styrofoam	Hg	Plastic Pollution	Plastic debris were collected from beach and street, and mercury content was an order of magnitude greater than beach sands. Up to 3,863 ng g^{-1} Hg detected in the debris[33]
PS, PVC	Cu, Zn	Plastic Pollution	Adsorption of Cu was greater by PVC compare to PS under marine environment[34]
PE (nr)	Am	Labware	The amount of metal adsorbed increased by10-90% with increasing pH, Am^{+3}concentration, and decreased in the presence of $NaClO_4$, $NaNO_3$, and $CaCl_2$ salts[35]
LDPE, PP	Pd, Pt, Rh	Labware	LDPE had the greatest adsorption and PP demonstrated intermediate adsorption. Increasing water pH (>5) caused greater metal sorption to polymers[36]
PS	Pb, Cd	Plastic Modification	Polystyrene waste was sulfonated and converted into cation exchange resin. Cation exchange capacity was 50 and 130 mq/100 g for Pb and Cd respectively[37]

nr=not reported; PVC=Polyvinylchloride; PTFE=Polytetrafluoroethylene; FEP=Fluorinated Ethylene Polypropylene; FRE=Fiberglass Resin Forced Epoxy; PE=Polyethylene; HDPE=High density polyethylene; LDPE=Low density polyethylene, PS=Polystyrene

Studies were not found that compared the oxidative condition of plastic pipes within a single plumbing system, and prior studies show disinfectants can chemically attack PEX pipes[19, 38-40]. To protect PEX pipes from degradation, antioxidants are added during pipe manufacture. When antioxidants are depleted, the PEX pipe's oxidative resistance, or oxidation induction time (OIT), approaches zero, and polymer chain scission can be expedited[19, 37, 38, 41, 42]. For pressurized water pipes, chain scission can culminate in pipe mechanical failure. Due to chlorinated water exposure, >C=O and >C-O-C< bonds can form on the PEX pipe's surface[19, 38-40]. Surface oxidation may be important in understanding metal-plastic pipe interaction because a few studies have shown that oxidized polyethylene materials sorbed a greater amount of Cd, Co, Cr, Cu, Ni, and Pb compared to new material[24, 30]. To better understand metal deposition and scale formation on plastic plumbing pipes, the condition of the plastic pipes should be investigated.

This study was conducted to examine metal abundance on plastic plumbing pipes and to determine if plastic surfaces influence metal scale formation. The specific research objectives were to: (1) Quantify the surface and bulk oxidative condition of PEX pipes removed from a residential building after one year of use, (2) Determine metal loading on the pipes removed, and (3) Conduct bench-scale metal nucleation experiments to determine if a plastic surface can allow metals to adsorb and act as nucleation sites.

4.3 Experimental

In 2015, potable water pipes from a residential building (2,863 ft^2, four bedroom, two bath home) were removed for this study. Plastic pipe condition and metal loading on their inner pipe walls were investigated. Based on field results from the present study, a bench-scale experiment was conducted to better understand iron crystal formation on a polyethylene surface.

4.3.1 Characteristics of the Exhumed Plumbing System

An entire one year old residential PEX (type A) pipe plumbing system was removed in July 2015 (Indiana, USA). The residential building was initially constructed

in the 1920s and renovated in 2014. The building contained 0.75 in and 0.5 in diameter PEX pipe with a trunk-and-branch design (**Figure 4-2**).

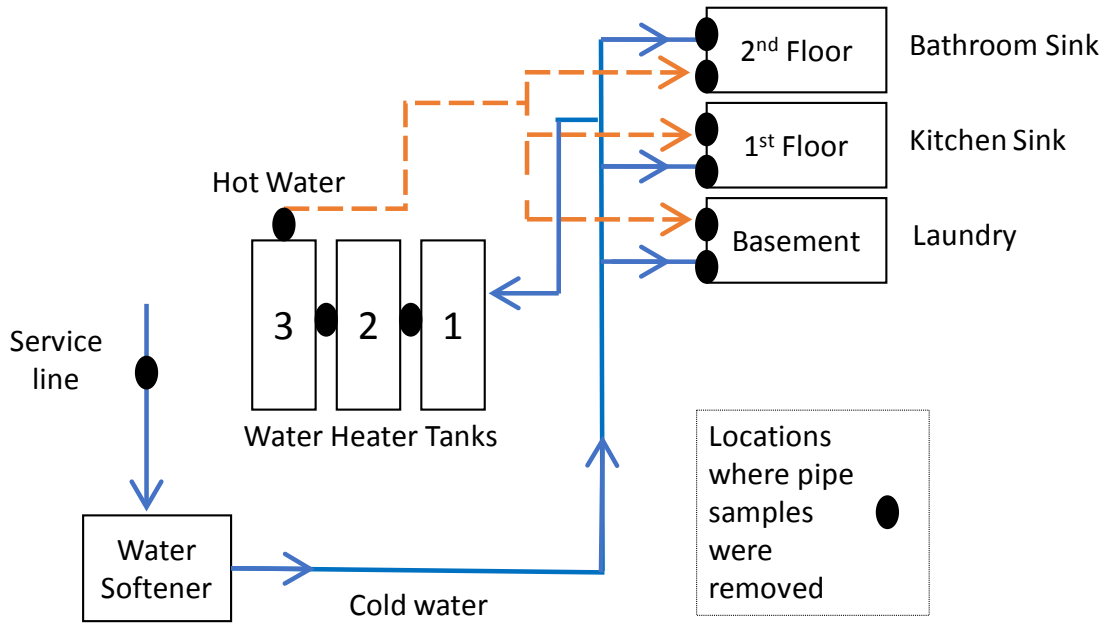

Figure 4-2 The schematic diagram of the plumbing system

All water entering the house, passed through a whole-house water softener (Whirlpool model WHES33 LE33) after the service line sampling point. Brass valves and fittings and also faucets were used in the plumbing system. A 5 ft section of corroded galvanized iron pipe conveyed hot water from the basement to 1st and 2nd floors. A Hersey 420 composite water meter with copper service line was connected to the PEX service line. Three 409 L glass lined water heaters were present in series with carbon steel heat exchangers. All heaters contained a magnesium coated anode rod. Pipes were collected from 10 different locations from both cold and hot water plumbing: the service line, pipes exiting three domestic water heater tanks in series (1, 2, 3), and pipes immediately before the basement laundry fixture (cold and hot), 1st floor kitchen sink fixture (cold and hot), and 2nd floor bathroom sink fixture (cold and hot). All pipes were capped and stored at 4 °C until characterization. After plumbing system removal, a new PEX-A plumbing system was installed (i.e., pipes, fixtures, and fittings). The water utility

that supplied drinking water to the building relied on a groundwater source, and provided its finished water chemical testing results (**Table 4-2**). Groundwater was chlorinated for oxidation, aerated, filtered, chlorinated for secondary disinfection, and a corrosion inhibitor was added before distribution (70% orthophosphate and 30% polyphosphate).

Table 4-2 Finished water quality reported by the local water treatment plant

Water Quality Parameter	**2016 Value**
pH	7.0 to 7.5
Alkalinity (mg/L as $CaCO_3$)	nr
Ca (mg/L)	104.0
Mg (mg/L)	34.0
Mn (mg/L)	0.02
P (mg/L)	nr
Zn (mg/L)	nd
Al (mg/L)	nd
Fe (mg/L)	0.05
Na (mg/L)	26.0
Pb (mg/L)	nd*
Cu (mg/L)	0.564*
As (mg/L)	0.004
Cr (µg/L)	nd to 0.14
Ni (mg/L)	0.005

* 90^{th} percentile results; nd = Not detected; nr = Not reported; Hardness is typically 248 to 416 mg/L as $CaCO_3$ per the utility drinking water 2016 Consumer Confidence Report

4.3.2 Characterization of Plastic Pipe Samples

For all pipes, the inner pipe wall was characterized to determine the surface morphology and elemental composition. Field emission scanning electron microscopy

(FESEM-EDX) was applied (FEI Nova Dual Beam, Oxford 80 EDX detector), and this technique has been used for other pipe scale investigations[20]. In the present study, pipe samples were coated with gold/palladium under a vacuum condition before FESEM analysis. The service line pipe was also selected for X-ray photoelectron spectroscopy (XPS) analysis to further characterize the elements on the pipe surface. XPS measurements were conducted using a Kratos Axis Ultra DLD spectrometer with monochromatic Al Kα radiation (hυ=1486.6 eV). A charge neutralizer was used to achieve better resolution. Binding energy value refers to the Fermi edge and the energy scale was calibrated using Au 4f7/2 at 84.0 eV and Cu 2p3/2 at 932.67 eV. A Shirley background was subtracted from each region before quantification.

The surface and bulk oxidative condition of each pipe was examined using Attenuated Total Reflectance Fourier Transform Infrared (ATR FTIR) spectroscopy and differential scanning calorimetry (DSC), respectively. A Perkin-Elmer Spectrum 100 FT-IR Spectrometer was used with 4,000 to 800 cm^{-1} and 2 cm^{-1} resolution. The pipe's bulk oxidative resistance, indicated by the material's OIT, was obtained with DSC. Samples (5 to 9 mg) were placed in open aluminum sample pans under a nitrogen flow of 50 mL/min. Cell temperature was ramped from 50 to 200 °C at 10 °C/min. The final temperature was held constant for 5 min, then the nitrogen flow was exchanged with pure oxygen. Sample oxidation time was determined by drawing a tangent line to the isothermal baseline and the steepest exothermal slope[43].

The total amount of element on each pipe surface was determined by acidifying the inner pipe wall followed by quantification using a Perkin Elmer Elan-DRCE II Inductively Coupled Plasma Mass Spectrometer (ICP-MS). Pipes were exposed to acid solution (2% HNO_3) for 48 hr at 23 °C. Acidified solutions were analyzed for the following elements and their detection limits were: Al (5 µg/L), As (25 µg/L), Be (0.5 µg/L), Ca (50 µg/L), Cd (5 µg/L), Co (5 µg/L), Ni (0.5 µg/L), Cr (5 µg/L), Cu (50 µg/L), Fe (5 µg/L), Mg (5 µg/L), Mn (1 µg/L), Na (5 µg/L), P (50 µg/L), Pb (1 µg/L), Se (2.5 µg/L), V (1 µg/L), Zn (1 µg/L). Calibration curves were created using six mixed standards (0.5 to 500 µg/L) and a blank. Water produced by an Ultrapure Milli-Q™ (18 MΩ*cm) system was used for all experiments, and tests were conducted in triplicate.

4.3.3 $FeSO_4$ Nucleation and Crystal Growth on a Polyethylene Surface

Because Fe was most abundant metal detected on pipes in the present study, bench-scale experiments were conducted to determine if a plastic surface can allow Fe to adsorb and act as a nucleation site. LDPE was chosen as the model plastic because it has been used in plastic pollution metal adsorption studies[32, 36], was previously used for European drinking water pipe manufacture[44], and domestic and commercial irrigation applications[45]. $FeSO_4.7H_2O$ and LDPE pellets were purchased from Sigma Aldrich.

Experiments were conducted by immersing LDPE pellets in supersaturated Fe solutions for 48 hr. Solutions were prepared by dissolving $FeSO_4.7H_2O$ in water at 60 °C followed by filtration using 0.2 µm PTFE syringe filters. Next, the clear solution was cooled to 4 °C by refrigeration. After cooling, filtered supersaturated solution (1.5 mL) at various concentrations was added to 2 mL glass vials, and four LDPE pellets were added to each vial. The time required for crystals to form and be visually observed in solution was recorded. At the conclusion of the experiment, crystals were analyzed using X-ray powder diffraction (XRPD). A Rigaku SmartLab (XRD 6000) diffractometer (The Woodlands, TX) with Bragg−Brentano mode was applied.

4.4 Result and Discussion

4.4.1 Pipe Visual and Oxidative Condition

Some, but not all, pipe sections were discolored. The service line pipe's inner wall discoloration was due to material deposited on the pipe surface. Coloring was removed after exposing the inner pipe wall to a 2% HNO_3 solution exposure for 48 hr (**Figure 4-3**). Yellow coloring was observed on the inner wall of each pipe exiting the three water heaters. Coloring was more distinct on the pipe end closer to the brass fitting. After 10 days of exposing the pipe surfaces to 2% HNO_3 solution, the discoloration remained. Coloring is hypothesized to be due to pipe oxidation similar to other studies[46].

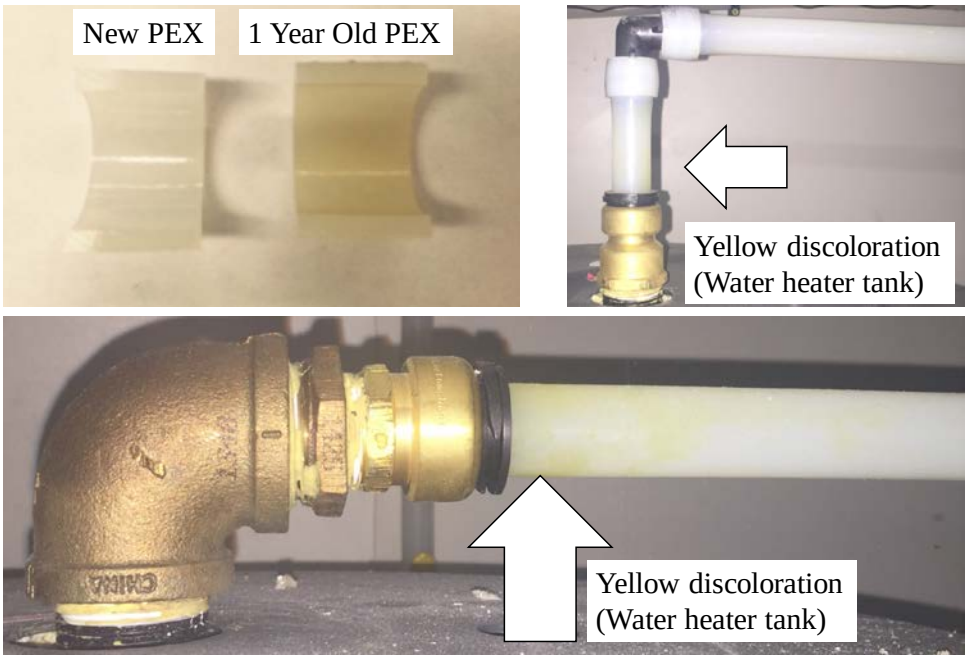

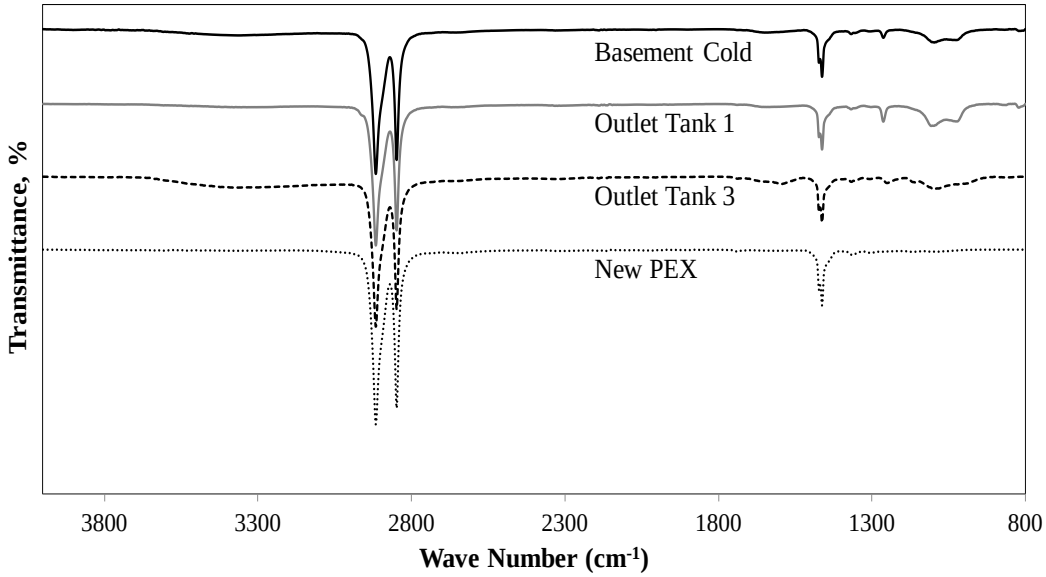

Figure 4-3 Images of (a) New and one year old PEX-a pipe service line and PEX pipes connected to brass fitting at the water heaters, and (b) ATR-FTIR spectra of new PEX-a (same brand) versus spectra for several exhumed PEX plumbing pipes. Outlet Tank 2 FTIR spectra was more similar to new PEX, than spectra for Outlet Tanks 1 and 3.

Pipes had a wide range of OIT values (antioxidant loadings), some pipes had oxidized surfaces, and no obvious trends were found based on in-building location or water temperature (**Table 4-3**). ATR-FTIR results showed that the surface of some,

plastic pipes was oxidized. An absorption peak at 1263 cm^{-1} (>C-O-C<) was observed for pipes exiting the water heater tank 1 and tank 3 and at the basement cold location. The >C-O-C< functional group can be caused by chlorinated water exposure[38]. No similar peak was detected for the pipe exiting water heater tank 2. The only pipes that contained >C-O< stretch peaks were located at the water heater tank 3 and basement cold location (1024 cm^{-1} and 1100 cm^{-1}) (**Figure 4-3**). This functional group has also been attributed to chlorinated water exposure[38]. Functional groups indicative of surface oxidation were not detected on any other pipes. OIT and surface chemistry differences across pipes could be due to varying degrees of chemical or microbiological attack[47], initial antioxidant loading[48], antioxidant loss due to fixture water usage patterns, variability in pH and disinfectant levels, and exposure temperature, and possibly oxidation caused by copper present on the plastic pipe surface[49-51] (**Table 4-3**). Because the new, unexposed PEX-A pipe initially installed in the building was not available, the pipe's oxidative condition at the time of installation could not be evaluated. Study results show that PEX pipe surface and bulk degradation, including discoloration, can occur during the first year of use, and the degradation was not consistent based on pipe location or water temperature (cold vs. hot water plumbing).

Table 4-3 Oxygen induction time (OIT) for plastic pipe samples

Location	**OIT (min)**		**Location**		**OIT (min)**
	Cold	**Hot**			
Service line	34 ± 5	-	Water Heater Tanks	Tank 1, 65 °F	22 ± 7
Basement	16 ± 6	14 ± 9		Tank 2, 85 °F	7 ± 1
1st Floor	27 ± 5	45 ± 6		Tank 3, 100 °F	51 ± 11
2nd Floor	20 ± 14	30 ± 11			

OIT values for new PEX-a pipes have ranged from 33.5 ± 3.9 min[40] to 34.3 ± 4.9 min (this study), oxidation induction time (OIT) is "a qualitative assessment of the level (or degree) of stabilization of the material tested"[43].

4.4.2 Metal Loading on Pipes at the Water Heaters in Series

Since building owners installed three water heaters in series, metal loading for the three pipes in this multi-heater system was examined. Plastic pipe inner walls were characterized to identify the role of the water heaters on pipe metal loading. As water temperature increased from the first to the third heater, pipe metal loading (i.e., Al, Cu, Fe, Mn) and scale morphology differed. A greater amount of metal was found on the pipe that exited the first water heater (43.2 mg/m^2) and the least amount of metal was detected on the pipe that exited the third water heater (3.4 mg/m^2) (**Figure 4-4a**). The magnesium coated water heater anode rod did not seem to influence metal loadings; Mg levels were highest exiting the first heater (3.9 mg/m^2) and lowest exiting the third heater (0.2 mg/m^2). Pipe wall coverage and deposit morphology differed between the water heaters. As Figure 4 shows, less pipe wall coverage but a greater number of spherical-like deposits were found for the third water heater pipe. Temperature and water flow may have influenced crystal structure formation, scale mass, and morphology[52-55].

(a)

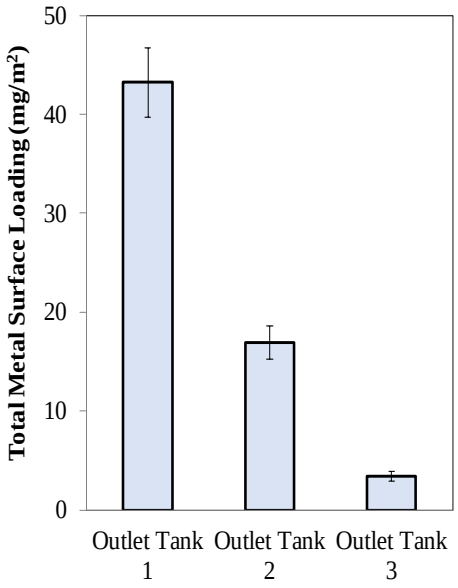

Element	Surface Loading			
	Outlet Tank 1	Outlet Tank 2	Outlet Tank 3	New PEX
Milligram Amounts of Metals (mg/m^2)				
Fe	26.5 ± 2.3	9.3 ± 1.1	0.3 ± 0.0	BDL
Mn	5.4 ± 0.3	1.9 ± 0.1	1.1 ± 0.3	BDL
Mg	3.9 ± 0.3	1.1 ± 0.1	0.2 ± 0.1	BDL
Na	2.1 ± 0.4	1.4 ± 0.2	1.0 ± 0.1	0.4 ± 0.2
Cu	1.7 ± 0.3	1.0 ± 0.1	BDL	BDL
Zn	1.3 ± 0.1	0.9 ± 0.1	1.2 ± 0.0	BDL
Al	1.1 ± 0.1	0.3 ± 0.0	0.1 ± 0.0	BDL
P	1.0 ± 0.2	0.5 ± 0.0	BDL	BDL
Ca	0.4 ± 0.1	BDL	BDL	BDL
Microgram Amounts of Metals (µg/m^2)				
Co	423.0 ± 35.3	550.4 ± 86.7	43.4 ± 2.4	BDL
Ni	173.0 ± 57.2	48.2 ± 27.0	7.8 ± 1.5	BDL
Pb	87.0 ± 20.4	59.3 ± 3.8	10.8 ± 8.5	BDL
Se	110.8 ± 27	34.1 ± 24.1	12.7 ± 17.9	10.7 ± 9.7

(b)

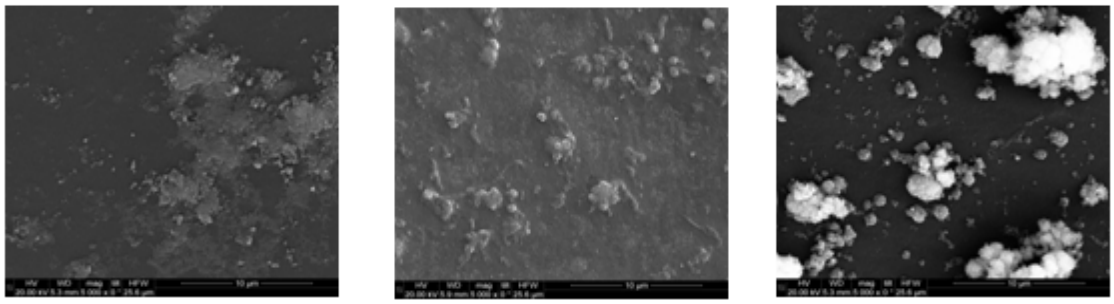

Figure 4-4 (a) Total metal surface loading and (b) FESEM images of outlet pipe samples at water heater tanks and their P and metals surface loadings, BDL: below detection limit

4.4.3 The Most Abundant Metals Found on the Pipes: Water Heaters Not Included

For pipes removed from the plumbing periphery, the greatest metal loading was found on the service line pipe (28.4 mg/m^2) (**Figure 4-5**). Very hard water entered the service line and this pipe had the greatest loading of Ca (1.6 ± 0.2 mg/m^2), Mg (0.6 ± 0.0 mg/m^2), Mn (5.9 ± 0.4 mg/m^2), as well as Pb (0.5 ± 0.0 mg/m^2). The whole-house water softener removed cations before water entered the rest of the plumbing. Ca (BDL to 0.55 mg/m^2), Mg (0.08 to 0.30 mg/m^2), and Mn (0.1 to 1.51 mg/m^2) loadings were found on pipes located after the water softener (i.e., basement, 1st floor, 2nd floor pipes). Pb was detected on pipe segments throughout the house (BDL to 0.4 mg/m^2). P is not a metal but was at greatest abundance on the service line (2.3 ± 0.1 mg/m^2) and BDL to 1.35 mg/m^2 throughout the house. P may be due to the water utility's corrosion inhibitor. Zn was not detected in water leaving the water treatment plant, but Zn plumbing pipe loading ranged from 0.37 to 2.0 mg/m^2.

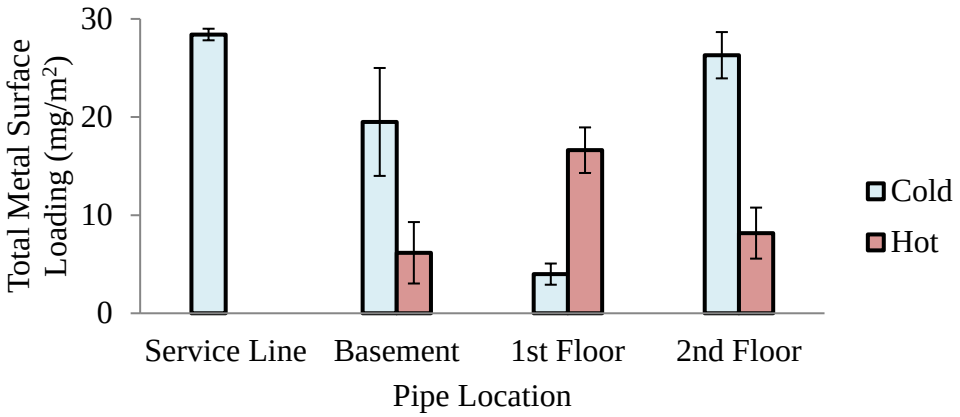

Figure 4-5 Total metal surface loading on cold and hot water pipe samples (mean and standard deviation shown for digestions of three replicate pipe segments). Service line did not have hot water, only cold water.

Metals detected on PEX hot water pipe surfaces on the 1st and 2nd floors could have originated from the 5 ft section of corroded galvanized iron pipe that conveyed hot water from the basement to 1st and 2nd floors. Galvanized iron pipes are coated with Zn,

contain Pb and Cd impurities, and can accumulate other metal species such as Pb[56, 57]. Excluding the three pipes that exited the water heaters, Fe was the most abundant metal found on the other pipes (5 of 7 pipes) and Na was the second most abundant metal detected (5 of 7 pipes) (**Figure 4-6**). The finding that Fe was the most abundant metal is important and Fe could have originated from multiple sources. While Fe concentration leaving the water treatment plant was only 0.05 mg/L, Fe loading on the pipe samples varied by orders of magnitude (0.67 to 19.69 mg/m^2). Water mains near the house were ductile iron and PVC. After the plumbing was replaced, building residents observed brown water through the house and the utility attributed this discolored water event to nearby water distribution system flushing. Additional work is needed to understand the contribution of metals on plumbing pipe surfaces due to routine drinking water use and poor water quality events caused by flushing.

4.4.4 Trace Metals Detected on Pipe Surfaces: Water Heater Not Included

Low quantities of other metals (µg/m^2) were also detected. Excluding pipes that exited each water heater tank, Se loading was greatest on the service line (98.1 ± 5.1 µg/m^2), and its loading was less throughout the house: BDL (cold) and 44.9 ± 40.7 µg/m^2 (hot) at 1st floor, 18.0 ± 12.7 µg/m^2 (cold) and 32.5 ± 35.0 µg/m^2 (hot) 2nd floor. Nickel was detected on the service line, basement hot, basement cold, and 1st floor hot water pipe at $\leq$ 15.6 ± 20.9 µg/m^2. The 1st floor hot water pipe (150.7 ± 19.1 µg/m^2) contained the greatest level of Co and its abundance varied through the building (BDL to 53.1 µg/m^2).

Differences between metal loading on plastic pipes could be due to a number of phenomena. Per the building owner, water usage frequency and water stagnation time varied at various locations throughout the house. Metal loadings may be influenced by water temperature, precipitation reactions, and the metal-plastic adsorption process. No study was found that examined the effect of temperature on heavy metal adsorption onto plastic pipe.

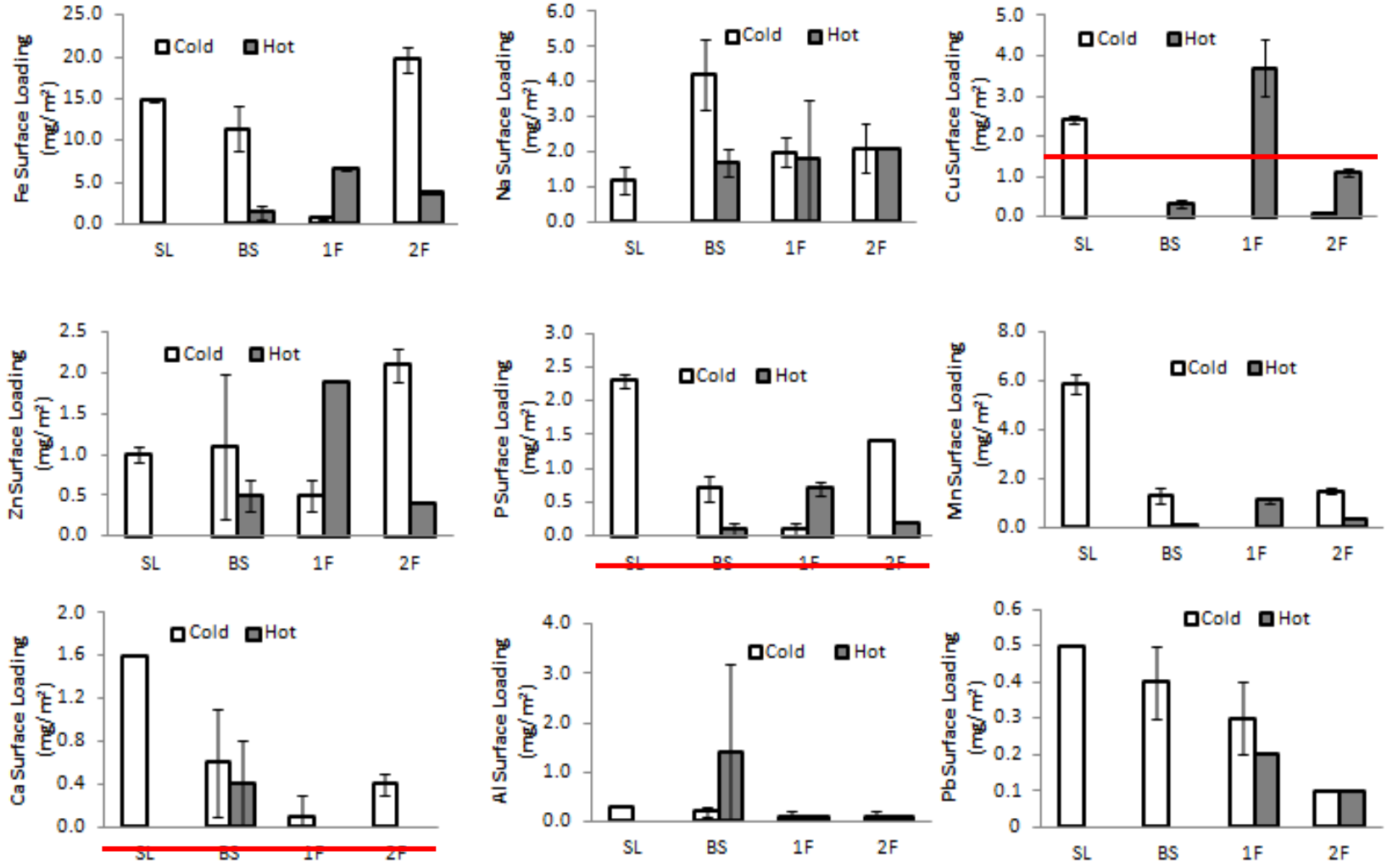

Figure 4-6 Metal and phosphorous surface loadings on pipe samples (SL: Service Line, BS: Basement, 1F: 1st Floor, 2F: 2nd Floor). Horizontal lines show the detection limits: Fe 0.03 mg/m^2, Na 0.03 mg/m^2, Cu 0.33 mg/m^2, Zn 0.01 mg/m^2, P 0.33 mg/m^2, Mn 0.01 mg/m^2, Ca 0.33 mg/m^2, Al 0.03 mg/m^2, Pb 0.01mg/m^2.

4.4.5 Plastic Pipe Scale Microstructural and Surface Elemental Analysis

4.4.5.1 Differences in Scale Coverage through the Plumbing

Scale coverage and element composition differed across pipe samples throughout the plumbing. For all pipes, C was the most abundant element detected and is due to the plastic pipe's organic nature. After C, Fe was the most frequently detected element for all pipes (0.2 wt% to 8.8 wt%) except for the basement and 1st floor cold water pipes where O abundance (7.6 wt%, 26.2 wt%) was greater than Fe (1.9 wt%, 7.2 wt%). Oxygen could be due to the presence of inorganic oxides[2]. Mn was only detected on the 1st floor and 2nd floor hot water pipes. Cl was present on the service line, and basement, 1st floor, 2nd floor hot water pipes. Na and Cu were found on 2nd floor cold water pipes, and Si was only detected on 1st floor cold water pipe. XPS analysis of the service line pipe revealed C, O, Si, Al, Ca, Cl, Fe, Mn, P and S. Differences between SEM-EDX and XPS results could be due to XPS's penetration depth (5 nm) compared to SEM-EDX (500 nm), and the difference in method detection limits. Prior PVC water distribution pipe characterization[2] using SEM-EDX revealed C, Cl, O, Pb and a very small percentage of other metals.

Pipe scale morphology differed throughout the plumbing (**Figure 4-7**). For hot water pipes, the scale area coverage was less than that of cold water pipes. Generally, most solids except $CaCO_3$ are more soluble in warmer water. $CaCO_3$ pipe scale morphology can be influenced by water temperature, water flow condition and water chemistry[54]. In a prior study, at temperature less than 30 °C and a supersaturated condition, compact calcite layers were formed on the inner pipe surface. However for greater than 30 °C, weak dendritic aragonite patterns formed on the pipe surface[52]. Additional work should be considered to understand differences between pipe scale formation and composition in plastic plumbing systems.

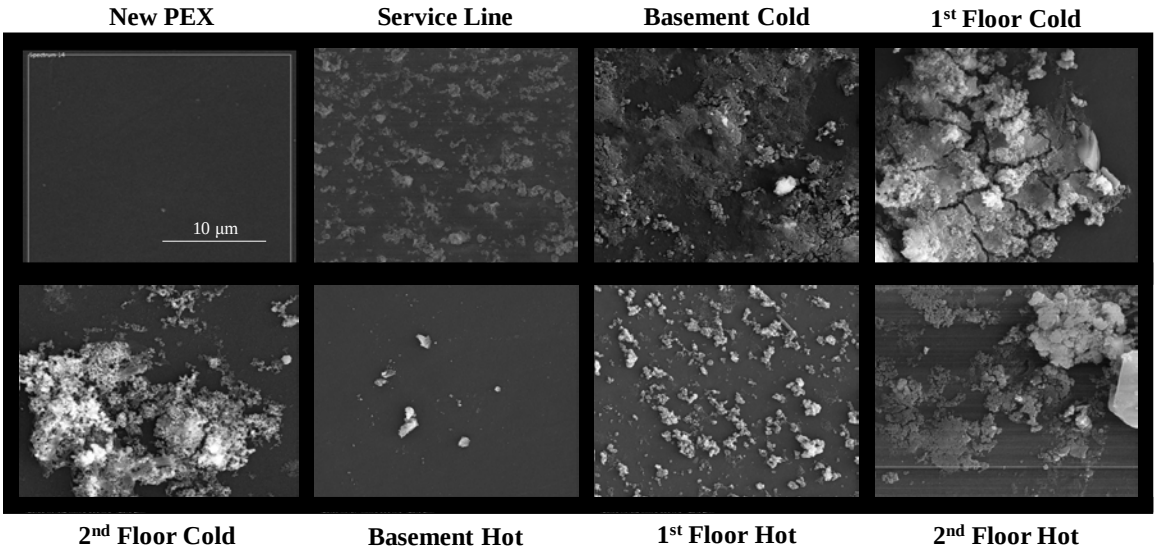

Figure 4-7 SEM scans of new PEX, service line and hot/cold water pipes at basement (Laundry Faucet), 1st Floor (Kitchen Sink), 2nd Floor (Lavatory Faucet)

4.4.6 $FeSO_4$ Nucleation and Crystal Growth on Polyethylene

Because field results showed that Fe accumulated on PEX pipes, the crystal nucleation process was studied. Bench-scale results showed that the polyethylene surface provided crystal nucleation sites, and expedited the crystal formation process (**Table 4-4, Figure 4-8**). XRPD analysis revealed that $FeSO_4$ crystals formed in solution in the absence of LDPE. Also found was that the crystals, Melanterite ($FeSO_4.7H_2O$), formed on LDPE pellets suspended in the solution. Crystal formation was a function of initial concentration, and crystals were not observed for the lowest concentration evaluated (400 mg/mL). A potential hypothesis is that the initial Fe species that adsorbed onto the LDPE surface acted as a nucleation site for Fe crystal growth. Studies have shown that metal atoms can associate with low energy polymer surfaces[58, 59]. These surfaces can include surface impurities, attractive local arrangements of polymer chains or polymer terminal groups. For example, $CaCO_3$ nucleation was facilitated through complexation between Ca^{2+} and carboxylic acid groups present on a grafted HDPE surface[60].

Table 4-4 Time required to visually recognize crystals in the samples

$FeSO_4.7H_2O$ Concentration (mg/mL)	**Time required for crystal formation**	
	With LDPE pellet	**No LDPE pellet**
400	No crystal after 48 hr	No Crystal after 48 hr
600	Crystal formed after 1 hr	No Crystal after 48 hr
700	Crystal formed < 1hr	No Crystal after 24 hr
760	Crystal formed < 1hr	5 hr < Crystal formed > 24 hr
800	Crystal formed < 1hr	Crystal formed < 1hr

Scale formation on plastic pipes has received limited study, but scale can increase the pipe surface's chlorine demand, facilitate bacterial regrowth and biofilm formation. Heavy metals adsorbed to scale can be problematic because they can be released into drinking water, cause discoloration, and result in conditions that exceed drinking water standards [4, 60-62]. To better understand and predict drinking water metal levels, the processes that control metal-plastic interactions should be further investigated.

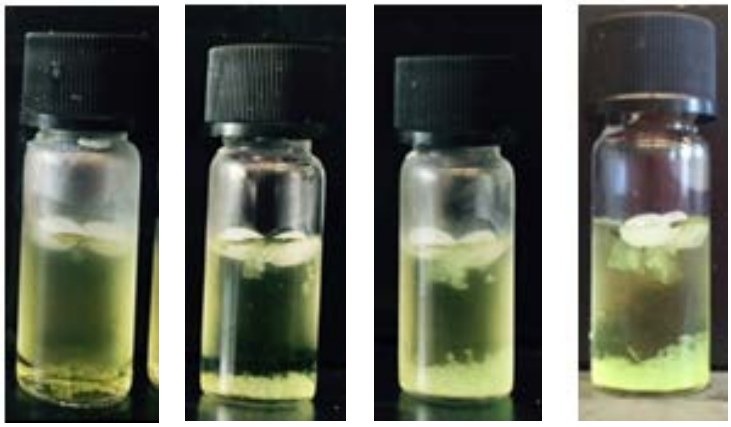

60 min 100 min 110 min 130 min

Figure 4-8 Crystal growth on new LDPE pellets over the time ($FeSO_4.7H_2O$ concentration 760 mg/mL)

4.5 Conclusion

Results of this study provide insight into metal scale formation for a one year old residential PEX plumbing system. Heavy metals that have health based, treatment technique based, and aesthetic drinking water standards such as Cu, Fe, Mn, Pb, and Zn deposited onto the plastic pipes. Iron was the most abundant contaminant detected on pipe surfaces. Metal loadings (mass/surface area) varied across in-building locations, sometimes by metal type and orders of magnitude. Detection metal compounds on residential plumbing pipe implies drinking water provided to the building can contribute to pipe scales in residential buildings. Bench-scale studies with LDPE showed plastics can act as nucleation sites for iron species. More research is needed to examine the influence of water source characteristics, water distribution system materials, and water temperature on metal deposition onto plastic materials. Metal release from plastic plumbing materials should be investigated as a factor of water pH, organic content and water flow conditions. As results of this study show, plastic drinking water pipes can accumulate metals on their surface. To better understand and predict drinking water metal levels, the processes that control metal-plastic interactions should be further investigated.

4.6 Acknowledgement

This research was funded by National Science Foundation grant CBET-1228615 and the Birck Nanotechnology Center. The authors appreciate the analytical assistance provided by Dr. Chloe De Perre, Dr. Rosa Diaz, Gamini Mendis, Mitul Patal Kumar. Additional thanks are extended to Dr. Lia Stanciu for FTIR spectrophotometer access. Tony Hahn and Whirlpool Corporation are acknowledged for removing the old PEX pipes and providing them to the authors. Dr. Keith Chadwick is thanked for his insight about nucleation experiments. Additional thanks are extended to the surface science analysis staff at Birck Nanotechnology center at Purdue University.

4.7 References

1. Malassa H, Al-Qutob M, Al-Khatib M, Al-Rimawi F. Determination of Different Trace Heavy Metals in Ground Water of South West Bank / Palestine by ICP / MS. *Journal of Environmental Protection*. 2013, 4(8), 818-827.

2. Cerrato JM, Reyes LP, Alvarado CN, Dietrich AM. Effect of PVC and Iron Materials on Mn(II) Deposition in Drinking Water Distribution Systems. *Water Res. 2006,* 40(14), 2720-2726.

3. Sandvig A, Kwan P, Kirmeyer G, Maynard B, Mast D, Trussell RR, Trussell S, Cantor A, Prescott A. *Contribution of Service Line and Plumbing Fixtures to Lead and Copper Rule Compliance Issues*, 2008. Water Research Foundation (Formerly AWWA Research Foundation). Denver, CO USA.

4. McNeill LS, Edwards MA. Iron Pipe Corrossion in Distribution Systems. *Journal of the American Water Works Association*. 2001, *93*(7), 88-100.

5. US EPA (Environmental Protection Agency), 2015. *Secondary Drinking Water Standards: Guidance for Nuisance Chemicals.* Accessed May 9, 2017. Retrieved from https://www.epa.gov/dwstandardsregulations/secondary-drinking-water-standards-guidance-nuisance-chemicals

6. Edwards M, Triantafyllidou S, Best D. Elevated Blood Lead in Young Children Due to Lead-Contaminated Drinking Water: Washington, D.C., 2001-2004. *Environmental Science & Technology*. 2009, 43(5), 1618-1623.

7. Hanna-Attisha M, LaChance J, Sadler RC, Schnepp AC. Elevated Blood Lead Levels in Children Associated with the Flint Drinking Water Crisis: A Spatial Analysis of Risk and Public Health Response. *American Journal of Public Health*. 2016, *106*(2), 283-290.

8. Pieper KJ, Tang M, Edwards MA. Flint Water Crisis Caused By Interrupted Corrosion Control: Investigating "Ground Zero" Home. *Environmental Science & Technology*. 2017, *51*(4), 2007-2014.

9. Petersen LR, Denis D, Brown D, Hadler JL, Helgerson SD. Community Health Effects of a Municipal Water Supply Hyperfluoridation Accident. *American Journal of Public Health*. 1988, *78*(6), 711-713.

10. Kroll D. *Securing Our Water Supply: Protecting a Vulnerable Resource*. PennWel Book, 2006.

11. Colorado Department of Public Health and Environment, Water Quality Control Division. *Colorado Cross-Connection Control Manual, 5th Edition*. 2004. Denver, CO USA.

12. AWWA (American Water Works Association). 1979. The Use of Plastics in Distribution Systems. Committee Report. *Journal of the American Water Work Association, 71*(7), 373-375.

13. American National Standards Institute (ANSI)/AWWA. *Standard C900-07, Polyvinyl Chloride (PVC) Pressure Pipe and Fabricated Fittings, 4 in. through 12 in. for Water Transmission and Distribution.* Denver, CO. 2007.

14. Le Gouellec YA, Cornwell DA. *Installation, Condition assessment, and reliability of service lines, #2927 Final Report.* 2007. Water Research Foundation (Formerly AWWA Research Foundation). Denver, CO, USA.

15. ANSI/AWWA. *Standard C906-15, Polyethylene (PE) Pressure Pipe and Fittings, 4 in. through 65 in. for Waterworks.* Denver, CO, 2015.

16. Martel KD, Klewicki K. *State of the Science: Plastic Pipe, # 4680 Final Report.* 2016. Water Research Foundation. Denver, CO USA.

17. Kim S. Pyrolysis Kinetics of Waste PVC Pipe. *Waste Management*. 2001, 21(7), 609-616.

18. Lytle DA, Sorg TJ, Frietch C. Accumulation of Arsenic in Drinking Water Distribution Systems. *Environmental Science & Technology*. 2004, 38(20), 5365-5372.

19. Campbell CE, Whelton AJ, Polera R, Dietrich AM. 2008. The Characteristics and Chemical Performance of Polyethylene and Poly (1-Butene) Pipes Removed from a Water Distribution System. *VWRRC Special Report SR43-2008*, 1-13. Blacksburg, VA USA.

20. Friedman MJ, Hill AS, Reiber SH, Valentine RL, Larsen G, Young A, Korshin GV, Peng CY. *Assessment of Inorganics Accumulation in Drinking Water System Scales and Sediments WRF #3118.* 2010. Water Research Foundation. Denver, CO USA.

21. Ginige MP, Garbin S, Wylie J, Bal Krishna KC. Effectiveness of Devices to Monitor Biofouling and Metals Deposition on Plumbing Materials Exposed to a Full-Scale Drinking Water Distribution System. *PLoS ONE.* 2017.

22. Varaprasad BJS, Vishwanadh GK. Investigations on Thickness of Deposits in PVC Pipes. *International Journal of Sustainable Civil Engineering*. 2011, *3*(1), 25-33.

23. Copeland RC, Lytle DA, Dionysiou DD. Desorption of Arsenic from Drinking Water Distribution System Solids. *Environmental Monitoring & Assessment*. 2007, *127*(1), 523-535.

24. Holmes LA, Turner A, Thompson RC. Interactions Between Trace Metals and Plastic Production Pellets Under Estuarine Conditions. *Marine Chemistry*. 2014, 167, 25-32.

25. Ranney TA, Parker LV. Comparison of Fiberglass and Other Polymeric Well Casings, Part III. Sorption and Leaching of Trace-Level Metals. *Ground Water Monitoring & Remediation*. 1998, 18(3), 127-133.

26. Hewitt AD. Potential of Common Well Casing Materials to Influence Aqueous Metal Concentrations. *Ground Water Monitoring & Remediation*. 1992, 12(2), 131-136.

27. Parker LV, Hewitt AD, Jenkins TF. Influence of Casing Materials on Trace-Level Chemicals in Well Water. *Ground Water Monitoring & Remediation*. 1990, 10(2), 146-156.

28. Robertson DE. The Adsorption of Trace Elements in Sea Water on Various Container Surfaces. *Analytica Chimica Acta*. 1968, 42(C), 533-536.

29. Fischer C, Kroon JJ, Verburg TG, Teunissen T, Wolterbeek HT. On The Relevance of Iron Adsorption to Container Materials in Small-Volume Experiments on Iron Marine Chemistry: ^{55}Fe-Aided Assessment of Capacity, Affinity and Kinetics. *Marine Chemisry*. 2007, 107(4), 533-546.

30. Holmes LA, Turner A, Thompson RC. Adsorption of Trace Metals to Plastic Resin Pellets in the Marine Environment. *Environmental Pollution*. 2012, *160*, 42-48.

31. Ashton K, Holmes L, Turner A. Association of Metals with Plastic Production Pellets in the Marine Environment. *Marine Pollution Bulletin*. 2010, 60(11), 2050-2055.

32. Rochman CM, Hentschel BT, Teh SJ. Long-term Sorption of Metals is Similar Among Plastic Types: Implications for Plastic Debris in Aquatic Environments. *PLoS ONE*. 2014, *9*(1), e85433.

33. Graca B, Bełdowska M, Wrzesień P, Zgrundo A. Styrofoam Debris as a Potential Carrier of Mercury within Ecosystems. *Environmental Science & Pollution Research.* 2014, 21(3), 2263-2271.

34. Brennecke D, Duarte B, Paiva F, Caçador I, Canning-Clode J. Microplastics as vector for heavy metal contamination from the marine environment. *Estuarine, Coastal & Shelf Science*, 2014, 1-7.

35. Weijuan L, Fuming Z, Zuyi T. Adsorption and Desorption of Am(III) on Calcareous soil and its parent material. *Journal of Radioanalytical & Nuclear Chemistry*. 2005, 265(3), 431-439.

36. Cobelo-Garcia A, Turner A, Millward GE, Couceiro F. Behaviour of Palladium(II), Platinum(IV), and Rhodium(III) in Artificial and Natural Waters: Influence of Reactor Surface and Geochemistry on Metal Recovery. *Analytica Chimica Acta*. 2007, 585(2), 202-210.

37. Bekri-Abbes I, Bayoudh S, Baklouti M. Converting Waste Polystyrene into Adsorbent: Potential Use in the Removal of Lead and Cadmium Ions from Aqueous Solution. *Journal of Polymers & the Environment.* 2006, 14(3), 249-256.

38. Castillo Montes J, Cadoux D, Creus J, Touzain S, Gaudichet-Maurin E, Correc O. Ageing of Polyethylene at Raised Temperature in Contact with Chlorinated Sanitary Hot Water. Part I - Chemical Aspects. *Polymer Degradation & Stability*. 2012, *97*(2), 149-157.

39. Whelton, A. J., Dietrich, A. M. (2009). Critical Considerations for the Accelerated Aging of Polyethylene Potable Water Materials. *Polymer Degradation & Stability*, 94, 1163-1175.

40. Whelton AJ, Dietrich AM, Gallagher DL. Impact of Chlorinated Water Exposure on Contaminant Transport and Surface and Bulk Properties of High-Density Polyethylene and Cross-Linked Polyethylene Potable Water Pipes. *Journal of Environmental Engineering*. 2011, 137(7), 559-568.

41. Thompson DM, Weddle SA, Maddaus WO. *Water Utility Experiences with Plastic Service Lines WRF#414*, 1992. Water Research Foundation. Denver, CO USA.

42. Hoàng EM, Lowe D. Lifetime Prediction of a Blue PE100 Water Pipe. *Polymer Degradation & Stability*. 2008, 93(8), 1496-1503.

43. ASTM (American Society for Tesing and Materials International). 2015. *ASTM D3895-14, Standard Test Method for Oxidative-Induction Time of Polyolefins by Differential Scanning Calorimetry*. West Conshohocken, PA USA.

44. Brocca D, Arvin E, Mosbæk H. Identification of Organic Compounds Migrating from Polyethylene Pipelines into Drinking Water. *Water Res*. 2002, 36(15), 3675-3680.

45. Ollick AM, Al-Amir AM. Weathering Effects on Mechanical Properties of Low Density Polyethylene (LDPE) and High Density Polyethylene (HDPE) Pipes Used in Irrigation Networks. *Alexandria Engineering Journal*. 2003, 42(6), 659-667.

46. Gorbunova TL, Gaevoi NV, Gerasimov KV, Chalykh AE, Kalugina EV. Effect of chlorinated water on peroxide-crosslinked polyethylene PEX-a. *Plasticheskie Massy*. 2009, 9, 40-46.

47. Rożej A, Cydzik-Kwiatkowska A, Kowalska B, Kowalski D. Structure and Microbial Diversity of Biofilms on Different Pipe Materials of A Model Drinking Water Distribution Systems. *World Journal of Microbiology & Biotechnology*. 2015, 31(1), 37-47.

48. Denberg M, Mosbæk H, Hassager O, Arvin E. Determination of the Concentration Profile and Homogeneity of Antioxidants and Degradation Products in a Cross-Linked Polyethylene Type A (Pexa) Pipe. *Polymer Testing*. 2009, 28(4), 378-385.

49. George G. 2012. Performance of Polyolefin (PP-R , PEX and PB) Piping and Fittings in Recirculating Hot Water Systems Under Australian Operating Conditions. *Expert Opinion*, Queensland University of Technology. Rockdale, NSW, AU.

50. Wagner D, Siedlarek H, Kropp M, Fischer WR. *Proceedings of the IOM Plastics Pipes IX Conference*, Edinburgh, U.K. 1995, p.497.

51. Wright D. *Failure of Plastics and Rubber Products: Causes, Effects and Case Studies Involving Degradation.* Rapra Publishing, 2001. Shropshire, U.K. ISBN185957517X, 9781859575178

52. Andritsos N, Karabelas AJ, Koutsoukos PG. Morphology and Structure of $CaCO_3$ Scale Layers Formed under Isothermal Flow Conditions. *Langmuir*. 1997, 13(10), 2873-2879.

53. Chen T, Neville A, Yuan M. Calcium Carbonate Scale Formation - Assessing the Initial Stages of Precipitation and Deposition. *Journal of Petroleum Science & Engineering*. 2005, 46(3), 185-194.

54. Muryanto S, Bayuseno AP, Ma'mun H, Usamah M, Jotho. Calcium Carbonate Scale Formation in Pipes : Effect of Flow Rates, Temperature, and Malic Acid as Additives on the Mass and Morphology of the Scale. *Procedia Chemistry*. 2014, *9*, 69-76.

55. Muryanto S, Bayuseno AP, Sediono W, Mangestiyono W, Sutrisno. Development of a Versatile Laboratory Project for Scale Formation and Control. *Education for Chemical Engineers*. 2012, 7(3), e78-e84.

56. Masters S, Edwards E. Increased Lead in Water Associated with Iron Corrosion. *Environmental Engineering Science*. 2015, 32(5), 361-369.

57. Clark BN, Masters SV, Edwards, MA. Lead Release to Drinking Water from Galvanized Steel Pipe Coatings. *Environmental Engineering Science*. 2015, *32*(8), 713-721.

58. Zaporojtchenko V, Strunskus T, Behnke K, Bechtolsheim CV, Thran A, Faupel F. Formation of Metal-Polymer Interfaces by Metal Evaporation: Influence of Deposition Parameters and Defects. *Microelectronic Engineering*. 2000, *50*(1-4), 465-471.

59. Zaporojtchenko V, Zekonyte J, Biswas A, Faupel F. Controlled Growth of Nano-Size Metal Clusters on Polymers by Using VPD Method. *Surface Science*. 2003, *532-535*, 300-305.

60. Zhang Z, Stout JE, Yu VL, Vidic R. Effect of Pipe Corrosion Scales on Chlorine Dioxide Consumption in Drinking Water Distribution Systems. *Water Res.*2008, 42(1-2), 129-136.

61. Sarin P, Snoeyink VL, Bebee J, Jim KK, Beckett MA, Kriven WM, Clement JA. Iron Release from Corroded Iron Pipes in Drinking Water Distribution Systems: Effect of Dissolved Oxygen. *Water Res.* 2014, 38, 1259-1269,

62. Zhu Y, Wang H, Li X, Hu C, Yang M, Qu J. Characterization of Biofilm and Corrosion of Cast Iron Pipes in Drinking Water Distribution System with UV/Cl_2 Disinfection, *Water Res*. 2014, 60, 174-181.

LIMITATIONS AND FUTURE WORK

The limitations of this dissertation research and recommendations for future work are briefly described.

Chapter1: Polyester composite water uptake and organic contaminant release

In this study inclusion of CNF into polyester composites enhanced water sorption and organic contaminant release to water during the short exposure period (30 day). Additional studies could be conducted to examine the impact of enhanced water sorption on CNF-polyester composite mechanical and long-term durability properties. A knowledge-gap found in the literature was that little information exist that describe chemical leaching by FRP materials. The long-term water quality impacts caused by CNF reinforced polyester composites to water quality should to be investigated.

Chapter2: Link between Fixture Water Use and Drinking Water Quality

Chemical and microbiological drinking water quality varied within a single family residential plumbing system. The complexity observed in this plumbing system mimicked the complexity of drinking water quality exhibited by large water distribution systems. To better understand the carbon source in building drinking water, assimilable organic carbon and biodegradable dissolved organic carbon analysis should be considered in future work. Adsorption of organics, metals, and bacteria onto and release from plumbing materials under different water chemistry, temperature, and flow conditions may also have influenced study results and could be investigated in future work. The plumbing product testing protocol used for the PEX piping that was installed currently considers 16 hr and 24 hr stagnation periods but should be revised to account for worst-case more realistic stagnation periods identified in the present work (72 hr).

While water flow at each fixture was measured with a one-second resolution, many fewer drinking water chemical and bacteria measurements were conducted. To better identify the relationships between fixture use and water quality more frequent water chemical and microbiological analysis would be required. The authors propose conducting more frequent water sampling over a short duration (1 week) and couple these results with service line pressure and fixture flow monitoring for the development of

integrated water quality-hydraulic plumbing models. This process has been implemented to better design water distribution systems and should be considered for building plumbing.

In the U.S., residential building plumbing is designed to deliver a certain volume of water to fixtures based on number of building inhabitants. Factors such as drinking water chemical and microbiological levels are not explicitly considered in plumbing design. Future work should consider how different design characteristics (i.e., plumbing designs for multi-story vs. long single story buildings) influence drinking water quality. Identification and examination of plumbing branches to include residence time, disinfectant decay, chemical leaching, and microbiological growth kinetics should be considered. This information will be useful to better avoid lower-flow, hot spots of degraded drinking water quality.

Chapter 3: Investigation of the Factors that Influence Lead Accumulation onto Polyethylene

The influence of polymer aging, water chemistry, and aqueous Pb concentration causing Pb deposition onto low density polyethylene (LDPE) were investigated. In this study Pb precipitation over the time was tested under no oxygen condition and using the ultrapure water, however in future the experimental conditions could be modified to be more representative of tap water real characteristics. In this research due to our time limitations we applied accelerated ozone aging method to oxidized LDPE surface. However future research could investigate Pb precipitation kinetics onto LDPE aged with chlorinated hot or cold water. Ozone aged LDPE chemical and physical properties could be compared later with hot water chlorinated aged LDPE. The influence of plastic and heavy metal type on precipitation kinetics could be investigated. Natural organic matter (NOM) is known to form complexes with heavy metals present in water, the influence of NOM type and concentration on heavy metal precipitation on plastic materials should be examined. Future research should be conducted to examine the water quality parameters and plastic surface characteristics which influence heavy metal release from new and aged plastic materials.

Chapter 4: Accumulation of Metals in Plastic Drinking Water Plumbing Systems

Results of this study provide insight into heavy metal scale formation for a one-year-old residential PEX plumbing system. This study quantified the metal abundance only for one building drinking water plumbing systems. More research needed to examine the influence of water source characteristics, water distribution system materials and water temperature on metal deposition abundance onto the plastic materials. Also with increasing plastic pipe installation, additional work is needed to understand the conditions that cause metal scale formation. Metal release from these plumbing materials should be investigated as a factor of water pH, organic content and water flow conditions.

APPENDIX A

METHODS

Contaminant Biodegradability Testing. A five day biochemical oxygen demand (BOD_5) concentration was determined according to SM 5210B for water from the first three day exposure period[45]. BOD_5 testing involved quantifying the amount of oxygen consumed over a five day exposure period seeded with 24 h stabilized primary influent from a local activated sludge wastewater treatment facility.

RESULTS

Results. TGA was utilized to quantify the components of each composite and facilitate comparisons based on the mass of resin in each composite (**Figure A1**). TGA scans were compared between two distinct groups: composites that contained glass fiber and composites that did not contain glass fiber. Thermal decomposition of the P/O resulted in a 0.012 mg/mg mass fraction residual char at 700 °C. The mass fraction of glass fiber ranged from (0.36 to 0.40) mg/mg.

In the case of the P/CNF composite, the decrease in mass fraction at the ramp to 700 °C was approximately (0.006 $\pm$ 0.002) mg/mg. This is approximately half the 0.01 mg/mg mass fraction expected from sample manufacture. The residual mass of the P/CNF was 0.014 mg/mg mass fraction, similar to the P/O decomposition. Thermogravimetric analysis showed the glass fiber composites contained approximately 0.62 mg/mg mass fraction of glass fiber. The P/GF/CNF composite had a smaller detectable CNF mass fraction of (0.0007 $\pm$ 0.0004) mg/mg. This was an order of magnitude less than the 0.01 mg/mg mass fraction expected and the variation in CNF content between samples was much higher. The CNF slightly oxidizes at 500 °C, but the mass loss measured for raw CNF at 500 °C would not account for the missing CNF material.

Table A1 Composite Mass Loss Due to Water Desorption

Composite	P/O	P/GF	P/CNF	P/GF/CNF
Mass Loss%	-0.54 ± 0.06	-0.16 ± 0.04	-0.59 ± 0.08	-0.43 ± 0.16

Table A2 TOC and COD Leaching Rates for the Studied Composites.

Contaminant	**Composite and leaching Rate (mg contaminant/L-mg resin-day)**			
	P/O	P/GF	P/CNF	P/GF/CNF
Total Organic Carbon (TOC)	-0.0017	-0.0002	-0.0058	-0.0024
Chemical Oxygen Demand (COD)	-0.0070	-0.0008	-0.0217	-0.0048

Table A3 Contaminant Biodegradability Indicators for Organic Contaminants Released during the First Three Day Exposure Period.

Composite	**Contaminant Biodegradability Indicators**	
	BOD5, mg/L	**COD/BOD5 Ratio**
P/O	10.2 + 5.2	7.5 + 3.6
P/GF	1.4 + 0.7	8.9 + 4.6
P/CNF	9.1 + 5.2	7.0 + 2.6
P/GF/CNF	1.6 + 0.7	6.9 + 0.0

* Mean and standard deviation values shown for two replicate specimens.

Biodegradability of Organic Contaminants Released. A small fraction of the organic contaminants released from each composite were biodegradable and no difference was found between the biodegradability of the contaminants released from all composites (**Table 3A**) based on the COD/BOD_5 ratio. The COD/BOD_5 ratio was applied

because it has been used in the wastewater treatment industry to gauge the biodegradability of organic compounds present in water. A wastewater or stormwater which contains a large quantity of biodegradable material has a COD/BOD_5 ratio typically between 1 and 4[50]. BOD_5 results and COD/BOD_5 ratios for polyester composites were in the order of magnitude of release characteristics for the same water that contacted a polyurea stormwater pipe coating at 23 °C for three days (9.2 mg/L BOD_5; 10.2 COD/BOD_5 ratio)[51]. Generally, contaminants released by each composite were not readily biodegradable. CNF did not impact the biodegradability of contaminants present in contact water.

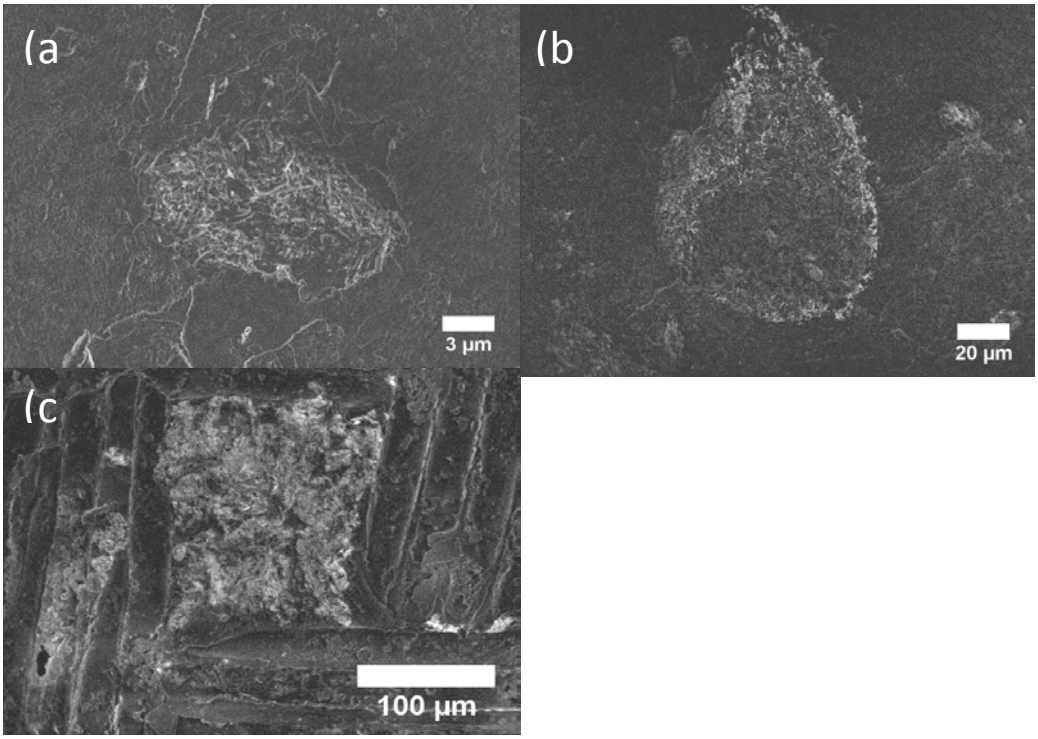

Figure A1 SEM images of CNF fiber agglomerates in the different composites. (a), (b) Large scale agglomerates found on the fracture surface of the P/CNF composite showing the dense CNF bundles. (c), (d) Dense CNF bundles found within resin rich regions on the top surface of the composite. These areas would have formed during the VARTM processing as the resin moved through distribution media placed on the top of the glass fiber mat.

APPENDIX B

B.1.0 MATERIALS AND METHODS

B.1.1 Plumbing System Disinfection

After plumbing installation, the system (hot and cold water lines, and tanks) was shock chlorinated with approximately 100 mg/L as Cl_2 prepared in municipal tap water and the solution stagnated for 24 hr. STERILENE™ was used for superchlorination and the product was comprised of 60-100% $C_3Cl_2N_3NaO_3$ (Design Water Technologies, Inc; Shorewood, MN)[48]. Before superchlorination, the authors collected cold water samples exiting the water softener, from the basement clothes washer hose valve, first floor kitchen sink, and second floor bathroom sink. Water was analyzed for pH, temperature, and free chlorine concentration. The first location where water samples could be collected was immediately following the water softener. After superchlorination water was flushed from the plumbing, municipal tap water stagnated for 18 hr. Then, water was flushed for 30 min from all fixtures and the authors initiated the three month water quality monitoring study.

B.1.2 Building Plumbing System

The hot water system included a recirculation pump that was operated only when a building inhabitant physically pushed the hot water recirculation button in the upstairs bathroom or underneath the kitchen sink. The recirculation pump withdrew water from the fourth water heater and distributed it through the hot water lines that conveyed water from the heater to the shower and/or kitchen sink, and then back to the water heater. The recirculation pump shut-off when the pump inlet temperature was 4.4 to 5.5 degrees Celsius greater than ambient temperature. All fixtures were new and are low-flow type. Three 409 L [108 G] glass lined hot water storage tanks were installed with carbon steel heat exchangers and magnesium coated anode rods. The fourth, electrically-driven, water heater (151 L [40 G] capacity) had a magnesium coated anode rod. The large in-building water storage volume was primarily designed to support the rooftop solar, thermal-photovoltaic systems. While bypassing the three 409 L tanks to use only the 151 L tank was possible, all water tanks were in operation during this study. At the water softener

sampling point, water was flushed for approximately 3 min before a water sample was taken. This action was taken to obtain fresh city water.

B.1.3 Water Quality Monitoring: Free Chlorine, pH, Alkalinity, TOC, UV_{254}, Metal, and qPCR Analysis

Free chlorine concentration was determined using a HACH® 131 Pocket Colorimeter (DPD Free Chlorine). Water pH and temperature was measured using an Orion Star A329 portable pH meter (Thermo Scientific). Water samples were collected in 1 L nitric acid washed amber vials for water quality analysis. Water samples for inorganic analysis were first draw and collected in 15 mL polypropylene tubes. Alkalinity concentration was determined by titration in accordance with Standard Method (SM) 2320B.[49] TOC concentration was measured using a Shimadzu TOC-L CPH/CPN in accordance with USEPA method 415.1.[50] The instrument was calibrated from 0 to 75 mg TOC/L using $HOOCC_6H4COOK$ (r^2 0.99). One 25 mL sample was removed from 1 L bottle for TOC analysis. UV_{254} absorbance was measured using a CARY 300-Bio UV-Vis Spectrophotometer in accordance with USEPA method 415.3. The TOC and UV_{254} limits of detection were 0.004 mg/L and 0.000 cm^{-1}, respectively. Specific Ultraviolet Absorbance (SUVA) was calculated by dividing UV_{254} absorbance to TOC concentration.

Metals were quantified by collecting water samples in 15 mL polypropylene tubes, acidified using 2% HNO_3, and were analyzed with a Perkin Elmer Elan-DRCE II Inductively Coupled Plasma Mass Spectrometer (ICP-MS). Water was analyzed for the following metals: Al, Mn, Mg, Ca, Na, Fe, Zn, Cu, Pb, Cd, Cr, Co, As, Se, Ni, Be, V, Hg. The instrument was calibrated using seven mixed standards and a blank (**Table B3** and **B4**).

Olfactory water properties were described using the TON Standard Method (SM), 2150B at 55 °C.[49] Ultrapure Milli-Q™ water (18Ω) was used as an odor-free reference water and also to dilute water samples. Prior to odor analysis, premise water samples were dechlorinated with $Na_2S_2O_3$. Approval for the human subject research was obtained from the Institutional Review Board (IRB) at Purdue University. At least five participants participated in each test.

DNA was extracted from the membrane with the MO Bio PowerWater DNA Isolation Kit (MO BIO Laboratories, Carlsbad, CA) according to the manufacturer's instructions. DNA extract yields and purities were quantified with a NanoDrop 2000c UV-Vis Spectrophotometer (Thermo Fisher Scientific, Waltham, MA). 16S rRNA genes were amplified by qPCR using universal bacterial primers Eub338Fw (5'ACTCCTACGGGAGGCAGCAG3') and Eub518Rv (5'ATTACCGCGGCTGCTGG3').[47] The total volume of each reaction was 20 µL, which contained 10 µL 2X iTaq universal SYBR Green supermix (Bio-rad, Hercules, CA), 0.4 µL individual primer (10 µM), 2 uL of DNA templates, and 7.2 µL sterile nanopure water. All reactions were performed in a CFX96 Real-time PCR detection system (Bio-rad, Hercules, CA) with the following thermal conditions: an initial denaturation at 95 ºC for 3 min, followed by 40 cycles of 30 sec at 95 ºC, 30 sec at 59.9 ºC, and 30 sec at 72 ºC. Subsequently, melt curve analysis was performed by the increasing temperature from 65 ºC to 95 ºC. DNA templates, negative control (DNA template replaced by sterile nanopure water), and 10-fold serial dilutions of standard were analyzed in triplicate per qPCR experiment. The presence of only one peak in the melt curve, the authors concluded non-specific amplification did not occur. For PCR analysis the water samples were not diluted. Triplicate wells in every real-time PCR test was used and when the coefficient of variation of triplicate wells was over 25%, the data was rejected.

B.1.4 Water Usage Calculations

Figure S1 describes the basis for these calculations. The recorded number of usage events determined the fixture use frequency. The elapsed time since the last fixture use event represented the stagnation time (**Figure B1, B**). As mentioned, there were some missing records in the data, which required a modified approach for calculating the maximum stagnation time and the average stagnation time over the duration of the study. Because it is unknown whether there was usage during the missing records periods, they were excluded from the analysis. Each continuous segment of missing records was assigned an artificial event called missing records event (**Figure B1, A**). When a period of non- usage fell between two missing records events (**Figure B1, C**), the stagnation time was calculated only as the duration of the recorded non-usage period without consideration of the missing records event. Similarly, when a period of non-usage was

recorded between a missing records event and an actual usual event (**Figure B1, D**), only the recorded period of non-usage was calculated as the stagnation time. Therefore, the calculated stagnation time for the first event after a missing records event before a usage event (**Figure B1, D**) might be considered shorter in duration than the actual stagnation time. All the calculated stagnation times regardless of whether they were bounded by missing records events (**Figure B1, B, C, D**) were included in the calculation of the maximum stagnation time. However, the calculation of average stagnation time excluded the stagnation times bounded by r the missing event records (**Figure B1, C and D**) to avoid biasing the results towards shorter elapsed periods.

B.2.1 Flushing Superchlorinated Water from the Plumbing

Water samples collected from various fixtures at the completion of superchlorination and before flushing out the superchlorinated water revealed slight differences in water quality: pH: 6.6 to 6.8; temperature: 21 to 22 °C; Free chlorine: 74 to 110 mg/L as Cl_2; TOC: 13 to 22.5 mg/L (**Table S5**). A chlorinous odor was detectable at all taps. Based on STERILINE chemical formula ($C_3Cl_2N_3NaO_3$) and its concentration, it was estimated that 9.8 to 16.4 m/L of carbon was added to the water by STERILINE reagent used to create the superchlorinated water. Water collected exiting the water softener, which was not superchlorinated, contained pH 7.3, 1.1 mg/L TOC, temperature and chlorine level were 21.0 °C and 0.5 mg/L as Cl_2, respectively. Water pH, chlorine and temperature were again characterized after water was allowed to sit for 18 hr and also after flushing again for 30 min (**Table B6**).

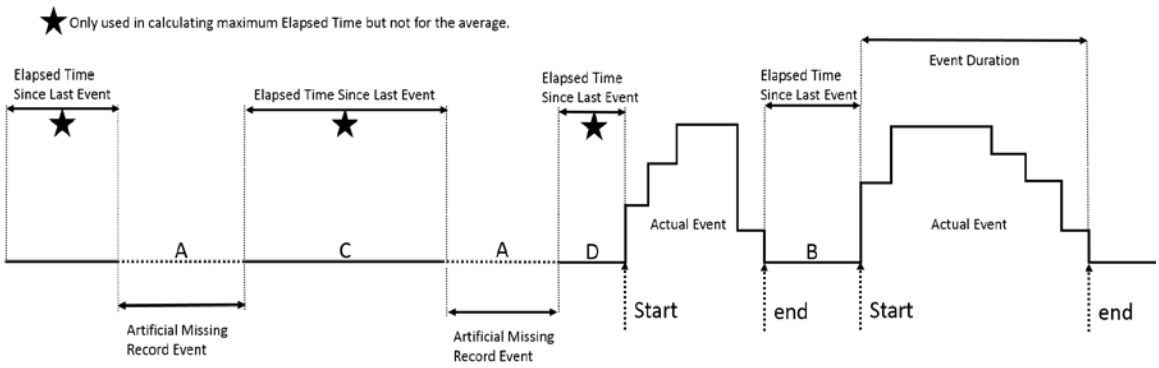

Figure B1 Defining Start/End, Elapsed time since last event, and duration of each event

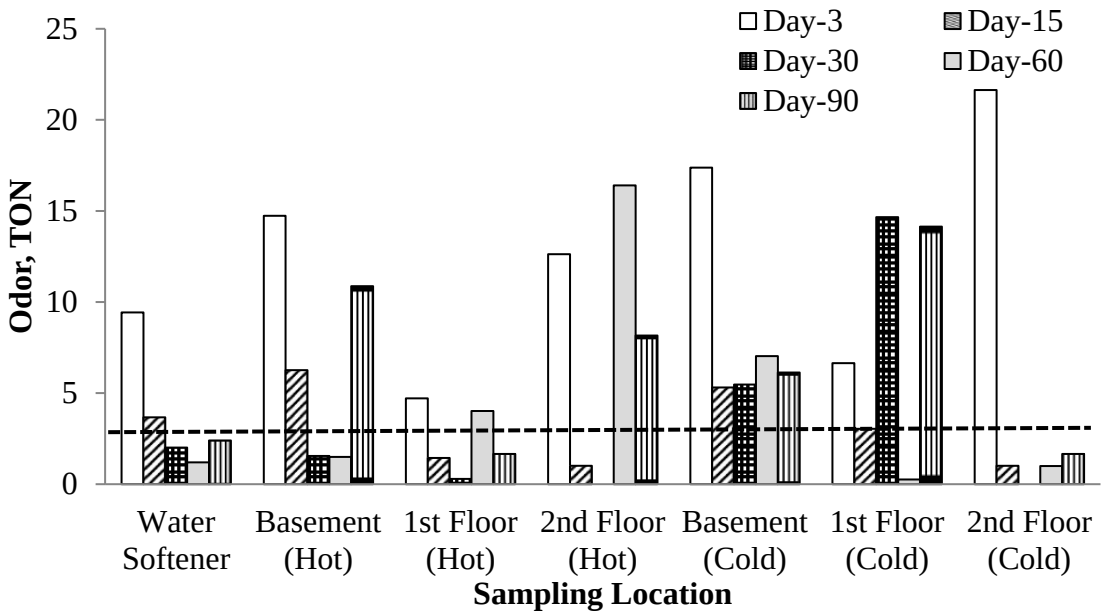

Figure B2 Odor monitoring results for hot and cold water samples at different exposure periods. Results shown represent one water sample per fixture per sampling period. The USEPA SMCL is 3 TON.

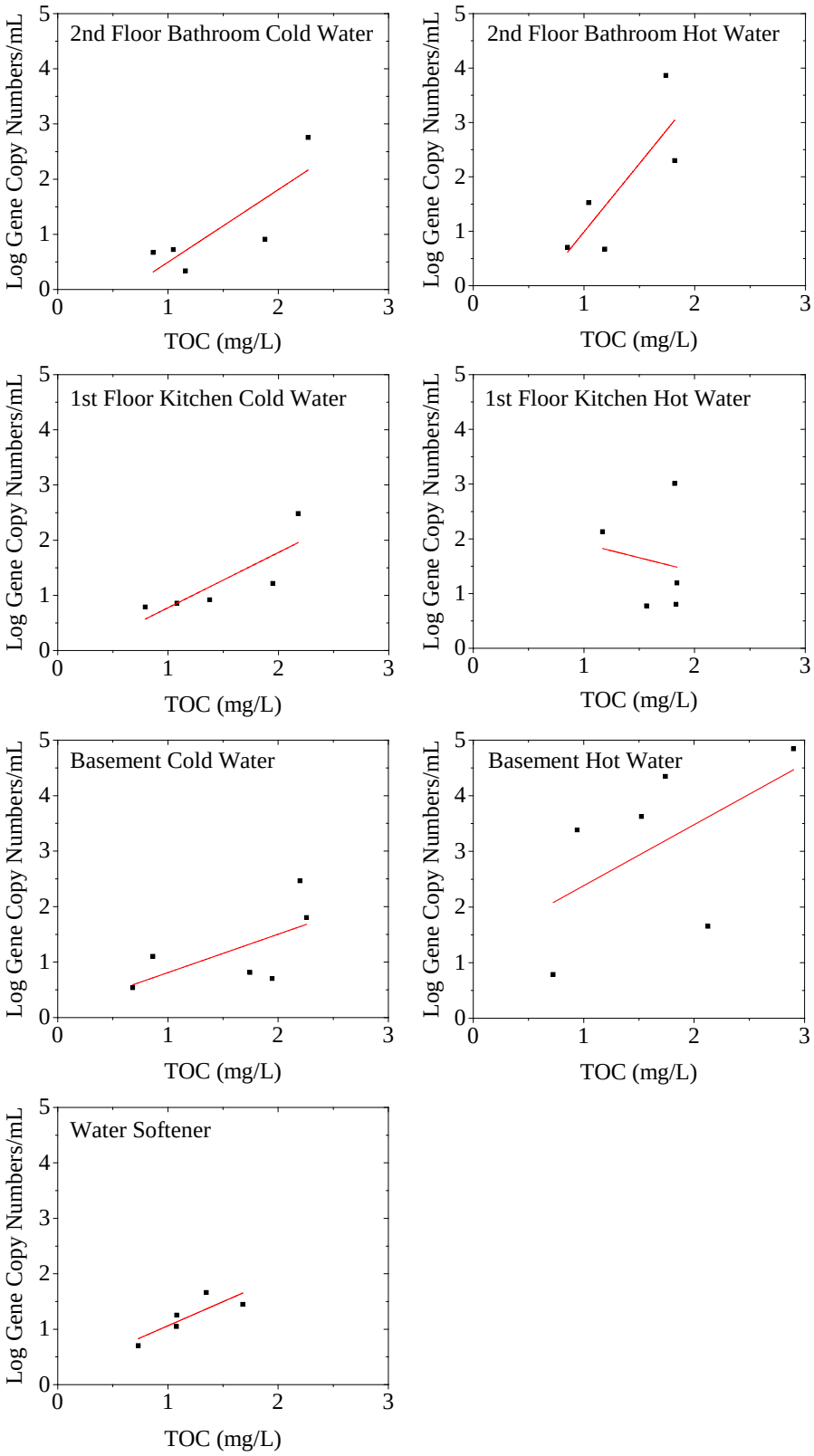

Figure B3 Correlations between TOC and bacterial concentrations at seven locations during 90 days

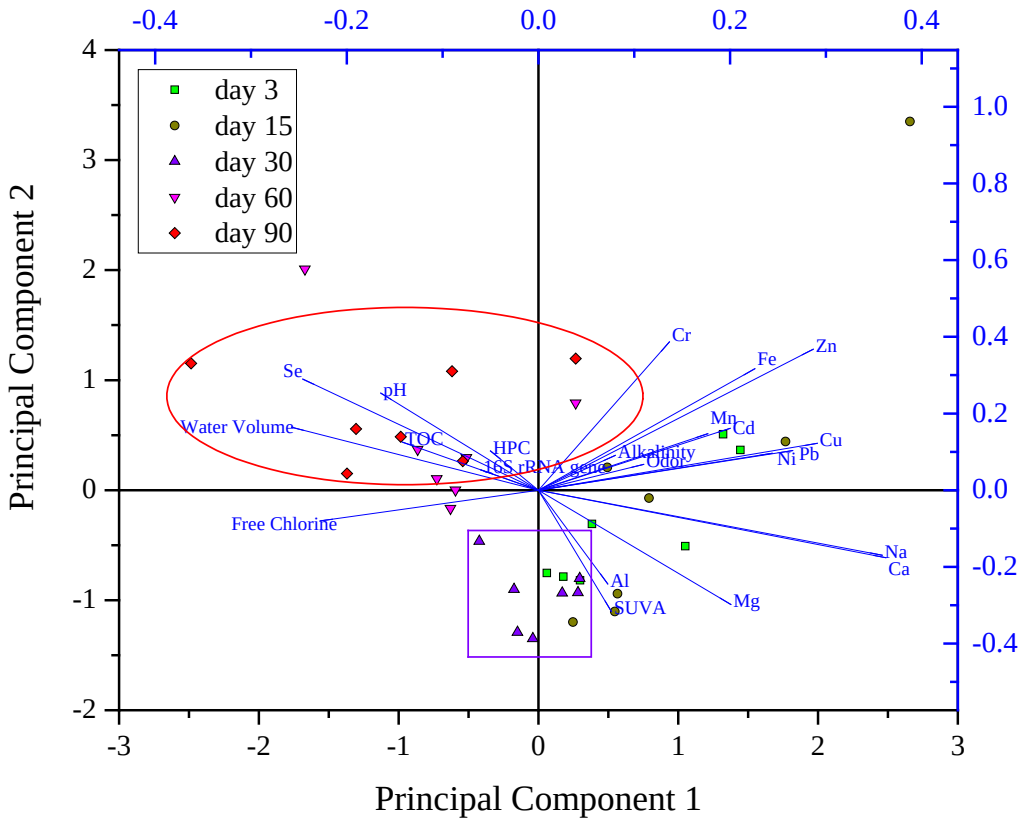

Figure B4 Principal component analysis of plumbing water quality parameters

Table B1 Diameter and length of pipes present in the house

Pipe Type	Diameter (ID), cm	Length, m	Total Internal Surface Area, m^2
Cold	1.2	41.9	0.3
Hot		40.9	0.3
Cold	1.7	35.8	0.3
Hot		38.3	0.4
Total in home		156.9	1.3
Total Cold		77.7	
Total Hot		79.2	

Table B2 Finished water quality reported by the local water treatment plant

Water Quality	Value
pH	7.0-7.5
TOC (mg/L)	nr
Alkalinity (mg/L as $CaCO_3$)	nr
Ca	104.0
Mg	34.0
Mn	0.02
P	nr
Zn	nd
Al	nd
Fe	0.05
Na	26.0
Pb	nd*
Cu	0.564*
As	0.004
Cr	nd-0.14 µg/L
Ni	0.005

* 90th percentile results; nd=not detected; nr=not reported

Table B3 Standards used for ICP-MS analysis µg/L

Element	(1)	(2)	(3)	(4)	(5)	(6)	(7)
Al	250	100	66.7	50	25	10	5
Cr	250	100	66.7	50	25	10	5
Pb	250	100	66.7	50	25	10	5
Se	125	50	33.3	25	12.5	5	2.5
As	125	50	33.3	25	12.5	5	2.5
Co	250	100	66.7	50	25	10	5
Mn	250	100	66.7	50	25	10	5
V	250	100	66.7	50	25	10	5
Be	25	10	6.7	5	2.5	1	0.5
Cu	250	100	66.7	50	25	10	5
Hg	12.5	5	3.4	2.5	1.25	0.5	0.25
Zn	250	100	66.7	50	25	10	5
Cd	250	100	66.7	50	25	10	5
Fe	125	50	33.3	25	12.5	5	2.5
Ni	125	50	33.3	25	12.5	5	2.5

Table B4 Standards used for ICP-MS analysis mg/L

Element	(1)	(2)	(3)	(4)	(5)	(6)
Ca	150	120	100	75	60	30
Mg	50	40	33.3	25	20	10
Na	50	40	33.3	25	20	10
Zn	5	4	3.33	2.5	2	1
Fe	0.5	0.4	0.33	0.25	0.2	0.1

Table B5 Water quality characteristics at the end of superchlorination and before flushing

Location	**Water pH**	**Free chlorine, mg/L as Cl_2**	**Temperature, °C**	**TOC, mg/L**
Service Line	7.35	0.5	21.0	1.1±0.1
Basement	6.68	92	21.9	22.2 ± 0.4
1st Floor	6.63	92	21.4	21.1 ± 0.6
2nd Floor	6.84	110	21.2	21.0 ± 0.8

Table B6 Water quality characteristics for basement water samples at day 0 before and after flushing

Location	**Water Quality**						
	Water pH		Free chlorine, mg/L		Temp, °C		TOC, mg/L
Flushing	Before	After	Before	After	Before	After	Before
Basement Cold	7.29	7.94	1.3	0.9	21.3	17.1	0.68
Basement Hot	7.22	7.92	1.2	1.0	21.9	38.2	0.72
Water heater tank	7.3		0.9				

Table B7 Water pH at different fixtures and exposure durations

Location / Exposure Duration		3d	15d	30d	60d	90d
Soften Water		7.61	7.57	7.31	7.95	7.75
Cold	Basement	7.73	7.64	7.31	7.14	7.52
	1st-Floor	7.46	7.47	7.40	7.99	7.84
	2nd-Floor	7.64	7.47	7.29	7.59	7.76
Hot	Basement	7.42	7.58	7.37	7.17	7.72
	1st-Floor	7.42	7.43	7.35	7.63	7.81
	2nd-Floor	7.62	7.43	7.27	7.64	7.72

Table B8 Water alkalinity at different fixtures and exposure durations

Location / Exposure Duration		3d	15d	30d	60d	90d
Soften Water		285.0	270.0	280.0	280.0	283.7
Cold	Basement	282.5	267.5	277.5	270	278.7
	1st-Floor	285.0	276.2	275.0	280.0	265.0
	2nd-Floor	285.0	282.5	270.0	272.5	247.5
Hot	Basement	270.o	280.0	272.5	267.5	280.0
	1st-Floor	265.0	277.5	275.0	280.0	276.2
	2nd-Floor	280.0	275.0	260.0	265.0	277.5

Table B9 Water free chlorine concentration, mg/L

Location/Exposure Duration		3d	15d	30d	60d	90d
Soften Water		0.4	1.0	1.4	1.1	1.6
Cold	Basement	0.3	nd	0.2	0.2	0.4
	1st-Floor	0.3	0.1	1.3	0.7	0.6
	2nd-Floor	0.5	0.3	0.8	0.3	0.2
Hot	Basement	0.3	nd	0.6	0.3	0.3
	1st-Floor	0.2	0.3	1.1	0.5	1.1
	2nd-Floor	0.6	0.1	0.8	0.4	0.3

nd: not detected

Table B10 Statistical significance of exposure duration, location and water temperature for TOC, UV_{254} and SUVA levels

Effect	Factor	TOC mg/L		UV_{254} Absorbance cm^{-1}		SUVA, L-mg/M	
		Sig?	*p*	Sig?	*p*	Sig?	*p*
Main Effect	Exposure Duration	Yes	<0.005	Yes	<0.001	Yes	<0.001
	Location	No	0.186	Yes	<0.001	Yes	<0.001
	Hot/Cold	No	0.322	Yes	<0.001	Yes	<0.001
Interaction Effects	Time and Location	No	0.787	Yes	<0.001	Yes	<0.001
	Time and Hot/Cold	No	0.279	Yes	<0.001	Yes	<0.001
	Location and Hot/Cold	No	0.132	Yes	<0.001	No	0.863
	Location & Hot/Cold & Time	No	0.730	Yes	<0.001	Yes	<0.001

Table B11 Specific UV Absorbance (SUVA) values, L-mg/M

Location/Exposure Duration		3d	15d	30d	60d	90d
Soften Water		3.4 ± 0.7	2.7 ± 0.1	5.3 ± 0.0	1.2 ± 0.0	1.1 ± 0.0
Cold	Basement	3.8 ± 0.3	0.8 ± 0.0	1.4 ± 0.0	1.1 ± 0.0	0.5 ± 0.0
	1st Floor	3.6 ± 0.1	1.1 ± 0.1	2.9 ± 0.0	1.2 ± 0.0	0.9 ± 0.0
	2nd Floor	2.6 ± 0.2	1.3 ± 0.2	5.2 ± 0.1	0.2 ± 0.0	0.6 ± 0.0
Hot	Basement	2.7 ± 0.2	0.8 ± 0.1	1.6 ± 0.0	0.5 ± 0.0	1.1 ± 0.0
	1st Floor	2.7 ± 0.1	1.1 ± 0.1	2.5 ± 0.0	0.9 ± 0.0	1.1 ± 0.0
	2nd Floor	3.0 ± 0.8	1.2 ± 0.1	3.0 ± 0.0	0.9 ± 0.1	0.7 ± 0.0

Table B12(a) Correlation between water quality parameters

		16S	HPC	Zn	Fe	Pb	Cu	Cr	Cd
16S rRNA	Pearson Corr.	1.000	0.259	0.022	-0.054	-0.019	-0.049	0.008	0.070
	p-value	--	0.133	0.900	0.759	0.914	0.782	0.962	0.691
HPC	Pearson Corr.	0.259	1.000	0.151	-0.037	-0.037	0.004	0.014	-0.049
	p-value	0.133	--	0.387	0.833	0.833	0.983	0.936	0.782
Zn	Pearson Corr.	0.022	0.151	1.000	0.781	0.343	0.556	0.632	0.569
	p-value	0.900	0.387	--	0.000	0.044	0.001	0.000	0.000
Fe	Pearson Corr.	-0.054	-0.037	0.781	1.000	0.143	0.221	0.837	0.066
	p-value	0.759	0.833	0.000	--	0.414	0.203	0.000	0.707
Pb	Pearson Corr.	-0.019	-0.037	0.343	0.143	1.000	0.398	0.146	0.399
	p-value	0.914	0.833	0.044	0.414	--	0.018	0.403	0.018
Cu	Pearson Corr.	-0.049	0.004	0.556	0.221	0.398	1.000	0.105	0.551
	p-value	0.782	0.983	0.001	0.203	0.018	--	0.549	0.001
Cr	Pearson Corr.	0.008	0.014	0.632	0.837	0.146	0.105	1.000	0.035
	p-value	0.962	0.936	0.000	0.000	0.403	0.549	--	0.843
Cd	Pearson Corr.	0.070	-0.049	0.569	0.066	0.399	0.551	0.035	1.000
	p-value	0.691	0.782	0.000	0.707	0.018	0.001	0.843	--
Ni	Pearson Corr.	-0.033	-0.054	0.227	-0.004	0.782	0.572	0.055	0.382
	p-value	0.851	0.758	0.190	0.981	0.000	0.000	0.754	0.023
Al	Pearson Corr.	0.027	0.004	-0.146	0.033	-0.164	0.100	-0.092	-0.074
	p-value	0.878	0.980	0.402	0.849	0.346	0.569	0.600	0.672
Se	Pearson Corr.	-0.009	0.030	-0.044	-0.040	-0.230	-0.114	0.323	-0.008
	p-value	0.957	0.866	0.803	0.818	0.184	0.516	0.059	0.964
Mn	Pearson Corr.	-0.123	-0.093	0.437	0.749	0.140	-0.022	0.688	-0.066
	p-value	0.480	0.595	0.009	0.000	0.424	0.900	0.000	0.708
Ca	Pearson Corr.	-0.230	-0.198	0.208	0.224	0.360	0.331	0.107	0.027
	p-value	0.184	0.254	0.230	0.197	0.034	0.052	0.539	0.876
Mg	Pearson Corr.	-0.095	-0.122	-0.055	0.030	0.004	0.316	-0.097	-0.054
	p-value	0.587	0.484	0.755	0.862	0.983	0.064	0.580	0.756
Na	Pearson Corr.	-0.221	-0.191	0.196	0.229	0.305	0.246	0.137	0.080
	p-value	0.202	0.272	0.260	0.186	0.075	0.155	0.432	0.648
pH	Pearson Corr.	-0.220	0.148	-0.054	0.032	-0.168	-0.067	0.220	-0.239
	p-value	0.190	0.396	0.759	0.857	0.334	0.701	0.205	0.167
Free Chlorine	Pearson Corr.	-0.143	-0.097	-0.405	-0.206	-0.158	-0.404	-0.098	-0.300
	p-value	0.400	0.578	0.016	0.236	0.365	0.016	0.575	0.080
Water Volume	Pearson Corr.	-0.085	-0.061	-0.199	-0.066	-0.103	-0.365	0.196	-0.277
	p-value	0.629	0.728	0.252	0.708	0.556	0.031	0.258	0.107
Odor	Pearson Corr.	-0.077	0.145	0.191	0.023	0.179	-0.019	0.007	0.225
	p-value	0.652	0.406	0.272	0.894	0.304	0.912	0.967	0.194
Alkalinity	Pearson Corr.	-0.040	0.114	0.217	0.130	0.023	0.114	0.171	0.018
	p-value	0.814	0.514	0.210	0.456	0.898	0.515	0.325	0.917
SUVA	Pearson Corr.	-0.209	-0.094	-0.275	-0.198	0.016	-0.236	-0.211	-0.128
	p-value	0.214	0.590	0.109	0.253	0.929	0.173	0.223	0.464
TOC	Pearson Corr.	0.337	0.111	0.070	0.026	-0.047	0.062	-0.016	0.131
	p-value	0.041	0.525	0.688	0.880	0.789	0.722	0.927	0.453

Table B12(b) Correlation between water quality parameters

		Mn	Ca	Mg	Na	pH	Free Chlorine	Water Volume
16S	Pearson Corr.	-0.123	-0.230	-0.095	-0.221	-0.220	-0.143	-0.085
	p-value	0.480	0.184	0.587	0.202	0.190	0.400	0.629
HPC	Pearson Corr.	-0.093	-0.198	-0.122	-0.191	0.148	-0.097	-0.061
	p-value	0.595	0.254	0.484	0.272	0.396	0.578	0.728
Zn	Pearson Corr.	0.437	0.208	-0.055	0.196	-0.054	-0.405	-0.199
	p-value	0.009	0.230	0.755	0.260	0.759	0.016	0.252
Fe	Pearson Corr.	0.749	0.224	0.030	0.229	0.032	-0.206	-0.066
	p-value	0.000	0.197	0.862	0.186	0.857	0.236	0.708
Pb	Pearson Corr.	0.140	0.360	0.004	0.305	-0.168	-0.158	-0.103
	p-value	0.424	0.034	0.983	0.075	0.334	0.365	0.556
Cu	Pearson Corr.	-0.022	0.331	0.316	0.246	-0.067	-0.404	-0.365
	p-value	0.900	0.052	0.064	0.155	0.701	0.016	0.031
Cr	Pearson Corr.	0.688	0.107	-0.097	0.137	0.220	-0.098	0.196
	p-value	0.000	0.539	0.580	0.432	0.205	0.575	0.258
Cd	Pearson Corr.	-0.066	0.027	-0.054	0.080	-0.239	-0.300	-0.277
	p-value	0.708	0.876	0.756	0.648	0.167	0.080	0.107
Ni	Pearson Corr.	-0.116	0.354	-0.035	0.371	0.048	-0.255	-0.151
	p-value	0.506	0.037	0.842	0.028	0.786	0.139	0.386
Al	Pearson Corr.	0.156	-0.001	0.550	0.246	-0.351	0.004	-0.321
	p-value	0.371	0.995	0.001	0.155	0.039	0.982	0.060
Se	Pearson Corr.	-0.107	-0.442	-0.354	-0.460	0.464	0.187	0.685
	p-value	0.540	0.008	0.037	0.005	0.005	0.283	0.000
Mn	Pearson Corr.	1.000	0.264	0.121	0.260	-0.120	0.190	0.096
	p-value	--	0.126	0.490	0.132	0.493	0.275	0.584
Ca	Pearson Corr.	0.264	1.000	0.616	0.794	-0.299	-0.262	-0.307
	p-value	0.126	--	0.000	0.000	0.081	0.128	0.073
Mg	Pearson Corr.	0.121	0.616	1.000	0.353	-0.438	-0.083	-0.306
	p-value	0.490	0.000	--	0.038	0.009	0.634	0.074
Na	Pearson Corr.	0.260	0.794	0.353	1.000	-0.237	-0.304	-0.396
	p-value	0.132	0.000	0.038	--	0.170	0.075	0.019
pH	Pearson Corr.	-0.120	-0.299	-0.438	-0.237	1.000	0.037	0.316
	p-value	0.493	0.081	0.009	0.170	--	0.829	0.065
Free Chlorine	Pearson Corr.	0.190	-0.262	-0.083	-0.304	0.037	1.000	0.626
	p-value	0.275	0.128	0.634	0.075	0.829	--	0.000
Water	Pearson Corr.	0.096	-0.307	-0.306	-0.396	0.316	0.626	1.000
	p-value	0.584	0.073	0.074	0.019	0.065	0.000	--
Odor	Pearson Corr.	-0.015	0.100	-0.334	0.284	0.196	-0.160	-0.190
	p-value	0.931	0.569	0.050	0.098	0.244	0.345	0.275
Alkalinity	Pearson Corr.	0.203	0.235	-0.047	0.197	0.255	-0.040	0.231
	p-value	0.243	0.175	0.789	0.255	0.127	0.815	0.182
SUVA	Pearson Corr.	0.185	0.439	0.250	0.480	-0.270	0.366	0.002
	p-value	0.286	0.008	0.147	0.004	0.106	0.026	0.990
TOC	Pearson Corr.	-0.175	-0.539	-0.166	-0.505	0.033	-0.073	-0.057
	p-value	0.316	0.001	0.339	0.002	0.846	0.667	0.744

Table B12(c) Correlation between water quality parameters

		Ni	Al	Se	Odor	Alkalinit	SUVA	TOC
16S rRNA	Pearson Corr.	-0.033	0.027	-0.009	-0.077	-0.040	-0.209	0.337
	p-value	0.851	0.878	0.957	0.652	0.814	0.214	0.041
HPC	Pearson Corr.	-0.054	0.004	0.030	0.145	0.114	-0.094	0.111
	p-value	0.758	0.980	0.866	0.406	0.514	0.590	0.525
Zn	Pearson Corr.	0.227	-0.146	-0.044	0.191	0.217	-0.275	0.070
	p-value	0.190	0.402	0.803	0.272	0.210	0.109	0.688
Fe	Pearson Corr.	-0.004	0.033	-0.040	0.023	0.130	-0.198	0.026
	p-value	0.981	0.849	0.818	0.894	0.456	0.253	0.880
Pb	Pearson Corr.	0.782	-0.164	-0.230	0.179	0.023	0.016	-0.047
	p-value	0.000	0.346	0.184	0.304	0.898	0.929	0.789
Cu	Pearson Corr.	0.572	0.100	-0.114	-0.019	0.114	-0.236	0.062
	p-value	0.000	0.569	0.516	0.912	0.515	0.173	0.722
Cr	Pearson Corr.	0.055	-0.092	0.323	0.007	0.171	-0.211	-0.016
	p-value	0.754	0.600	0.059	0.967	0.325	0.223	0.927
Cd	Pearson Corr.	0.382	-0.074	-0.008	0.225	0.018	-0.128	0.131
	p-value	0.023	0.672	0.964	0.194	0.917	0.464	0.453
Ni	Pearson Corr.	1.000	-0.199	-0.098	0.177	0.042	-0.062	-0.089
	p-value	--	0.252	0.576	0.309	0.809	0.722	0.611
Al	Pearson Corr.	-0.199	1.000	-0.312	-0.243	-0.187	0.116	0.128
	p-value	0.252	--	0.068	0.160	0.281	0.508	0.463
Se	Pearson Corr.	-0.098	-0.312	1.000	-0.192	0.018	-0.285	0.177
	p-value	0.576	0.068	--	0.269	0.917	0.098	0.310
Mn	Pearson Corr.	-0.116	0.156	-0.107	-0.015	0.203	0.185	-0.175
	p-value	0.506	0.371	0.540	0.931	0.243	0.286	0.316
Ca	Pearson Corr.	0.354	-0.001	-0.442	0.100	0.235	0.439	-0.539
	p-value	0.037	0.995	0.008	0.569	0.175	0.008	0.001
Mg	Pearson Corr.	-0.035	0.550	-0.354	-0.334	-0.047	0.250	-0.166
	p-value	0.842	0.001	0.037	0.050	0.789	0.147	0.339
Na	Pearson Corr.	0.371	0.246	-0.460	0.284	0.197	0.480	-0.505
	p-value	0.028	0.155	0.005	0.098	0.255	0.004	0.002
pH	Pearson Corr.	0.048	-0.351	0.464	0.196	0.255	-0.270	0.033
	p-value	0.786	0.039	0.005	0.244	0.127	0.106	0.846
Free	Pearson Corr.	-0.255	0.004	0.187	-0.160	-0.040	0.366	-0.073
	p-value	0.139	0.982	0.283	0.345	0.815	0.026	0.667
Water	Pearson Corr.	-0.151	-0.321	0.685	-0.190	0.231	0.002	-0.057
	p-value	0.386	0.060	0.000	0.275	0.182	0.990	0.744
Odor	Pearson Corr.	0.177	-0.243	-0.192	1.000	0.149	0.148	-0.243
	p-value	0.309	0.160	0.269	--	0.379	0.382	0.147
Alkalinity	Pearson Corr.	0.042	-0.187	0.018	0.149	1.000	0.085	-0.067
	p-value	0.809	0.281	0.917	0.379	--	0.618	0.693
SUVA	Pearson Corr.	-0.062	0.116	-0.285	0.148	0.085	1.000	-0.217
	p-value	0.722	0.508	0.098	0.382	0.618	--	0.197
TOC	Pearson Corr.	-0.089	0.128	0.177	-0.243	-0.067	-0.217	1.000
	p-value	0.611	0.463	0.310	0.147	0.693	0.197	--

Table B13 Drinking water Ni and Mn concentrations at different fixtures and exposure duration

Location		**Ni, µg/L**					**Mn, µg/L**				
Exposure, days		3d	15d	30d	60d	90d	3d	15d	30d	60d	90d
Soften Water		3.1	3.5	3.2	5.6	3.0	11.1	5.4	37	20	<5
Cold	Basement	3.2	46.7	3.0	7.8	8.4	5.9	<5	<5	<5	<5
	1st Floor	13.1	6.7	4.4	4.8	3.0	10.4	<5	26.9	<5	<5
	2nd Floor	22.9	4.0	4.1	4.8	4.4	<5	5.4	<5	<5	<5
Hot	Basement	3.4	5.8	3.7	7.3	4.8	11.3	59.9	13.5	<5	<5
	1st Floor	3.3	14.4	7.2	4.8	3.1	13.9	<5	25.5	6.1	<5
	2nd Floor	23.8	4.4	4	4.1	4.2	8.7	5.2	<5	<5	<5

Table B14 Drinking water Ca, Mg, Na concentrations at different fixtures and exposure durations

Location/ Exposure		Ca, mg/L					Mg, mg/L					Na, mg/L				
		d-3	d-15	d-30	d-60	d-90	d-3	d-15	d-30	d-60	d-90	d-3	d-15	d-30	d-60	d-90
Soften Water		124.9	135.1	119.9	98.3	89.0	37.9	44.1	39.8	36.7	34.5	38.4	31.9	29.6	27.5	25.5
Cold	Basement	123.7	127.5	113.5	100.7	100.7	37.1	38.5	38.7	36.3	36.6	37.5	37.5	29.2	28.0	28.0
	1st Floor	117.3	124.9	107.1	99.5	94.5	38.6	42.1	39.6	38.3	35.4	38.8	31.5	33.3	28.9	27.1
	2nd Floor	126.2	123.7	113.5	102	93.2	37.5	41.2	41.0	38.8	37.3	39.1	36.5	34.3	29.0	27.8
Hot	Basement	108.4	124.9	112.2	99.5	96.5	39.1	38.9	40.5	37.8	37.1	38.9	37.3	33.9	28.0	27.3
	1st Floor	124.9	118.6	110.9	99.5	93.4	37.0	41.0	39.8	37.7	35.5	37.5	31.5	33.1	28.0	27.3
	2nd Floor	123.7	121.1	109.7	98.3	100.7	37.4	41.9	40.3	37.3	38.4	38.4	36.5	33.9	27.4	28.2

Table B15 Drinking water Cr, Al, Se concentrations at different fixtures and exposure duration

Location/ Exposure		Cr, µg/L					Al, µg/L					Se, µg/L				
		3d	15d	30d	60d	90d	d3	d15	d30	d60	d90	d3	d15	d30	d60	d90
Soften Water		nd	nd	nd	19.7	nd	nd	<5	<5	nd	nd	2.9	3	3.1	6.7	5.5
Cold	Basement	<5	<5	nd	nd	nd	nd	<5	1.4	nd	nd	3.4	3.1	3.6	3.6	3.5
	1st Floor	nd	nd	nd	nd	nd	11.7	<5	16.6	10.2	nd	3.2	3.9	2.6	4.5	3.9
	2nd Floor	nd	nd	nd	nd	nd	nd	15.7	16.2	7.4	8.0	3.1	3	3.5	3.3	4.4
Hot	Basement	<5	31.0	nd	<5	<5	18.5	8.5	17.5	6.7	7.0	3.7	3.4	3	3.5	3.7
	1st Floor	nd	nd	nd	nd	nd	nd	5.1	17.8	8.9	nd	3.4	4.7	2.8	3.3	3
	2nd Floor	6.7	nd	nd	nd	nd	nd	15.7	16.2	7.4	9.0	3.3	2.8	3.2	3.5	3.6

Table B16 Bacterial gene copy numbers and HPC Results

Location	Time (Day)	Gene Copy Numbers/mL	HPC (CFU/mL)
Water Softener	3	5.77 ± 2.04	NA[a]
	15	20.99 ± 7.58	1
	30	15.83 ± 6.04	0
	60	46.94 ± 7.17	0.0013 ± 0.0013
	90	31.64 ± 11.62	0.2490 ± 0.0468
Basement Cold Water	0	3.85 ± 1.03	NA
	3	15.44 ± 5.50	NA
	15	5.98 ± 1.97	0
	30	9.50 ± 5.86	0.0480 ± 0.0140
	60	309.44 ± 68.41	0.0013 ± 0.0013
	90	100.98 ± 34.13	0.3727 ± 0.1294
Basement Hot Water	0	6.86 ± 1.84	NA
	3	2707.01 ± 682.04	NA
	15	49.09 ± 11.69	NA
	30	4469.44 ± 1074.25	NA
	60	74002.44 ± 16231.31	0.3267 ± 0.1386
	90	22509.20 ± 1947.79	856.6667 ± 40.9607
1st Floor Kitchen Cold Water	3	7.39 ± 2.36	NA
	15	15.99 ± 10.51	0.0010
	30	10.01 ± 5.02	0
	60	18.47 ± 5.72	0
	90	313.67 ± 48.19	0.1100 ± 0.0519
1st Floor Kitchen Hot Water	3	149.95 ± 33.33	NA
	15	8.89 ± 5.26	NA
	30	6.60 ± 2.23	0.0160 ± 0.0080
	60	16.37 ± 3.47	0.2553 ± 0.1266
	90	1115.17 ± 284.54	0.8667 ± 0.5041
2nd Floor Bathroom Cold Water	3	5.27 ± 1.52	NA
	15	2.67 ± 0.88	0
	30	5.08 ± 1.10	0.0010 ± 0.0010
	60	8.24 ± 0.84	0
	90	597.61 ± 104.89	0.0660 ± 0.0065
2nd Floor Bathroom Hot Water	3	6.40 ± 3.19	NA
	15	7.08 ± 3.41	0.0070
	30	38.42 ± 15.00	0.0120 ± 0.0120
	60	203.17 ± 26.90	0.0840 ± 0.0462
	90	7422.21 ± 828.21	0.4167 ± 0.0678

NA: not available. No HPC tests were performed on day 0 and day 3 at all locations, and on day 15 at some locations.

Table B17 Correlation analysis between bacterial gene copy numbers and TOC levels

Sample location	**Pearson's correlation coefficients**	***p***
Water Softener	0.83	0.08
Basement Cold Water	0.63	0.18
Basement Hot Water	0.55	0.25
1st Floor Kitchen Cold Water	0.82	0.09
1st Floor Kitchen Hot Water	-0.15	0.81
2nd Floor Bathroom Cold Water	0.82	0.09
2nd Floor Bathroom Hot Water	0.81	0.10

Table B18 Water usage parameters correlation with TOC and bacterial concentrations, threshold for correlation was considered as 0.50

Fixture	Correlation with TOC			Correlation with Bacterial Concentration		
	Number of Events	Total Volume	Average Elapsed Time	Number of Events	Total Volume	Average Elapsed Time
Whole House Water Softener	0.84	0.81	0.63	0.97	0.93	0.47
Basement Cold	0.89	0.11	0.61	0.41	0.51	0.19
Basement Hot	0.71	-0.13	0.87	0.22	-0.28	0.50
1st Floor Cold	0.85	0.75	0.21	0.34	0.21	0.01
1st Floor Hot	0.68	0.52	0.86	0.36	0.39	0.03
2nd Floor Cold	0.64	0.53	0.75	0.12	-0.06	0.67
2nd Floor Hot	0.83	0.84	-0.03	0.07	0.85	0.09

APPENDIX C

Table C1 The chemical equilibrium and constant used to determine Pb speciation (Brezonic & Arnold, 2011)

Chemical Equilibrium	Equilibrium Constant
$Pb^{2+} + H_2O \leftrightarrow PbOH^+ + H^+$	$\log\beta_1^* = -7.597$
$Pb^{2+} + 2\,H_2O \leftrightarrow Pb(OH)_{2\,(aq)} + 2\,H^+$	$\log\beta_2^* = -19.988$
$Pb^{2+} + 2\,H_2O \leftrightarrow Pb(OH)_3^- + 3\,H^+$	$\log\beta_3^* = -28.091$
$Pb^{2+} + 2\,H_2O \leftrightarrow Pb(OH)_4^{2-} + 4\,H^+$	$\log\beta_3^* = -39.699$
$Pb(OH)_{2\,(s)} + 2\,H^+ \leftrightarrow Pb^{2+} + H_2O$	$K_s^* = 8.15$

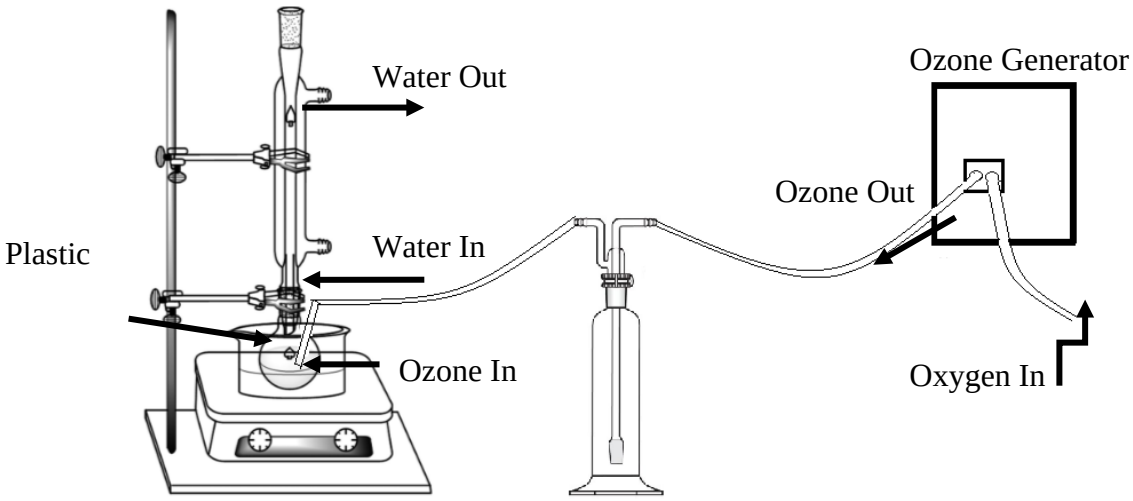

Figure C1 The schematic outline of ozonation setup

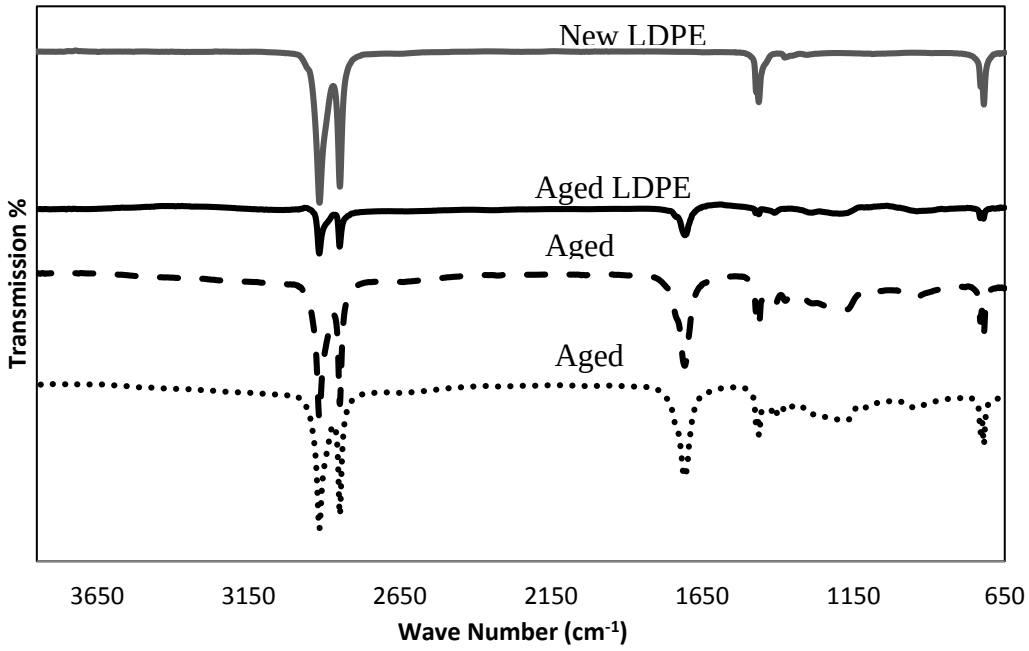

Figure C2 ATR-FTIR spectra for new LDPE pellet and 10 hr aged LDPE sheet, pellet and film

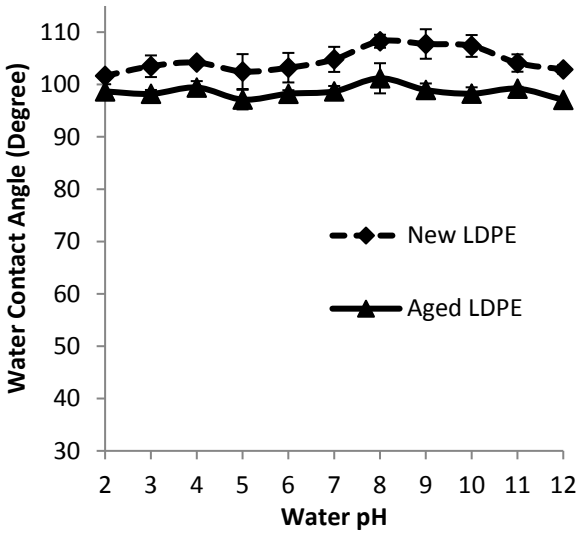

Figure C3 Static water contact angle for new and 10 hr aged LDPE versus pH

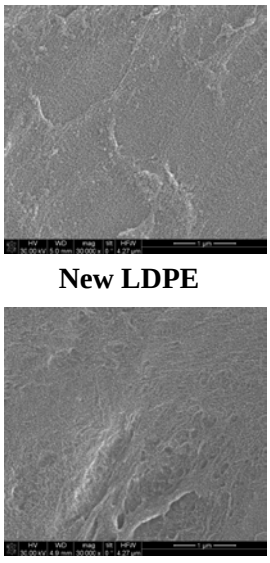

Figure C4 FE-SEM scans of new and aged LDPE

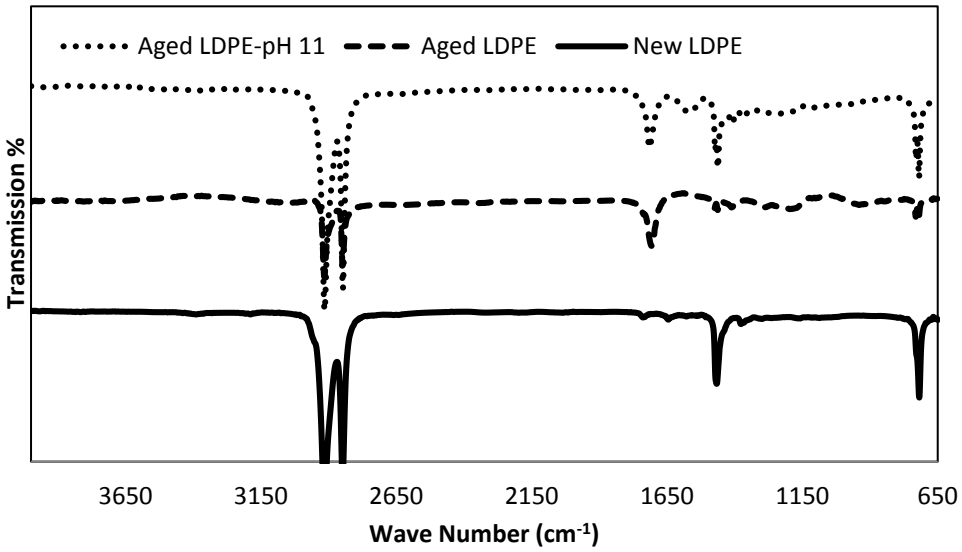

Figure C5 ATR-FTIR spectra of aged LDPE and aged LDPE exposed to pH 11 water for 5 days

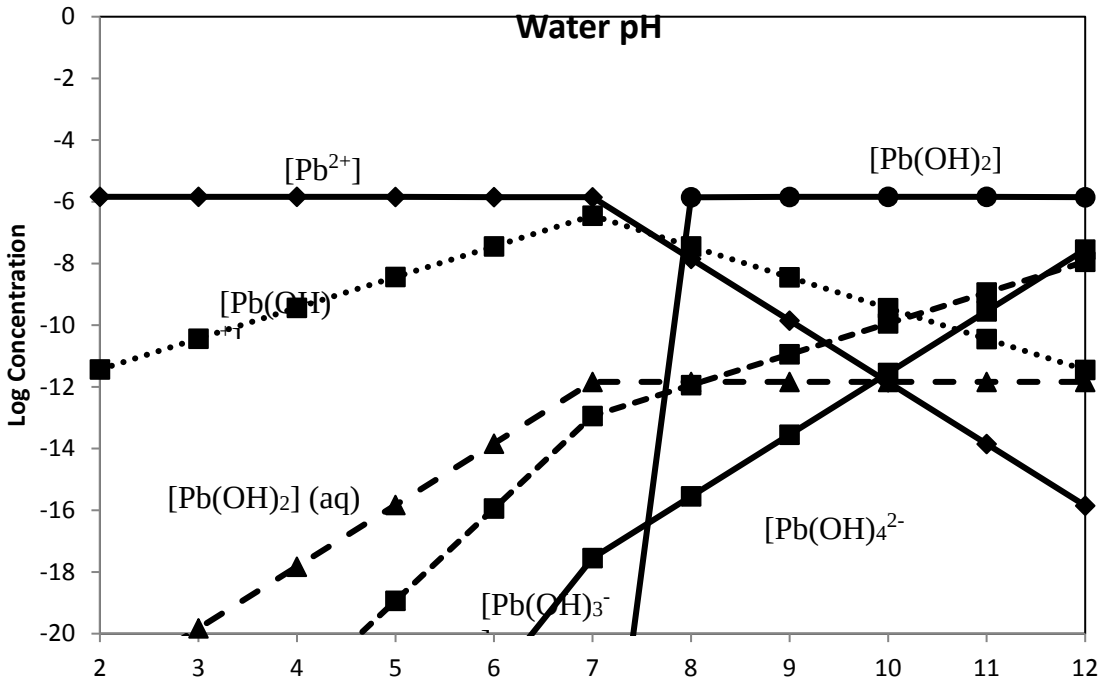

Figure C6 Log Pb species concentration versus water pH, [Pb]t=300 µg/L, no oxygen, room temp

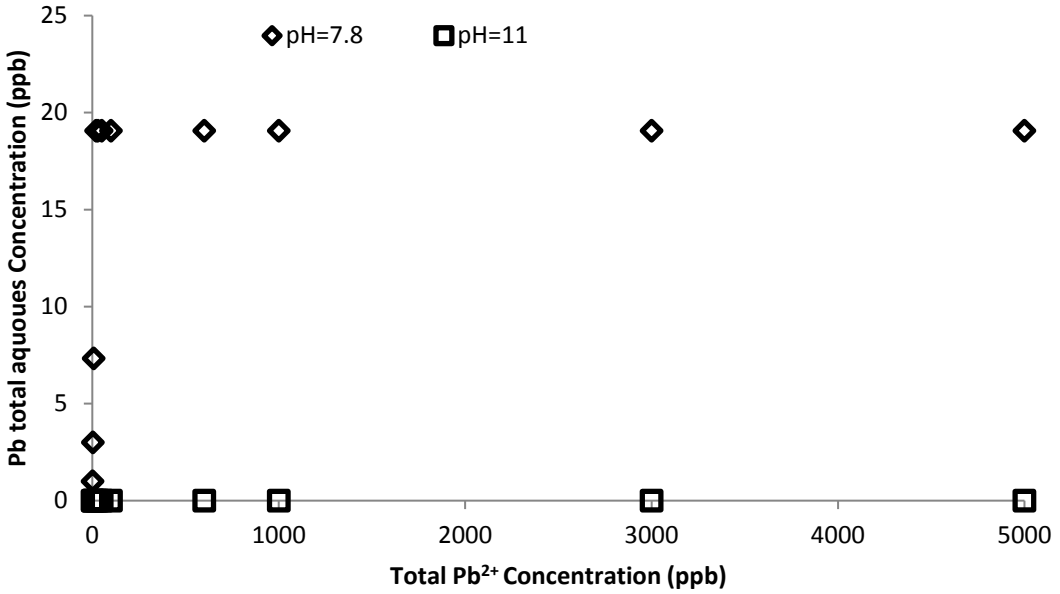

Figure C7 Aqueous Pb concentration versus Total Pb concentration at pH 7.8 and 11

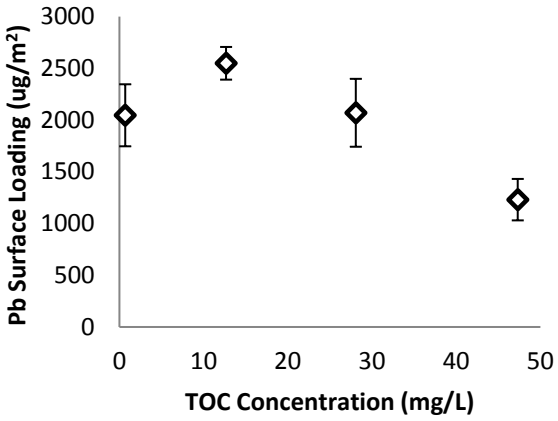

Figure C8 Influence of TOC concentration on Pb surface loading (aged LDPE, pH 7.8, after 48 hr)

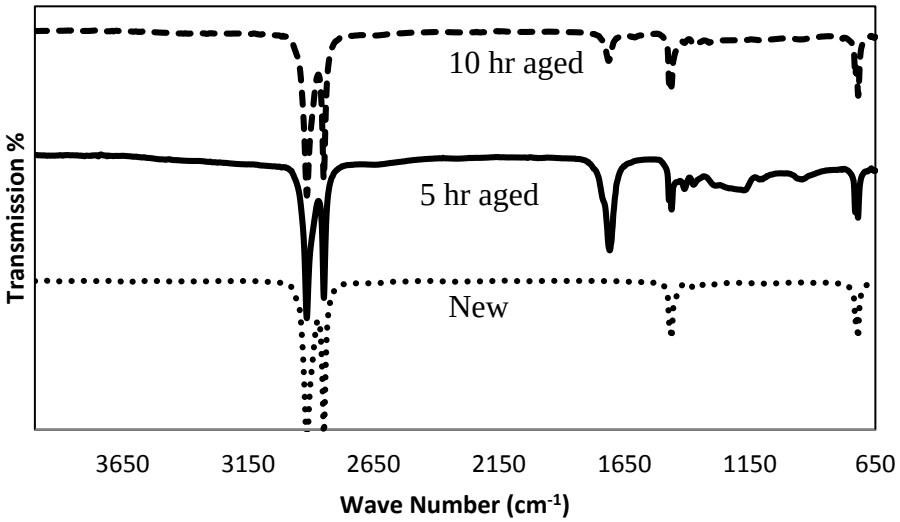

Figure C9 ATR-FTIR spectra of New, 5 hr and 10 hr aged LDPE films

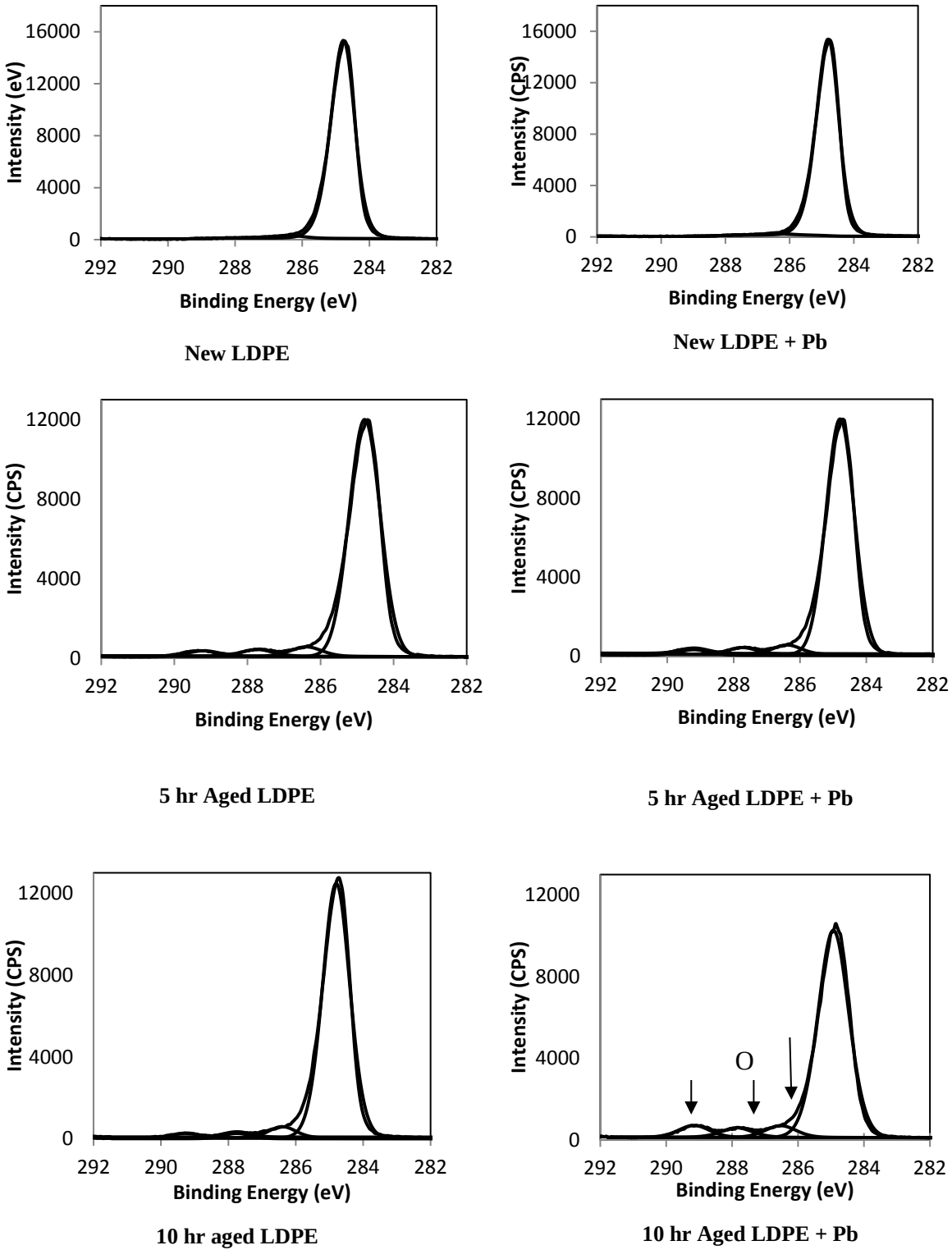

Figure C10 High resolution XPS spectra of C1s for LDPE samples

.

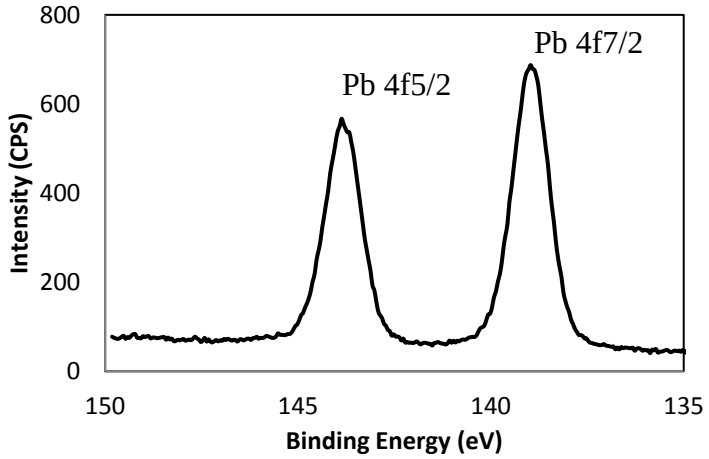

Figure C11 Pb high resolution XPS spectra for 5 hr aged LDPE exposed to Pb